

**AQUEOUS PRECIPITATION OF CRYSTALLINE SVABITE  
(Ca<sub>5</sub>(AsO<sub>4</sub>)<sub>3</sub>F) AND SVABITE/FLUORAPATITE (Ca<sub>5</sub>(AsO<sub>4</sub>)<sub>x</sub>(PO<sub>4</sub>)<sub>3-x</sub>F)  
COMPOUNDS AND EVALUATION OF THEIR STABILITY**

Marie-Christine Noel

Department of Mining and Materials Engineering

McGill University

Montreal

Canada

May 2018

A thesis submitted to McGill University in partial fulfilment of the requirements of the  
degree of Master of Engineering

© Marie-Christine Noel, 2018

## ABSTRACT

Precipitation of insoluble arsenic compounds from aqueous process solutions is an option for arsenic-rich waste stabilisation. This work aimed to determine the suitability of the calcium arsenate apatite svabite ( $\text{Ca}_5(\text{AsO}_4)_3\text{F}$ ) and mixtures/solid-solutions of svabite and the phosphate apatite fluoroapatite ( $\text{Ca}_5(\text{PO}_4)_3\text{F}$ ) as compounds for the long-term storage of arsenic. This work includes the development of a procedure for synthesizing the compounds using aqueous precipitation, and preliminary stability testing of the produced solids, to establish the arsenic release under different equilibration conditions. The operating range for the precipitation of the solids was investigated by varying the precipitation temperature, pH, reaction time, and the order of the procedure steps. Solids with differing arsenate contents were characterized using XRD and SEM. Concentrations in solutions sampled during precipitation were analysed using ICP-OES. The precipitation of the calcium arsenate apatite compounds required a moderately basic pH, but an alkaline pH greater than 9 resulted in the formation of johnbaumite ( $\text{Ca}_5(\text{AsO}_4)_3\text{OH}$ ). Formation of crystalline apatite required temperatures greater than  $60^\circ\text{C}$ , and aging times greater than four hours. It was also necessary that the fluoride be added to the precipitation solution after the arsenic and calcium components to avoid the interfering formation of fluorite ( $\text{CaF}_2$ ). Solids with varying arsenic and phosphate content were subjected to a preliminary stability test. The solids were kept in solution that was adjusted to pH 9 for three days, then the solution pH was allowed to drift for a further three days (reaching solution pHs ranging from 8.25 to 8.75), before the addition of  $\text{NaHCO}_3$  to investigate the effect of carbonate on arsenical apatite stability. Overall, the mixed arsenate/phosphate fluoroapatite solids with the 15% arsenate content released the least arsenic ( $\sim 15$  mg/L in  $\text{CO}_3$ -free water of pH 9 and 3 days equilibration). Even under these conditions however, the extent of dissolution was greater than what would be acceptable for the long-term storage of arsenical solids.

## RÉSUMÉ

La précipitation des composés insolubles de l'arsenic à partir de solution aqueuse est une option pour la stabilisation de résidus ayant une concentration élevée d'arsenic. Cette étude vise à déterminer la pertinence d'utiliser l'apatite svabite ( $\text{Ca}_5(\text{AsO}_4)_3\text{F}$ ) et des solides composés de svabite et de fluorapatite ( $\text{Ca}_5(\text{PO}_4)_3\text{F}$ ) pour l'entreposage à long terme de l'arsenic. Cette étude comprend le développement d'une procédure de synthèse pour la précipitation des composés en milieu aqueux et des essais préliminaires de stabilité des solides qui en découlent afin d'établir la quantité d'arsenic relâchée sous différentes conditions d'équilibration. La gamme opératoire des précipitations fut étudiée en variant certains paramètres, incluant la température, le pH, la durée de la réaction et la séquence des étapes de la synthèse. Des solides avec différentes teneurs d'arséniate furent caractérisés par diffraction X et microscopie électronique avec balayage MEB et les concentrations durant la précipitation furent analysées avec un spectromètre d'émission ICP-OES. La précipitation des composés de calcium arséniate apatite nécessite un pH modérément alcalin (7-9), mais un pH plus alcalin entraîne la formation de johnbaumite ( $\text{Ca}_5(\text{AsO}_4)_3\text{OH}$ ). La précipitation de l'apatite cristalline nécessite des températures de plus de  $60^\circ\text{C}$  et un temps de maturation de plus de quatre heures. Il est aussi nécessaire d'ajouter le fluorure à la solution de précipitation après l'ajout des composantes d'arsenic et de calcium. Les solides ayant diverses teneurs d'arsenic et de phosphate furent soumis à un test de stabilité préliminaire. Des solides furent conservés dans une solution ayant un pH de 9 pour une période de trois jours, puis cette solution fut laissée au repos pour une période de trois autres jours avant d'ajouter le  $\text{NaHCO}_3$  afin d'étudier l'effet du  $\text{CO}_3$  sur la stabilité de l'apatite. Les niveaux d'arsenic relâchés furent les plus élevés à un pH de 9, mais même sous ces conditions, le niveau de dissolution fut plus élevé que le niveau acceptable pour l'entreposage à long terme des solides d'arsenic, surtout en présence d'ions de carbonate. En général, les solides composés d'un mélange de fluorapatite arséniate/phosphate ayant une teneur d'arséniate de 15% relâchèrent le moins d'arsenic ( $\sim 15 \text{ mg/L}$ ) dans une solution sans carbonate ayant un pH de 9 et durant 3 jours d'équilibration.

## ACKNOWLEDGEMENTS

This thesis could not have happened without my supervisor Professor George P. Demopoulos, and I would like to thank him for his guidance, support, patience, and for all that he taught me.

Thanks are also due to my fellow McGill HydroMET group members – Matthew, Thomas, Christoph, Jessica, Ravi, Lying, Jay, Amrita, and the others. A special thank you also to Micah, for his support and friendship.

I would also like to thank Monique Riendeau, Andrew Gosztajn, and especially Ranjan Roy for their help with chemical analysis. Thanks also to Barbara Hanley and the rest of the Materials Engineering administrative team.

Thank you to NSERC and Teck for their funding support.

A big thank you also to all my friends and family who supported me throughout this time. Thank you to my parents, my sister, Eric, Nick, Charlotte, Nils, Ross, Andrea and Isaac for always being there.

## CONTRIBUTION OF AUTHORS

This dissertation is original, unpublished, independent work by the author, M-C Noel.

## Table of Contents

ABSTRACT.....	ii
RÉSUMÉ .....	iii
ACKNOWLEDGEMENTS.....	iv
1 Introduction .....	1
2 Literature Review.....	3
2.1 Introduction.....	3
2.1.1 Crystallization and Aqueous Chemistry .....	3
2.1.2 Arsenic Removal and Stabilization .....	4
2.1.3 Scorodite Precipitation and Stability .....	5
2.1.4 Apatite Minerals .....	6
2.2 Review of Calcium Arsenate Compounds.....	7
2.2.1 Formation of Calcium Arsenates in Aqueous Solution.....	8
2.2.2 Dissolution and Stability of Calcium Arsenates.....	12
2.2.3 Removal of Arsenic by Formation of Calcium Arsenate/Phosphate Apatite Solid Solutions .....	14
2.2.4 Dissolution and Stability of Calcium Arsenate/Phosphate Apatite Solid Solutions .....	15
2.3 Svabite.....	17
2.3.1 Synthesis of Svabite.....	17
2.1.1 Dissolution and Stability of Svabite .....	19
2.1.2 Synthesis and Stability of Svabite/Fluorapatite Solid Solutions .....	21
2.4 Fluoroapatite .....	23
2.4.1 Aqueous Synthesis of Fluoroapatite .....	24
2.4.2 Dissolution of Fluoroapatite .....	27
2.5 Conclusion .....	29

3	Objectives.....	31
4	Experimental Methods .....	33
4.1	Chemical Reagents.....	33
4.2	Procedure for Precipitation of Svabite and Svabite-Fluoroapatite Compounds .....	33
4.3	Characterization of Solids and Solutions.....	36
4.4	Stability Evaluation Procedure .....	36
5	Results and Discussion.....	39
5.1	Aqueous Precipitation of Svabite by Neutralization and Aging.....	39
5.1.1	Neutralization-Based Process for the Precipitation of Svabite.....	39
5.1.2	Effect of Aging on Svabite Formation .....	43
5.1.3	Effect of Neutralization pH on Svabite Formation.....	46
5.1.4	Effect of Neutralization Temperature on Svabite Formation .....	48
5.1.5	Effect of Initial As Concentration on Svabite Formation.....	50
5.1.6	Effect of Timing of Fluoride Addition to the Solution.....	52
5.2	Synthesis of Mixed Fluoroapatite/Svabite .....	55
5.3	Stability Evaluation.....	61
5.3.1	Effect of Washing.....	61
5.3.2	Stability at pH 9.....	63
5.3.3	Stability Evaluation Without pH Control .....	66
5.3.4	Stability Evaluation in the Presence of Carbonate in Solution.....	70
5.3.5	Comparison of Stability Data .....	73
6	Conclusions .....	75
7	Works Cited.....	78
	Appendix A: Duplicates of Synthesis Procedures .....	85
	Appendix B: Synthesis of Mixed Arsenate/Phosphate Apatites at Different pH .....	92

## List of Figures

Figure 2-1: Calcium arsenate phases at equilibrium with solution at 25°C (47).....	9
Figure 2-2: SEM image of johnbaumite (19) .....	11
Figure 2-3: SEM images of CaHAsO <sub>4</sub> •H <sub>2</sub> O (52) .....	11
Figure 2-4: SEM images of mixture of CaHAsO <sub>4</sub> •H <sub>2</sub> O and Ca(H <sub>2</sub> AsO <sub>4</sub> ) <sub>2</sub> (52) .....	12
Figure 2-5: Arsenic levels in solution after the dissolution of JBM/HAP (22). .....	16
Figure 2-6: Arsenic levels after the dissolution of solid solutions of JBM/HAP (55) .....	17
Figure 2-7: Svabite formed by precipitation from solution (65) .....	19
Figure 2-8: Morphology of mixed svabite/fluoroapatite solids (66) .....	21
Figure 2-9: Arsenic release during FAP/SVA solid solution dissolution (60) .....	23
Figure 2-10: TEM images of FAP synthesized at different temperatures (14) .....	26
Figure 2-11: Effect of initial F/Ca molar ratio on the morphology of FAP (75).....	26
Figure 2-12: Surface complexation model of fluoroapatite (76).....	28
Figure 5-1: Flowchart of developed procedure for the precipitation of crystalline svabite ..	40
Figure 5-2: XRD analysis of synthesized svabite compound.....	42
Figure 5-3: XRD characterization of svabite precipitates obtained from replicate tests .....	42
Figure 5-4: SEM image of svabite particles .....	43
Figure 5-5: XRD patterns of precipitates after 1 hour, 4 hours, 10 hours, and 24 hours of aging.....	44
Figure 5-6: Solution concentration profiles during aging.....	46
Figure 5-7: XRD patterns of solids precipitated by neutralization at different pH .....	47
Figure 5-8: XRD pattern for solids precipitated at 90°C after varying aging times.....	50
Figure 5-9: XRD patterns for solids precipitated at different arsenic concentrations .....	51
Figure 5-10: XRD patterns for solids precipitated at different arsenic concentrations at pH 6 .....	52
Figure 5-11: XRD patterns obtained by varying timing of fluoride addition at pH 8 .....	53
Figure 5-12: XRD patterns obtained by varying timing of fluoride addition at pH 6 .....	54
Figure 5-13: SEM images of svabite particles formed using different methods .....	55
Figure 5-14: XRD patterns of mixed arsenate-phosphate fluoroapatite solids .....	57
Figure 5-15: XRD patterns of solids formed with 50% arsenate content at different pH .....	58



Figure 5-16: Solution concentration profiles during aging of arsenate-phosphate fluoroapatites.....	59
Figure 5-17: SEM images of phosphate-arsenate solids with varying arsenate fraction.....	60
Figure 5-18: Evolution of concentrations of constituent elements and molar ratio of Ca: [P+As] during successive washing cycles.....	63
Figure 5-19: Stability testing of svabite and arsenate-substituted fluoroapatite samples at pH 9.....	65
Figure 5-20: Molar ratio of Ca:(P+As) concentrations during stability tests at pH 9 .....	66
Figure 5-21: pH drift during the uncontrolled equilibration tests.....	67
Figure 5-22: Stability testing of svabite and arsenate-substituted fluoroapatite samples during pH drift period .....	69
Figure 5-23: Solution molar ratios of Ca: (As+P) evolution during pH drift stability tests ..	70
Figure 5-24: pH evolution after addition of NaHCO <sub>3</sub> .....	71
Figure 5-25: Stability testing of svabite and arsenate-substituted fluoroapatite samples after addition of NaHCO <sub>3</sub> .....	72
Figure A-1: Svabite precipitation duplicates using synthesis at pH 8 .....	85
Figure A-2: Haideringite precipitation duplicates using synthesis at pH 6.....	86
Figure A-3: CaF <sub>2</sub> precipitation duplicates using synthesis at pH 4 .....	87
Figure A-4: Duplicates using synthesis at pH 10 .....	88
Figure A-5: Svabite precipitation duplicates fluoride added after neutralization,.....	89
Figure A-6: Duplicates of fluorapatite synthesis at pH 8 .....	89
Figure A-7: Duplicates of 25% Arsenate Svabite-Fluoroapatite Synthesis at pH 8.....	90
Figure A-8: Duplicates of 50% arsenate svabite-fluorapatite synthesis at pH 8 .....	90
Figure A-9: Duplicates of 75% arsenate svabite-fluorapatite synthesis at pH 8 .....	91
Figure B-1: XRD patterns for fluoroapatite synthesized at varied pH .....	92

## List of Tables

Table 2.1 Summary of synthesis methods of calcium arsenate compounds from solution ...	10
Table 2.2 Summary of stability investigations on calcium arsenates .....	13
Table 2.3: Stability testing results for synthetic svabite (60) .....	20
Table 2.4: Summary of methods developed to precipitate fluoroapatite from solution .....	24
Table 5.1: Chemical composition and BET area of solids formed at pH 8/70°C/24-hr .....	55
Table 5.2: BET surface area for mixed fluoroapatite solids with varying arsenic content ...	61
Table 5.3: Summary of released arsenic concentrations after stability tests .....	74

# 1 Introduction

Solubilized arsenic is a toxic by-product of metallurgical processes. The current Health Canada and WHO guideline for drinking water arsenic content is 0.01 mg/L (1). Canadian regulations also limit monthly average concentrations of arsenic in mining effluents to 0.50 mg/L (2). Arsenic can be removed from waste waters or process solutions by precipitation with calcium, co-precipitation/adsorption processes, using ferric or aluminum salts, electrocoagulation or through adsorption to media such as activated alumina, sand or ferric hydroxide (3). Although effective in the removal of arsenic from wastewater, these methods do not necessarily guarantee a stable arsenic-bearing residue, and are typically used for low arsenic concentration effluent streams only. Any arsenic-contaminated waste resulting from industrial processes must be disposed of in a manner that will ensure low arsenic concentrations in the environment below government-set limits. The prevalent treatment process for waste streams with low arsenic content is the combination of co-precipitation of arsenic(V) with ferric iron and lime neutralization. This method requires an iron(III):arsenic(V) molar ratio greater than 3, resulting in a high iron requirement (4), hence is not suitable for arsenic-rich process solutions or wastes.

Alternatively, precipitation of arsenic compounds is advocated. Such compounds include scorodite  $\text{FeAsO}_4 \cdot 2\text{H}_2\text{O}$  (5), and yukonite  $\text{Ca}_2\text{Fe}_{3-5}(\text{AsO}_4)_3(\text{OH})_{4-10} \cdot x\text{H}_2\text{O}$  (where  $x=2-11$ ) (6). Both minerals have been synthesized using an aqueous precipitation process by the McGill HydroMet group. The scorodite process developed by this group is currently commercially practiced in Chile (Ecometales Ltd.) (7) and piloted in Japan (Dowa Metals and Mining Company) (8). Scorodite is however soluble at pH greater than 7 and in anoxic conditions (9), (10)). As such other arsenate-containing compounds that are insoluble at  $\text{pH} > 7$  and even under anoxic conditions are worthy to investigate as means of stabilizing arsenical wastes. One such group of compounds are apatites, namely compounds with the formula  $\text{Ca}_5(\text{Z})_3\text{X}$ , where X is an anion of charge -1 (such as  $\text{OH}^-$ ,  $\text{F}^-$ ) and Z can be oxides such as  $\text{PO}_4$  or  $\text{AsO}_4$  (11).

Previous work by the McGill HydroMET group has included scorodite encapsulation research using hydroxyapatite ( $\text{Ca}_5(\text{PO}_4)_3\text{OH}$ ) and fluorapatite ( $\text{Ca}_5(\text{PO}_4)_3\text{F}$ ) (12), with the objective to increase the range of conditions (in terms of pH and redox potential) where scorodite is stable. This strategy proved effective as the release of arsenic from the coated scorodite particles decreased in slightly basic solutions under anoxic conditions (regulated with the

addition of sulfide ions) when compared to uncoated scorodite (12),. However, the apatite coating did not fully protect scorodite as it provided only partial coverage. Thus it was decided to pursue an alternative approach that of formation of calcium apatites with arsenate rather than phosphate and this is the subject of the present thesis. Furthermore, it was decided to focus on the study of fluoro-arsenate apatite known as svabite (13) rather than the hydroxy arsenate analogue as fluorapatite is known to have at least two orders of magnitude lower solubility than the hydroxyapatite compound (14) making it a more stable candidate to fix arsenic.

This thesis describes the development of an atmospheric aqueous precipitation process for the formation of the arsenate analogue of fluorapatite, svabite ( $\text{Ca}_5(\text{AsO}_4)_3\text{F}$ ) as well as mixed phosphate/arsenate analogues, and investigates the impact of different precipitation parameters on the phases formed. Preliminary dissolution tests were completed to determine the stability of these compounds and their potential as stable arsenate fixation media. This thesis consists of this introductory chapter and the following chapters:

**Chapter 2 – Literature Review** – Discusses aqueous precipitation of arsenic-containing solids, the phases and characteristics of the calcium-arsenate aqueous system, and previous work in the precipitation of calcium arsenates, the precipitation of fluorapatite, and the stability of these compounds.

**Chapter 3 – Objectives** – Discusses the objectives of the work presented in this thesis in the context of the current body of knowledge.

**Chapter 4 – Experimental Methods** – Describes chemicals and reagents used, experimental procedures for the precipitation of various solids, washing, and stability tests.

**Chapter 5 – Results and Discussion** – Describes the development of the precipitation process, the effect of different precipitation parameters on the evolutions of concentrations in solution and nature of the solids precipitated; and presents the results of the stability testing of solids with varying arsenate content.

**Chapter 6 – Conclusion** – Conclusions drawn from the work included in this thesis, and a discussion of the limitations of the current work and possible future work are presented here.

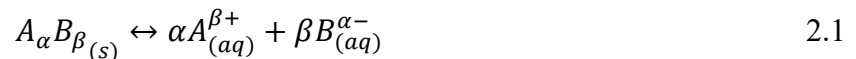
## 2 Literature Review

### 2.1 Introduction

#### 2.1.1 Crystallization and Aqueous Chemistry

To produce crystalline calcium arsenate compounds and solid solutions, it is necessary to understand aqueous chemistry and precipitation theory to select and manipulate the various system parameters.

A solid compound will equilibrate in water with its component ions:



The thermodynamic driving force of precipitation is the difference between the chemical potential of the crystal constituents in the supersaturated solution and in the precipitated solid.

The chemical potential ( $\mu$ ) of these ions is calculated using their activities ( $a_i$ ) as follows:

$$\mu_i = \mu_i^0 + RT \ln (a_i) \quad 2.2$$

The activities of the components are equivalent to the product of the concentration of the component and the activity coefficient of the component. The activity coefficients of ions will change depending on the overall dissolved component content in the water, or the ionic strength of the solution (15).

The solid will dissolve into water until the solution is saturated with respect to the solid. At saturation, the quotient of the activities of the components of the solid to the power of their stoichiometric coefficients will be equal to its solubility product, or  $K_{sp}$ , as seen in equation 2-3:

$$K_{sp} = (a_A)^{\alpha} (a_B)^{\beta} \quad 2.3$$

If the quotient of these activities is greater than the compound's solubility product, precipitation will occur. Should the quotient of the activities be greater than the compound's  $K_{sp}$ , the system is then considered supersaturated. Similarly, if the product of the component activities is less than  $K_{sp}$ , then the system is considered undersaturated. The saturation of a system is defined as (15):

$$S = \frac{\prod_i (a_i)^{v_i}}{K_{sp}} \quad 2.4$$

Where  $v_i$  is the stoichiometric coefficient of component  $i$ .

The supersaturation state of a system will influence the rate and nature of the precipitation process in terms of nucleation mechanism, growth and crystallinity of product (16). Depending

on the conditions of the precipitating solution (degree of supersaturation), different solid phases can be formed. According to Ostwald's law of stages, if nucleation is initiated in solution (rather than on a surface), a less thermodynamically stable (metastable) phase will be formed first, due to favorable kinetics. The thermodynamically favoured phase may evolve through secondary growth and/or phase transformations (16). Among the different key precipitation parameters affecting the quality of the product are pH and temperature as both can influence supersaturation given that the solubility of a compound ( $K_{sp}$ ) –at least those incorporating hydroxyl groups- depends on them. Manipulating the temperature will also affect the kinetics of crystallization and compound composition as it can lead to dehydration (15).

### 2.1.2 Arsenic Removal and Stabilization

Arsenic is a metalloid with four oxidation states: -3, 0, +3, +5. It occurs naturally in more than 300 different minerals in nature. 60% of these minerals occur as arsenates [As(V)], 20% as sulphides and sulphosalts and the remaining 20% is made up of arsenites [As(III)], arsenides, native elements and metal alloys (17). Arsenite as a rule is more toxic and more soluble than arsenate. This high solubility combined with the prevalence of arsenic-containing minerals leads to the contamination of soil and water with arsenic. Arsenic may also enter the environment through anthropogenic pathways, as it is a by-product of certain mineral and metallurgical processing operations (17). It is a toxic element for humans, animals and the majority of plant species (18). The current Health Canada and WHO guideline for drinking water arsenic content is 0.01 mg/L (1). Canadian regulations also limit mining effluent to monthly average concentrations of arsenic to 0.50 mg/L (2).

This low threshold leads to the necessity of treating any contaminated waste waters or materials. Various techniques exist for arsenic removal from waste waters (3). However, in the case of mineral/metallurgical processing effluents the most common methods are: (a) calcium is used to precipitate arsenic (using lime or hydrated lime, as the calcium source) as simple calcium arsenates (19) or (b) co-precipitation using ferric iron salts along with lime neutralization (4). The former method although effective in removing arsenic, it is not considered a viable method for long term stabilisation of arsenic as the generated calcium arsenate solids react over time with atmospheric  $CO_2$  releasing arsenic to environment (20) (21) (3). The latter method is effective in removing low concentration arsenic (few g/L As) with good evidence of long-term stability of the produced co-precipitated solids (4). Therefore, in selecting the appropriate arsenic

control process, not only must the effectiveness in arsenic removal from solution be given consideration, but the stability of the generated arsenic-bearing solids and their disposal must be considered. The disposal method must ensure no release of arsenic back in the environment (ground or surface waters). Alternatively, the waste solids may require further treatment before disposal. Therefore, the long-term stability of any arseniferous solid material generated must be an important consideration in designing safe waste management sites.

Multiple processes have been developed to generate insoluble forms of arsenic from high-concentration industrial sources such as metallurgical plant effluent or residues/dusts (20). One method is to take arsenic-containing solid wastes (such as flue dust or residues) and to stabilize them with a solid matrix. This can take the form of stabilization/solidification with cement, or vitrification (3). Another method is to form relatively stable crystalline compounds of arsenic similar to natural minerals such as scorodite ( $\text{FeAsO}_4 \cdot 2\text{H}_2\text{O}$ ) (22), yukonite ( $\text{Ca}_2\text{Fe}_3\text{-}5(\text{AsO}_4)_3(\text{OH})_{4-10} \cdot x\text{H}_2\text{O}$ ) (6) or johnbaumite ( $\text{Ca}_5(\text{AsO}_4)_3\text{OH}$ ) (19). These compounds are precipitated from solution by controlling crystallization parameters such as supersaturation. The stability of the generated arsenical waste materials destined for disposal is commonly evaluated using leachability tests involving equilibration of a known mass of solids with certain volume of water at different pH or redox potentials (oxidizing or reducing) ((9), (10)). By far the best known such stability evaluation method is that of the United States Environmental Protection Agency (EPA) Toxicity Characteristic Leaching Procedure (TCLP) (23). This leachability test involves contacting the solid with an extraction fluid having pH  $\sim 5$  in a 1:20 mass ratio at  $23 \pm 2$  °C for 1 day. At the end of the test, the slurry is filtered and the filtrate is analyzed. If the arsenic concentration in the filtrate exceeds the regulatory limit (this varies from one jurisdiction to the other between 1 and 5 mg/L As) the waste is considered hazardous and it requires special safe storage that implies high cost on a continuous basis. Hence the interest in identifying compounds with low solubility for safe disposal of arsenic.

### 2.1.3 Scorodite Precipitation and Stability

Scorodite is a secondary ferric arsenate mineral that has been found forming naturally due to the oxidation of primary arsenide minerals like arsenopyrite (17). Its solubility is relatively low making it a good form for arsenic immobilization. For example, water percolating through a column containing natural scorodite once a week yielded low As content ( $< 0.1$  mg/L As) 3 years later (22). Scorodite can be synthesized under hydrothermal conditions in an autoclave, or at

atmospheric pressure if supersaturation control is utilized, at very low pH, and a temperature below the boiling point of water (80-95°C) (24) (5). Since 2012 the atmospheric precipitation process of scorodite, originally developed at McGill University (25), is industrially applied by Ecometales Ltd. in Chile (26) (7).

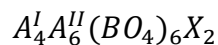
The solubility of scorodite is a function of pH, and it is quite unstable at pH greater than 7 (9). Scorodite is also soluble under anoxic conditions, as the arsenic and iron components will reduce to Fe(II) and As(III) (12) (27). Furthermore, scorodite placed in a gypsum-saturated solution has been found to partially form the calcium-ferric-arsenate mineral yukonite ( $\text{Ca}_2\text{Fe}_3(\text{AsO}_4)_4(\text{OH})\cdot 12\text{H}_2\text{O}$ ) (28). Synthetic and natural yukonites have a composition range of  $\text{Ca}_2\text{Fe}_3-5(\text{AsO}_4)_3(\text{OH})_4-10\cdot x\text{H}_2\text{O}$   $x=2-12$  (6). Equilibration of the partially transformed scorodite/yukonite at ambient temperature for up to 66 weeks released 3.55 mg/L As at pH 7, and 115 mg/L As at pH 9. Under the same conditions, scorodite released 5.89 mg/L at pH 7 and 386 mg/L at pH 9.

#### *Calcium phosphate coating of scorodite*

In alignment with the first option the McGill HydroMET group has investigated various coating techniques for scorodite to increase its stability (29), (30), (12), (31) (32). One such technique is the coating of scorodite particles with metal (aluminum or calcium) phosphate compounds. These compounds are not amenable to redox reactions therefore they have the potential to extend the range of stability for scorodite into anoxic conditions (29), (32). Calcium phosphate compounds with stable apatite structure, hydroxyapatite  $\text{Ca}_5(\text{PO}_4)_3\text{OH}$  (HAP), and fluoroapatite  $\text{Ca}_5(\text{PO}_4)_3\text{F}$  (FAP), were used to coat scorodite by Lagno first (29) (32) and later by Katsarou (10). Although the coatings on the scorodite particles were not fully developed, there was a significant improvement in arsenic retention, as compared to uncoated scorodite. At pH 9, uncoated scorodite released 22 mg/L arsenic, whereas scorodite coated with hydroxyapatite released 1.08 mg/L arsenic after 40 days (12). This suggests that apatite type compounds deserve further consideration in arsenic stabilization research.

#### 2.1.4 Apatite Minerals

The HAP and FAP compounds used to encapsulate scorodite are part of the apatite group of minerals. Apatites tend to have  $P6_3/m$  hexagonal symmetry (33), and a general formula of





In the case of HAP and FAP, the A sites are occupied by calcium, the B site by phosphorus and the X by a hydroxyl and fluoride ion respectively. Apatites are generally insoluble and very stable compounds (34). However, apatites can take a long time to equilibrate in an aqueous state, HAP in solution taking up to a year to equilibrate. They can be found not only as minerals, but also in living organisms, in material such as bones or teeth (35). All bone has an apatitic structure that is cross-linked with an organic material. The strongest of the apatites found in living things is FAP, specifically the FAP found in shark teeth (36).

Apatites containing arsenic exist, and include  $\text{Ca}_5(\text{AsO}_4)_3(\text{OH}/\text{F}/\text{Cl})$  and  $\text{Pb}_5(\text{AsO}_4)_3(\text{OH}/\text{F})$ ,  $\text{Sr}_5(\text{AsO}_4)_3\text{F}$ ,  $(\text{Sr}_{1.66}\text{Ba}_{0.34})-(\text{Ba}_{2.61}\text{Sr}_{0.39})(\text{AsO}_4)_3\text{Cl}$ ,  $\text{Cd}_5(\text{AsO}_4)_3\text{Sb}_{0.58}(\text{OH})_{0.42}$  (37),  $\text{Ba}_5(\text{P}_x\text{As}_{(1-x)}\text{O}_4)_3\text{Cl}$  (38) and  $\text{Cd}_5(\text{AsO}_4)_3\text{X}$  (where X is Cl or OH) (39). The inherent stability of phosphate apatites make arsenate apatites attractive candidates for the long-term storage of arsenic. In this thesis, in a departure from the earlier work that sought to enhance the stability of scorodite via its coating with calcium phosphate apatites (namely, hydroxyapatite-HAP and fluoroapatite-FAP) the arsenate analogue of fluoroapatite, svabite  $\text{Ca}_5(\text{AsO}_4)_3\text{F}$ , as well as solid solutions (composites) of the two (FAP and svabite) are investigated. In particular the present study focuses on determining the process parameters that favour formation of crystalline fluoro-arsenate apatites by precipitation from aqueous solution and evaluating their stability as alternatives to scorodite. The focus is arsenate-containing fluoroapatite as the latter apatite is known to have at least two orders of magnitude lower solubility than the hydroxyapatite compound (14). Twidwell and collaborators at Montana Tech have already investigated mixed (solid solution) arsenate-phosphate hydroxyapatite ( $\text{Ca}_5(\text{PO}_4)_{3-x}(\text{AsO}_4)_x\text{OH}$ ) precipitated from aqueous solution and found to be relatively stable at  $\text{pH} > 10$  if a high P/As molar ratio is used ( $> 7$ ) (40), (21). Given the lower solubility of FAP compared to HAP, the investigation of the svabite/fluoroapatite system becomes particularly interesting.

## 2.2 Review of Calcium Arsenate Compounds

Natural calcium arsenate minerals exist around the world. Calcium arsenates usually form naturally when an acidic solution with arsenate ions is exposed to calcium-containing minerals, such as carbonate rocks (41). Other calcium arsenate minerals have been observed to form in near neutral natural environments-such as arseniosiderite and yukonite. In Nevada, highly soluble weilite ( $\text{CaHAsO}_4$ ) and pharmacolite ( $\text{CaHAsO}_4 \cdot 2\text{H}_2\text{O}$ ) have been found in association

with haideringite ( $\text{CaHAsO}_4 \cdot \text{H}_2\text{O}$ ) (17). Johnbaumite ( $\text{Ca}_5(\text{AsO}_4)_3\text{OH}$ ), the arsenate analogue of hydroxyapatite, was first found in the Franklin Mine in New Jersey (42).

Calcium arsenates were originally used as pesticides in the USA, and as many as 15,000 tons were used per year. Sites where the pesticides were once used are now contaminated with arsenic (43).

### 2.2.1 Formation of Calcium Arsenates in Aqueous Solution

Various groups have treated arsenic-containing waste waters by precipitation with calcium, forming calcium arsenate apatites. The intent of these studies was not to investigate the long-term storage and stability of arsenic-containing precipitates through the intentional formation of stable calcium arsenate compounds, but rather the removal of arsenic from a waste stream.

Itakura et al. (44) used a hydrothermal process to treat a mixed arsenate/arsenite waste solution and precipitated johnbaumite, in the presence of  $\text{H}_2\text{O}_2$ , at pH 13, both after 10 hours at 150 °C and after 15 hours at 100°C. The arsenic content in solution was reduced to <0.5 mg/L from 2,000 mg/L. Dutre et al. (45) treated a solid waste from a copper refining process containing antimony, lead and arsenic (42 wt%) with calcium (through slaked lime addition) in a solidification/stabilisation system. All these methods required a neutral or basic pH for the formation of apatite solids. Itakura et al. (44) found that as the pH decreased, the residual arsenic concentrations increased.

Aqueous precipitation experiments can be classified into two categories. The first involves placing various components into solution and allowing them to reach equilibrium, and then analysing the solid phases present in the system. The second is the intentional precipitation of specific compounds. Table 2.1 summarizes the different compounds that have been precipitated, and the conditions used for their synthesis. The *Experiment Type* column identifies whether the experiments were to determine the equilibrium phase or an intentional precipitation.

A phase diagram developed by Magalhaes et al. (46) of calcium arsenate compounds generated from data produced by Bothe et al. (19) is presented in Figure 2-1.

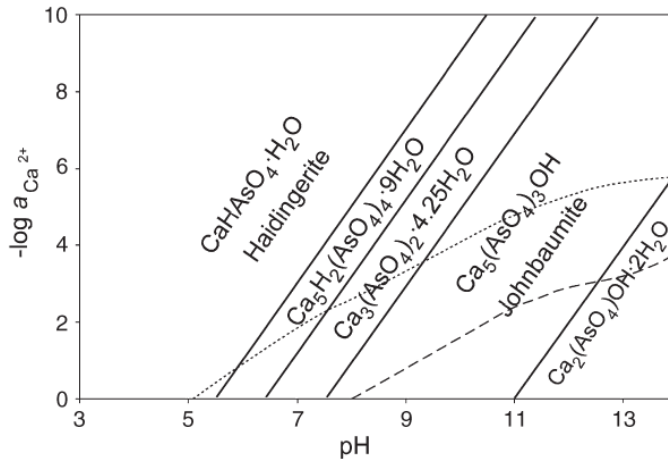


Figure 2-1: Calcium arsenate phases at equilibrium with solution at 25°C (46)

Figure 2-1 presents the specific operating pH range that yields johnbaumite. Examining Table 2.1, we see that all of the methods that yielded johnbaumite required a basic pH, which ranged from 9.73 (19) to 13 (47). This is due to the hydroxide ion in the johnbaumite matrix. There is also a general consensus that the initial ratio of calcium to arsenic in the solution directs which phase is precipitated. This is true of both types of experiments presented in Table 2.1. Most groups found that the stoichiometric ratio of 1.67 was necessary for the formation of the apatite. Other groups found different results; Moon et al. (48) formed the apatite at Ca:As ratio of 1.1, and Twidwell et al. (49) precipitated johnbaumite with excess calcium, notably a Ca:As ratio of 2.5. In Moon et al.'s case, this may be due to the use of a calcium arsenate precursor compound as the calcium source, rather than separate sources of calcium and arsenate ions.

**Table 2.1 Summary of synthesis methods of calcium arsenate compounds from solution**

Ref.	Solid formed	Ca source	As source	Ca:As	pH	pH control	Reaction Time	Temp (°C)	Experiment type
(44)	<b>Ca<sub>5</sub>(AsO<sub>4</sub>)<sub>3</sub>OH</b>	Ca(OH) <sub>2</sub> (s)	Na <sub>2</sub> HAsO <sub>4</sub> (s)	excess Ca	13	None	>10 hours	100, 150, 200	Treatment
(19)	Ca <sub>4</sub> (OH) <sub>2</sub> (AsO <sub>4</sub> ) <sub>2</sub> •4H <sub>2</sub> O	Ca(OH) <sub>2</sub> (s)	H <sub>3</sub> AsO <sub>4</sub> (s)	2-2.5	12.12	None	4 years	23	Equilibrium
	Ca <sub>3</sub> (AsO <sub>4</sub> ) <sub>2</sub> •3 2/3 H <sub>2</sub> O			1.67, 1.90	9.73				
	Ca <sub>3</sub> (AsO <sub>4</sub> ) <sub>2</sub> •4 ¼ H <sub>2</sub> O			1.67	11.18				
	CaHAsO <sub>4</sub> •H <sub>2</sub> O			1.5	7.3-7.5				
	Ca <sub>5</sub> H <sub>2</sub> (AsO <sub>4</sub> ) <sub>4</sub> •9H <sub>2</sub> O			1	6.2				
<b>Ca<sub>5</sub>(AsO<sub>4</sub>)<sub>3</sub>OH</b>	Pure Ca(OH) <sub>2</sub> (s)		1.2	7					
(48)	<b>Ca<sub>5</sub>(AsO<sub>4</sub>)<sub>3</sub>OH</b> , NaCaAsO <sub>4</sub> •7.5H <sub>2</sub> O Ca <sub>4</sub> (OH) <sub>2</sub> (AsO <sub>4</sub> ) <sub>2</sub> •4H <sub>2</sub> O	Ca(OH) <sub>2</sub> (s)	Na <sub>2</sub> HAsO <sub>4</sub> •7H <sub>2</sub> O (s)	1 1.5, 2, 2.5, 4		None	4 days	20	Equilibrium
(50)	Ca(AsO <sub>3</sub> ) <sub>2</sub> , CaH <sub>4</sub> (AsO <sub>4</sub> ) <sub>2</sub>	Ca(OH) <sub>2</sub> (s) CaO (s)	As <sub>2</sub> O <sub>5</sub> (s)	1			120 days	16	Equilibrium
	CaH <sub>4</sub> (AsO <sub>4</sub> ) <sub>2</sub> •H <sub>2</sub> O, CaHAsO <sub>4</sub>			2					
	Ca <sub>3</sub> (AsO <sub>4</sub> ) <sub>2</sub> , Ca <sub>5</sub> H <sub>2</sub> (AsO <sub>4</sub> ) <sub>2</sub>			3					
(51)	CaHAsO <sub>4</sub> •H <sub>2</sub> O, Ca(H <sub>2</sub> AsO <sub>4</sub> ) <sub>2</sub>	CaCO <sub>3</sub> (s)	As <sub>2</sub> O <sub>5</sub> •3H <sub>2</sub> O (s)	-	-	-	5 days	70	Equilibrium
(52)	CaHAsO <sub>4</sub> •H <sub>2</sub> O	CaO (s)	H <sub>3</sub> AsO <sub>4</sub> (aq)	1-1.36	5.7-7.4	None	30 days	25	Equilibrium
	Ca <sub>3</sub> (AsO <sub>4</sub> ) <sub>2</sub> •4H <sub>2</sub> O			1.33-1.68	7.4-11.6				
	Ca <sub>2</sub> AsO <sub>4</sub> OH•2H <sub>2</sub> O			1.68-4	11-12.5				
(53)	Ca <sub>3</sub> (AsO <sub>4</sub> ) <sub>2</sub>	CaCl <sub>2</sub> (aq)	Na <sub>2</sub> HAsO <sub>4</sub> (aq)	0.67	<10.6	Yes	-	25	Equilibrium
	CaNaAsO <sub>4</sub>				>10.6				
(54)	CaHAsO <sub>4</sub>	Ca(NO <sub>3</sub> ) <sub>2</sub> (aq)	(NH <sub>4</sub> ) <sub>2</sub> HAsO <sub>4</sub>	1	5	yes	15minutes	80	Precipitation
	<b>Ca<sub>5</sub>(AsO<sub>4</sub>)<sub>3</sub>OH</b>	Ca(NO <sub>3</sub> ) <sub>2</sub> (aq)	(NH <sub>4</sub> ) <sub>2</sub> HAsO <sub>4</sub>	1.67	12	yes	5 days	100	Precipitation
(49)	<b>Ca<sub>5</sub>(AsO<sub>4</sub>)<sub>3</sub>OH</b>	Ca(NO <sub>3</sub> ) <sub>2</sub> (aq)	H <sub>3</sub> AsO <sub>4</sub> (aq)	2.505	10	yes	5 days	95	Precipitation
	<b>Ca<sub>5</sub>(AsO<sub>4</sub>)<sub>3</sub>OH</b>				10	yes	5 days	25*, 95	
(47)	Ca <sub>3</sub> (AsO <sub>4</sub> ) <sub>2</sub> •xH <sub>2</sub> O, Ca <sub>4</sub> (OH) <sub>2</sub> (AsO <sub>4</sub> ) <sub>2</sub> •4H <sub>2</sub> O	Ca(OH) <sub>2</sub> (aq)	H <sub>3</sub> AsO <sub>4</sub> (aq)	1, 1.25	5,7	Initially	24 hours	50	Precipitation
	Ca <sub>3</sub> (AsO <sub>4</sub> ) <sub>2</sub>			1.5	5,7				
	Ca <sub>3</sub> (AsO <sub>4</sub> ) <sub>2</sub>			1.5	5,7				
	<b>Ca<sub>5</sub>(AsO<sub>4</sub>)<sub>3</sub>OH</b> , Ca <sub>3</sub> (AsO <sub>4</sub> ) <sub>2</sub> •xH <sub>2</sub> O			1.67, 4	12,13				
	Ca <sub>4</sub> (OH) <sub>2</sub> (AsO <sub>4</sub> ) <sub>2</sub> •4H <sub>2</sub> O			2	12,13				
(55)	amorphous <b>Ca<sub>5</sub>(AsO<sub>4</sub>)<sub>3</sub>OH</b>	CaO	H <sub>3</sub> AsO <sub>4</sub> (aq)	1.67	11.5	yes	24 hours	ambient	Precipitation

\*Compound precipitated at 25°C and aged at 95°C.

The calcium source did not otherwise seem to affect the formation of johbaumite, as  $\text{Ca}(\text{NO}_3)_2$  and  $\text{CaCl}_2$  have both been used successfully. However, the presence of magnesium was found to hinder apatite formation (19).

The formation of johbaumite also seems to be dependent on the aging temperature of the precipitate. All groups required at least the aging steps to be at elevated temperature ( $\geq 70^\circ\text{C}$ ). The only groups that did not age or precipitate at an elevated temperature yielded amorphous apatite (55). Bothe et al. (19) presented SEM images of the precipitated johbaumite (Figure 2-2), showing the needle-like morphology of this solid.

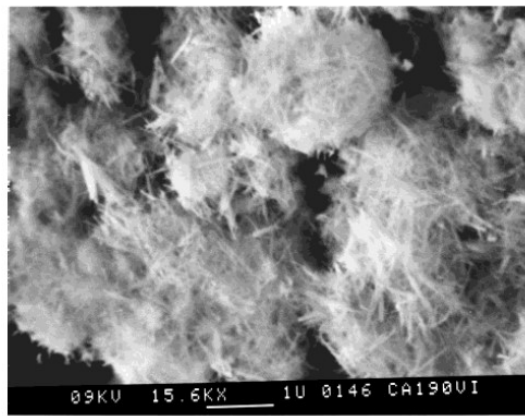


Figure 2-2: SEM image of johbaumite (19)

Taboada et al. (51) precipitated  $\text{CaHAsO}_4 \cdot \text{H}_2\text{O}$  (haidingerite) (SEM images in Figure 2-3) and  $\text{Ca}(\text{H}_2\text{AsO}_4)_2$ . An SEM image of a mixture of the two minerals is presented as Figure 2-4. The difference between these calcium arsenate morphologies and the needle-like morphology of arsenate apatites should be noted.

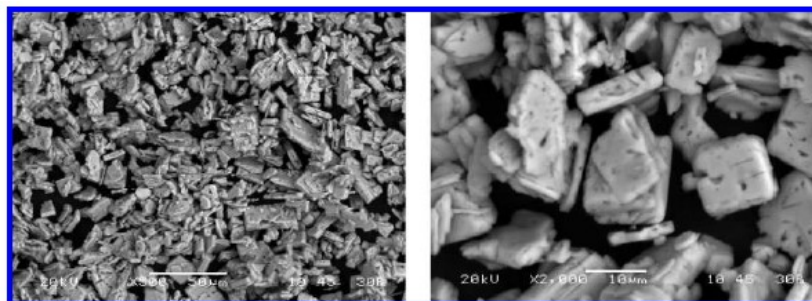


Figure 2-3: SEM images of  $\text{CaHAsO}_4 \cdot \text{H}_2\text{O}$  (51)

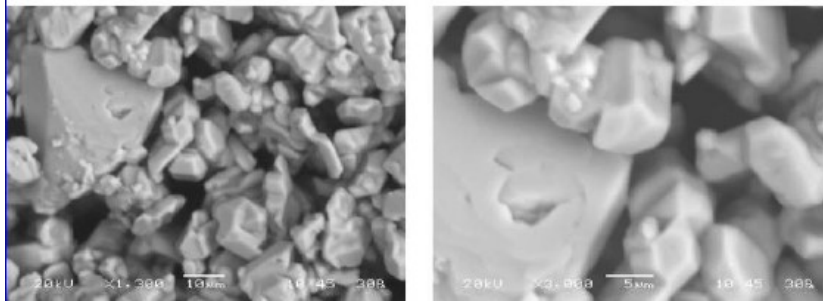


Figure 2-4: SEM images of mixture of  $\text{CaHAsO}_4 \cdot \text{H}_2\text{O}$  and  $\text{Ca}(\text{H}_2\text{AsO}_4)_2$  (51)

### 2.2.2 Dissolution and Stability of Calcium Arsenates

Table 2.2 summarizes the solubility results from various dissolution and precipitation tests. These experiments are categorized as precipitation tests when they involve placing sources of calcium and arsenate into solution and allowing the system to reach equilibrium; or as dissolution when they involve generating solid compounds, and placing them into fresh solution and finding the equilibrium concentrations.

In general, arsenic release increases with decreasing pH. Many compounds have been found to be stable at high pH ( $>10$ ), such as  $\text{Ca}_2\text{AsO}_4\text{OH} \cdot 2\text{H}_2\text{O}$ , which released as little as 0.001 mg/L at pH 12.5 (52). The only compound which released less than 100 mg/L at a pH below 9 is johnbaumite

This demonstrates the relatively greater stability of calcium arsenate apatites relative to simple calcium arsenates.

The presence of air and  $\text{CO}_2$  led to a significant increase in arsenic release (52). Twidwell (40) found that air sparging for 6 months of synthetic johnbaumite led to the release of 85 mg/L of arsenic (pH 8), which previously had only released 0.0155 mg/L after 5 years at pH 12.1. The presence of  $\text{CO}_2$  and subsequent incorporation into solution as  $\text{H}_2\text{CO}_3$  meant a decrease in pH, which also contributed to the increase in arsenic in solution.

**Table 2.2** Summary of stability investigations on calcium arsenates

Source	Type of Test	Material	As Solubility (mg/L)	Length	pH	pH control	T (°C)	CO2 Precautions	Agitation	
(47)	Dissolution	Ca <sub>3</sub> (AsO <sub>4</sub> ) <sub>2</sub> •3H <sub>2</sub> O	37,200	100 days	6.2	None	25	Sealed	Shaking	
		Ca <sub>3</sub> (AsO <sub>4</sub> ) <sub>2</sub> •2 ¼ H <sub>2</sub> O	2.39		7.4					
		<b>Ca<sub>5</sub>(AsO<sub>4</sub>)<sub>3</sub>OH</b>	2.04		13.4					
		Ca <sub>4</sub> (OH) <sub>2</sub> (AsO <sub>4</sub> ) <sub>2</sub> •4H <sub>2</sub> O	0.432		13.4					
(52)	Precipitation	CaHAsO <sub>4</sub> •H <sub>2</sub> O	6,240	1 month	5.7	None	25	Sealed	Shaking	
			3,680		6.1					
			2,540		6.5					
			1,400		7.25					
			1,270		7.33					
			Ca <sub>3</sub> (AsO <sub>4</sub> ) •4H <sub>2</sub> O		660					8
			61		10.2					
			0.17		11.6					
Ca <sub>2</sub> AsO <sub>4</sub> OH•2H <sub>2</sub> O	0.01	12.3								
		0.001	12.5							
(51)	Precipitation	CaHAsO <sub>4</sub> •H <sub>2</sub> O	1,300-1,500	2 days	-		50	Sealed	Stirring	
			1,100				70			
(19)	Precipitation	Ca <sub>4</sub> (OH) <sub>2</sub> (AsO <sub>4</sub> ) <sub>2</sub> •4H <sub>2</sub> O	0.12	823 days	12.1	None	23	Sealed	Shaking	
		<b>Ca<sub>5</sub>(AsO<sub>4</sub>)<sub>3</sub>OH</b>	19.5	674 days	9.77					
		Ca <sub>3</sub> (AsO <sub>4</sub> ) <sub>2</sub> •4¼ H <sub>2</sub> O	490.5	823 days	7.5					
(40)	Dissolution	<b>Ca<sub>5</sub>(AsO<sub>4</sub>)<sub>3</sub>OH</b>	0.0155	5 years	12.1	None	25	No air exposure	None	
			85	6 months	8			Air sparging		
			22	10 days	10.2			No air		
(54)	Dissolution	<b>Ca<sub>5</sub>(AsO<sub>4</sub>)<sub>3</sub>OH</b>	76.5	10 hours	4	yes	35	Sealed	Shaking	
			57.75		5					
			51		6					
			48		7					
			45.75		8					

### 2.2.3 Removal of Arsenic by Formation of Calcium Arsenate/Phosphate Apatite Solid Solutions

For calcium arsenate compounds to be successful as arsenic sequestration matrices, they must be stable in various environmental conditions. This includes stability in the presence of CO<sub>2</sub> and subsequent H<sub>2</sub>CO<sub>3</sub> formation.

The phosphate apatite hydroxyapatite is more stable than its arsenate apatite analogue, johnbaumite (40) (19). Since phosphate and arsenate are isostructural, the precipitation of mixed calcium arsenate/phosphate compounds or more precisely arsenate-substituted calcium phosphates otherwise called solid solutions (with the general formula Ca<sub>5</sub>(PO<sub>4</sub>)<sub>3-z</sub>(AsO<sub>4</sub>)<sub>z</sub>X, where X=OH, Cl or F) may prove more stable than compounds synthesised with arsenic only (Ca<sub>5</sub>(AsO<sub>4</sub>)<sub>3</sub>X). This section details previous work synthesising mixed hydroxyapatite-johnbaumite compounds and their stability and dissolution mechanisms.

The synthesis of an apatite solid solution (Ca<sub>5</sub>(PO<sub>4</sub>)<sub>3-x</sub>(AsO<sub>4</sub>)<sub>x</sub>X) by the replacement of phosphate with arsenate causes local distortions in the hydroxyapatite structure (56). A solid solution of hydroxyapatite and johnbaumite has proven to be more effective in arsenic retention than pure johnbaumite (49). Twidwell et al. (49) produced solid solutions of hydroxyapatite and johnbaumite by precipitation at 95°C and pH 10 at various arsenate and phosphate ratios. The same authors were also successful in producing solid solution of hydroxyapatite and johnbaumite by precipitating first at room temperature and afterwards aging the solids at an elevated temperature. The peaks of the resulting XRD analysis broadened with decreasing temperature, indicating a lower level of crystallinity. Even after an aging period, there is little to no indication of crystal growth as the XRD patterns remain the same, and this may suggest the importance of the initial precipitation concentration for the morphology of the resulting solid (49).

In another report Twidwell et al. (40) determined that for a stable compound (in terms of arsenic release) in the presence of CO<sub>2</sub>, the initial P/As molar ratio in solution must be larger than 5. They determined that for the formation of apatite-like compounds the Ca/(As+P) molar ratio in the initial solution must be greater than or equal to 1.5 (the stoichiometric molar ratio is 1.67). A pilot plant (40) (21) using this process was built to treat arsenic-contaminated waters. The plant used a P/As molar ratio of 7, at pH 12 and a residence time of 12 minutes effectively reduced arsenic in the effluent to 50ppb..



Lee et al. (55) have also described the synthesis of solid solution of hydroxyapatite and johnbaumite,  $\text{Ca}_5(\text{PO}_4)_x(\text{AsO}_4)_{(3-x)}\text{OH}$ , with various As/P molar ratios by precipitation from solution. In one approach, a solution of  $\text{KH}_2\text{PO}_4$  and  $\text{KH}_2\text{AsO}_4$  was added dropwise into a 75-80°C solution of  $\text{Ca}(\text{NO}_3)_2$  at pH 10 (using KOH as the controlling base). In another approach, they produced the mixed arsenate/phosphate apatite by reacting CaO with a solution of  $\text{Na}_2\text{HAsO}_4$  at 90°C.

Experiments run at room temperature produced amorphous solids as also observed by Twidwell and co-workers (49). The produced  $\text{Ca}_5(\text{PO}_4)_x(\text{AsO}_4)_{(3-x)}\text{OH}$  solids however were found to react with atmospheric  $\text{CO}_2$  leading to the formation of calcium carbonate and release of arsenic.

In another study, Zhu et al. (57) prepared mixed HAP/HAsP solids by mixing  $\text{Ca}(\text{OH})_2$  with solutions having varying ratios of phosphoric acid/arsenic acid, and keeping the molar ratio  $\text{Ca}/(\text{As}+\text{P})$  at 1.67. After the solutions were stirred for 10 min at room temperature, then were heated and stirred at 70 °C for a week. The precipitates were filtered, washed and then dried in a 110°C oven. The solids all had an apatite structure. The As/P molar ratios in the final product were very close to the initial solution ratio. Pure hydroxyapatite had morphology of large tabular crystals, which progressively changed to the small needle-like morphology of the pure johnbaumite.

Bothe et al. (19) followed the method used to precipitate johnbaumite (Section 2.2.1) by substituting the arsenate with various quantities of sodium phosphate.. The  $\text{Ca}/(\text{As}+\text{P})$  ratio was kept at the apatite ratio of 1.67. The final solids had a P/As ratio close to the initial ratio in the solution. These samples were monitored for 490 days, and showed that apatites are indeed the most thermodynamically favourable phase under these conditions. However, since the d-spacing of the XRD results showed discrete changes rather than a smooth transition between the arsenate and phosphate apatites, Bothe et al. concluded that they did not form solid solutions, i.e. arsenate substitution into the phosphate apatite crystal lattice, but rather a mixture of the two phases (hydroxyapatite and johnbaumite). They are the only group to reach this conclusion, and it may be due to the precipitation and aging at ambient temperature rather than at elevated temperature.

#### 2.2.4 Dissolution and Stability of Calcium Arsenate/Phosphate Apatite Solid Solutions

Twidwell et al. (49) found that HAP/HAsP compounds with P/As molar ratio of 7 to be very stable if not exposed to air - releasing less than 1 ppb of arsenic. The same solids exposed to air

sparging in the water leached arsenic to the solution after 18 months in the range of 5 ppb to 120 ppm depending on the arsenic content, or JBM/(JABM+HAP) as a percent, of the solid solution. The ability of the solids to retain arsenic indicates that the hydroxy arsenate/phosphate-containing apatite compounds with P/As molar ratios of 7 ( $\text{Ca}_4(\text{P}_x\text{As}_{(1-x)}\text{O}_4)_3\text{OH}$ ) are largely resistant to the formation of  $\text{CaCO}_3$ .

Similarly, Mahapatra et al. evaluated the stability of various arsenate hydroxyapatites with varying phosphate ratios in air-tight flasks and their results are shown in Figure 2-6. In general, the solubility decreased with increasing pH, mirroring the trend found with calcium arsenates. Higher solubility associated with higher arsenic content is possibly due to the alterations in lattice energy when replacing the phosphate ion with the larger arsenate ion. The lower concentrations reported by Mahapatra et al. compared to Twidwell et al. for solids with a higher proportion of JBM is likely explained by the presence of air and therefore carbon dioxide in the Twidwell tests.

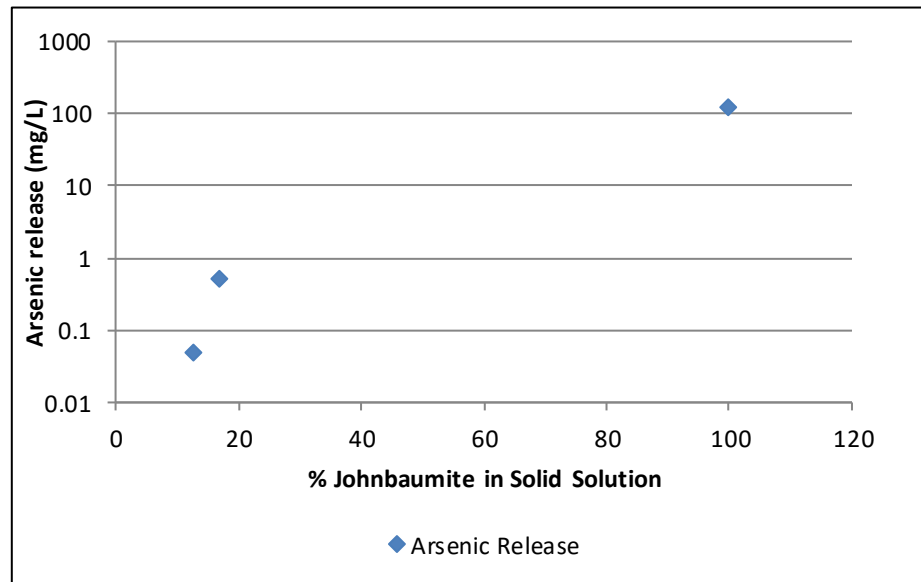


Figure 2-5: Arsenic levels in solution after the dissolution of solid solutions of JBM/HAP (40).

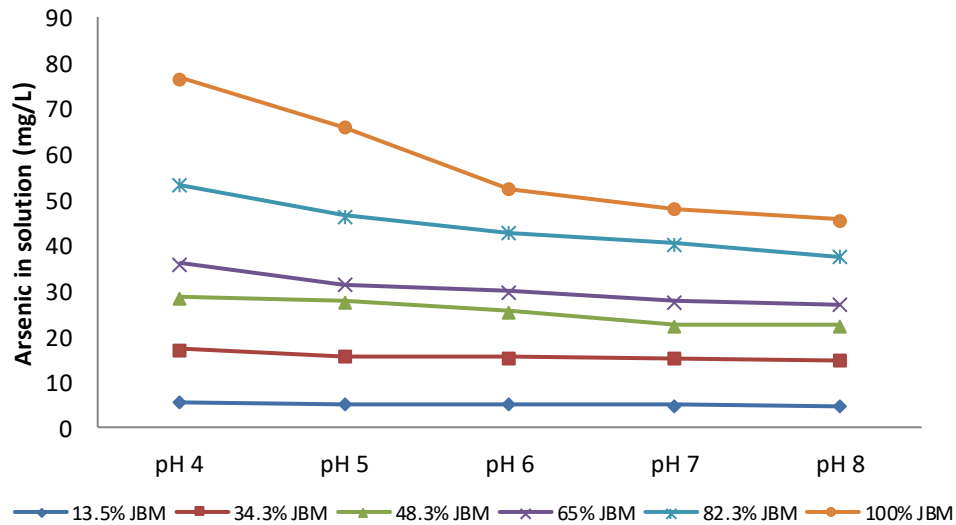


Figure 2-6: Arsenic levels after the dissolution of solid solutions of JBM/HAP (54)

## 2.3 Svabite

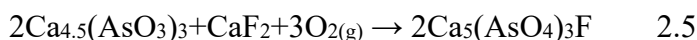
The arsenate analogue of fluorapatite, svabite,  $\text{Ca}_5(\text{AsO}_4)_3\text{F}$ , (FAsP) has been found occurring naturally in a few areas of the world, namely mines in Sweden (58). Fluorapatite deposits in Italy have shown to reduce the mobilisation of both fluoride and arsenic in soils and groundwater (59). Since fluorapatite is less soluble than hydroxyapatite (60), by analogy is thought that svabite will be less soluble than johnbaumite. Svabite has been successfully synthesized in two ways: by sintering and by hydrothermal precipitation.

### 2.3.1 Synthesis of Svabite

#### *Synthesis of Svabite by Sintering*

Two research teams have reported the synthesis of svabite using a high-temperature sintering process. White et al. (61) (62) synthesised “Xtaltite” (pronounced crystal-tight), from waste that contained arsenic (III) and lead that was mixed with excess fluorspar ( $\text{CaF}_2$ ) and lime ( $\text{CaO}$ ). This mixture was slurried in water for up to 12 hours, and the precipitation was catalyzed by using a diluted base ( $\text{NaOH}$ ) to solubilize the lime. This led to the formation of an initial finnemanite-like compound,  $\text{Ca}_{4.5}(\text{AsO}_3)_3$ , while mixing at room temperature. (It should be noted

that the fluorspar does not partake in this reaction, but is included in the slurry so it will react in further steps of the process.) The resulting solids were filtered, then dewatered at 100°C (to reach <5% water), and then sprayed with a dilute sodium silicate solution that acted as a binder. The dried solids were then fired at 1100-1200°C in air for 30 minutes, oxidizing both the arsenic and the lead. The final stabilized waste contained 22 wt% As(V). X-ray diffraction (XRD) analysis proved the presence of crystalline svabite phase, formed as per this reaction:



The resulting solids were used to create a refractory ceramic using the proprietary Synthetic Mineral Immobilization Technology (SMITE). The initial precipitation step was used to avoid the sublimation of arsenic during the high-temperature firing. The dried solid was crushed and mixed with Portland cement, which acts as a barrier to dissolution. This process is not a vitrification process, as the concentrations of contaminants are not dilute, and can rather be considered the manufacture of a glass ceramic.

This process has though certain drawbacks like a high volume of waste through the use of cement, a large overall environmental footprint, and this two-step, high temperature process has a high-energy demand (62).

A similar process was used by Kucharski et al. (58), although without encapsulating the waste into cement. A solution of stoichiometric ratios of As<sub>2</sub>O<sub>3</sub>, CaO, and CaF<sub>2</sub> were mixed at room temperature. Either 0.1M NaOH or 30% H<sub>2</sub>O<sub>2</sub> was added to catalyze the reaction, and both resulted in the formation of svabite. The mixture was stoppered and left for 18 hours before being filtered. Like White et al.'s procedure (62), the solid was first oven dried at 100°C for 16 hours, then sintered at 500°C for 18 hours, then 1300°C for 18 hours.

### *Precipitation from solution*

The only published method to precipitate svabite was presented by Zhu et al. in 2011 without offering much detail (63). More specifically, the authors reported that svabite was synthesized by mixing solutions with the individual precursor elements as follows: “A solution of 100 mL 0.5 M Ca(NO<sub>3</sub>)<sub>2</sub> and a solution of 60 mL 0.5 M Na<sub>3</sub>AsO<sub>4</sub> and a solution of 20 mL 0.5 M NaF, so that a Ca/As molar ratio in the mixed solution was 1.67.” The mixed solution was kept in a covered beaker for a week at 70°C. The precipitate was then filtered and dried for 24 hours at 110°C. The

work presented in this paper does not include how the procedure was developed, what was the pH, or how varying the precipitation conditions affected the compounds formed.

The precipitates formed were microcrystalline and did not demonstrate the same needle-like morphology of johnbaumite. An SEM image of the svabite formed by Zhu et al. (63) is presented in Figure 2-7.

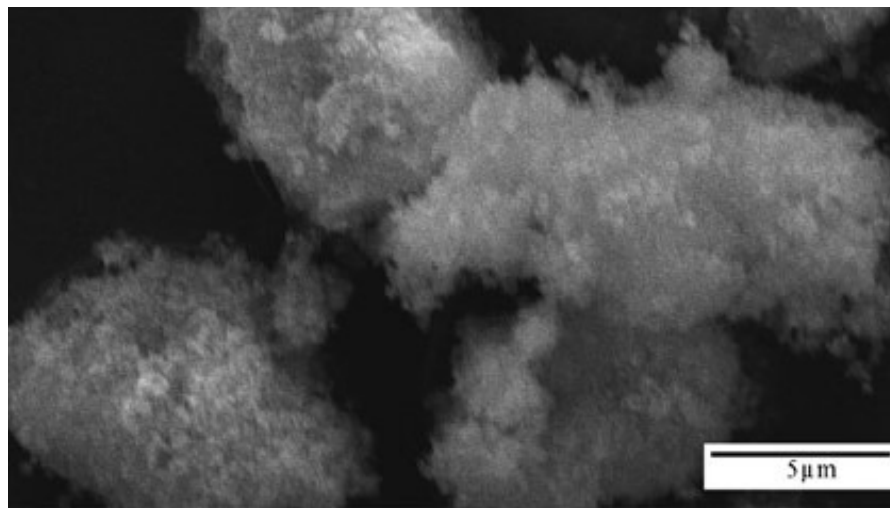


**Figure 2-7: Svabite formed by precipitation from solution (63)**

### 2.1.1 Dissolution and Stability of Svabite

Kucharski et al. (58), White et al. (61) and Zhu et al. (63) tested the stability of the different synthesised svabite solids. White et al. only tested the cement-encapsulated solids without presenting stability data for pure svabite. Stability was evaluated using the Environment Protection Agency (EPA) Toxicity Characteristic Leaching Procedure (TCLP) (23). This procedure involves contact of the solid with an extraction fluid having pH ~5 in a 1:20 mass ratio at  $23 \pm 2$  °C for ~24 hours. The cement-encapsulated material of White et al. (62), containing 24 wt% As released 2.5 ppm As. This however, does not represent the true solubility of svabite, as the solid –as already mentioned- was a cement-encapsulated mix of apatite and lead-containing crystalline solid, and 24 hours may not be long enough time to reach equilibrium.

Kucharski et al. (58) tested both synthetic svabite and a sample of natural svabite. The solid svabite was ground, then slurried (10g solids/ litre of liquid) at a pre-determined and controlled pH, and left to equilibrate for 14 days. The pH-dependent arsenic solubility results are reproduced in Table 2.3. As it can be seen, the more acidic the solution, the greater the arsenic

release. The results from this test seem to be promising for the use of svabite as a sequestration matrix for arsenic only above pH 9 a trend that is similar with the solubility of apatites (14).

Table 2.3: Stability testing results for synthetic svabite (58)

TABLE 3

The solubility of arsenic as a function of pH of leaching solution at  $20 \pm 2^\circ\text{C}$

Sample	pH at beginning	pH after test	As in solution, $\text{mg} \cdot \text{l}^{-1}$
Synthesised svabite	1.08	1.21	4410
	2.02	5.74	800
	2.99	7.22	54
	4.01	9.47	5.5
	5.02	9.65	4.0
	5.46	9.74	3.8
	6.00	9.73	3.5
	6.47	9.78	3.6
	6.98	9.75	3.5
	7.59	9.80	3.4
	7.96	9.82	3.45
8.98	9.83	3.20	
Natural svabite	0.97	1.00	2080
	0.99	1.10	530
	1.97	3.11	440
	2.01	3.05	450
	3.01	6.61	420
	3.01	6.15	77
	3.99	9.32	5.5
	5.01	9.66	2.9
	6.01	9.61	2.9
	6.98	9.85	2.4
	7.99	9.82	2.4
	8.99	9.83	2.5
	8.99	9.83	2.7

The dissolution tests conducted by Zhu et al. (63) found that after 125 days of equilibration, at pH 8 the arsenic release was at least one order of magnitude higher than the values of Kucharski et al., namely 37 mg/L at 45 °C and 60 mg/L at 25 °C. Their solubility results were used in the modelling software PHREEQC, with the MINTEQ.v4 database, to calculate the solubility product ( $K_{sp}$ ) of svabite. The average  $K_{sp}$  value for svabite was estimated to be  $10^{-39.21}$ .

There is a significant discrepancy between the results obtained by Zhu et al. (63) and Kucharski et al. (58), where at pH 8, 25°C, Zhu et al. obtained a solubility of 60 mg/L As, while Kucharski et al. reported a concentration of 54 mg/L at pH 7.22 and 4.0 mg/L for pH 9.60 for synthetic svabite or 2.9 mg/L As at pH 9.59 for natural svabite. Although both use a different solids/liquid ratio, both report an established steady-state before the end of the test. The difference in final concentrations may be partly explained by the difference in pH but also by a difference in the crystallinity of the two samples or their purity (presence of amorphous secondary phases), or perhaps the length of time between the two tests. The use of natural svabite

by Kucharski et al. to obtain the lowest concentrations may indicate that these tests are a better indication of the true solubility of pure svabite.

### 2.1.2 Synthesis and Stability of Svabite/Fluorapatite Solid Solutions

Zhu et al. also studied the stability of solid solutions of svabite and fluorapatite with varying composition (64). Synthesis involved the same precipitation method as in the case of svabite (63). The precursor solutions of individual components (100 mL of 0.5M  $\text{Ca}(\text{NO}_3)_2$ ; 60 mL of 0.5M  $\text{Na}_3\text{PO}_4/\text{Na}_3\text{AsO}_4$ ; and 20 mL of 0.5M NaF) were mixed slowly at their stoichiometric ratios ( $\text{Ca}/(\text{P}+\text{As})=1.67$ ) and stirred in covered beakers at  $70^\circ\text{C}$  for a week. The ratio of  $\text{P}/(\text{As}+\text{P})$  was varied in increments of 0.1 from 0 to 1 to prepare different composition solid solutions. The final precipitates were washed and dried at  $110^\circ\text{C}$  for 24 hours. It was found that the final ratio of arsenate and phosphate was highly dependent on the initial  $\text{P}/\text{As}$  ratio in the original solution. The  $\text{P}/(\text{As}+\text{P})$  ratio in the solid was slightly larger than the ratio in the starting solution. XRD analysis revealed a gradual change from cell parameters of fluorapatite to those of svabite with increasing arsenic content. Precipitated svabite and As-rich solid solution (90% As-10% P) was found to be made of needle-like crystals, while fluorapatite and As-poor solid solution (90% P-10% As) to be made of plate-like crystals. The crystal size decreased with increasing arsenic content. The transition is pictured in Figure 2-8.

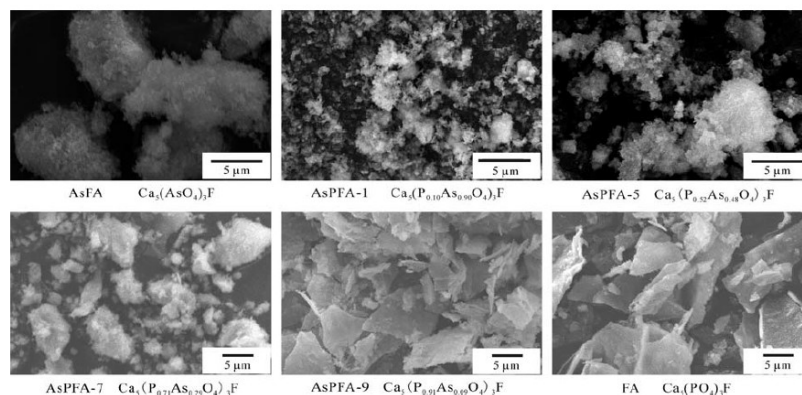


**Figure 2-8: Morphology of mixed svabite/fluoroapatite solids (64)**

The Zhu team also tested the stability of the solid solutions of svabite/fluoroapatite (65). Solids precipitated at  $50^\circ\text{C}$  were washed multiple times with ethanol, then dried at  $90^\circ\text{C}$  for 5 days. The solids were placed into aqueous solutions at pH 2, 6 and 9. The pH was not adjusted during the dissolution tests, but allowed to drift. They found that as the arsenic content in the

solid material increased, so did the release of arsenic into solution. The samples that began at pH 2 reached a range of pH 3.78 (9% As) which increased to 6.41 (91% As) after equilibration for 120 days. At initial pH 6, the samples reached pH 7.2 (9% As) to pH 8.08 (91% As) after equilibration. Finally, at pH 9, the samples reached pH 7.44 (9% As) to pH 8.08 (91% As) at the end of equilibration.

The reported arsenic release can be seen in Figure 2-9. The arsenic released in solution that began at pH 6 ranged from 68.24mg/L for solid which had 91% arsenic (final solution pH 7.20), to 4.8mg/L for 9% As (final solution pH 8.08). The difference in pH values would also impact the arsenic release, as a higher pH will lead to less dissolution, and should be considered when comparing the dissolution values. It should also be noted that these solids still released more arsenic into solution than was reported by Kucharski et al. with pure svabite (58) perhaps pointing to less well developed crystals.



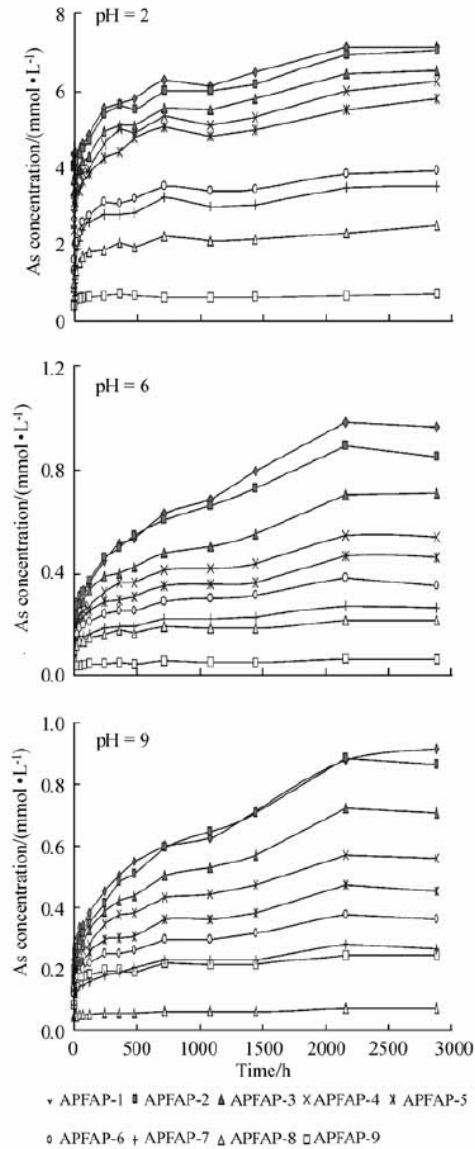


Figure 2-9: Arsenic release during FAP/SVA solid solution dissolution (58)

## 2.4 Fluoroapatite

Due to the limited research in the formation of svabite, it is beneficial to examine fluoroapatite precipitation systems given the similarity between the two mineral types. Fluoroapatite ( $\text{Ca}_5(\text{PO}_4)_3\text{F}$ ) has been the subject of much research since it is part of the bone structure in structure in certain animals, , but also because it has been considered in various industrial-environmental applications, such as precipitating lead (66), removing copper (67), cadmium, or zinc (68). Arsenate is isostructural and isoelectric with phosphate hence the tendency for the formation of solid solutions (64).

Arsenate has been known to partly replace phosphate in various apatites, including synthetic fluoroapatite (64) and natural fluorapatite deposits in the St. Marcel Praboma mine in Val d'Aosta in Italy (69). These properties mean that studying the fluorapatite system may give insight to the svabite system. Although this paper focuses on the synthesis of fluorapatite in aqueous systems, it is also possible to synthesise FAP by sintering of component precursor powders (70), (71) (72).

#### 2.4.1 Aqueous Synthesis of Fluoroapatite

Various groups have precipitated FAP in an aqueous solution. Their methods are summarized in Table 2.45. The range of precipitation conditions is wider for FAP than either johnbaumite (JBM) or svabite. Precipitation pH ranges from 4.6 to 9, and temperatures range from ambient to 80°C. However, it does seem that to obtain FAP at an acidic pH, temperatures greater than 50°C are required. Zhu et al. (73) specifically found that even at high temperatures, non apatitic compounds were formed at pH<8; although perhaps these were metastable in nature due to insufficient aging times for the transformation to stable apatite.

**Table 2.4: Summary of methods developed to precipitate fluoroapatite from solution**

Reference	Ca source	P source	Ca: P	pH	pH control	T ( °C)
(12)	CaCl <sub>2</sub>	NaH <sub>2</sub> PO <sub>4</sub>	1.67	7.6	yes	varied
(73)	Ca(NO <sub>3</sub> ) <sub>2</sub>	Na <sub>3</sub> PO <sub>4</sub>	1.67	>8	yes	30-90
(74)	Ca(NO <sub>3</sub> ) <sub>2</sub>	(NH <sub>4</sub> ) <sub>2</sub> HPO <sub>4</sub>	1.67	9	yes	100
(75)	Ca(NO <sub>3</sub> ) <sub>2</sub>	KH <sub>2</sub> PO <sub>4</sub>	1.67	4.6	yes	25-100
(76)	CaHPO <sub>4</sub> , Ca <sub>6</sub> (PO <sub>4</sub> ) <sub>2</sub> O		1.67	11	yes	25
(77)	CaCl <sub>2</sub>	Na <sub>2</sub> HPO <sub>4</sub>	1.67		yes	25
(78)	(NH <sub>4</sub> ) <sub>2</sub> HPO <sub>4</sub>	Ca(OH) <sub>2</sub>	1.67	6	yes	80
	NaH <sub>2</sub> PO <sub>4</sub>	Ca(C <sub>2</sub> H <sub>3</sub> O) <sub>2</sub>	1.67	5		75
(79)	KH <sub>2</sub> PO <sub>4</sub>	CaCl <sub>2</sub>	1.67	7.4	yes	37

Zhu et al. (73), Flora et al. (78), and McCann (75) all found that a higher temperature led to an increase in particle size. The F/Ca ratio also impacted morphology, with an increased ratio leading to longer elongated crystals. Fluoride also impacts the rate of precipitation. A higher fluoride concentration accelerated the precipitation reaction (76), but if the concentration was too high, only CaF<sub>2</sub> precipitated, decreasing the calcium levels available in solution and hindering apatite formation (78) (76). Fulmer et al. (76) found that CaF<sub>2</sub> precipitated first, and F<sup>-</sup> levels in

solution remained constant throughout the neutralization until the apatite began to form at a basic pH.

Other ions, such as  $Mg^{2+}$ , hindered the growth of FAP (77) which is like what was found in the JBM system by Bothe and Brown (80). However, even at basic pH, FAP was favored to HAP precipitation (78).

Katsarou (12) synthesised FAP by first preparing a metastable solution of Ca and P by slowly adding a solution of  $CaCl_2$  and a solution of NaF to a beaker containing  $NaH_2PO_4$ . The pH was adjusted and controlled to remain at pH 7.6 using 0.1M NaOH. After 30 minutes of equilibration, feed solutions of  $NaH_2PO_4$ , NaF and  $CaCl_2$  were added slowly to continue the precipitation.

Zhu et al. (14) synthesised FAP by the controlled mixing of  $Ca(NO_3)_2$ ,  $Na_3PO_4$  and NaF in stoichiometric ratios. The solution was mixed at room temperature for 10 minutes, and then the pH was adjusted to be between 7 and 8. Then, the solution was stirred for a week at various temperatures. The effect of temperature on morphology and crystal size is illustrated by the TEM images presented in Figure 2-10. The same procedure (at  $70^\circ C$ ) without NaF was used to precipitate HAP. After 1440 hours, the phosphorus level in solution became constant. Both solids were microcrystalline with an apatite structure.

Zhu et al. (73) mixed a solution containing  $(NH_4)_2HPO_4$ ,  $NH_4F$ ,  $Ca(NO_3)_2$  and  $NH_4OH$  at a controlled pH (7,8,9,10) for 3 hours. Various samples were synthesised at temperatures of 5, 30, 60 and  $90^\circ C$ . The solution was stirred for 3 hours, then aged for 24 hours at room temperature. The solids were filtered, washed and dried in an oven at  $110^\circ C$ . All crystals precipitated were nano-sized, and the lower temperature synthesis gave short, rod-like crystals, and higher temperatures yielded longer rods. The higher the temperature, the larger the precipitated crystal size is (Figure 2-10). The F/Ca molar ratio in the initial solution also affected the morphology of the solid formed, with longer rods being precipitated with a larger F/Ca molar ratio in the initial solution (Figure 2-11). At a  $pH > 8$ , apatitic-like compounds were precipitated, whereas at a pH lower than this other calcium phosphate minerals were synthesised.

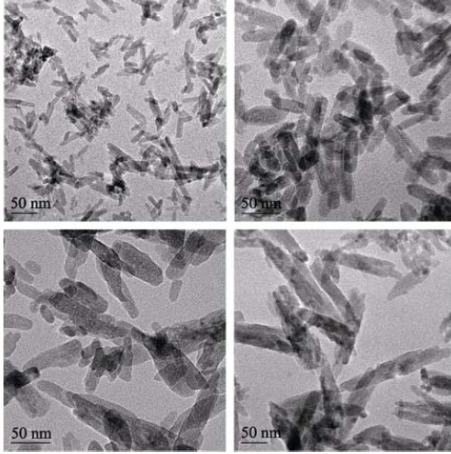


**Figure 2-10: TEM images of FAP synthesized at different temperatures (clockwise from top left: 5, 30, 60, 90°C) (14)**

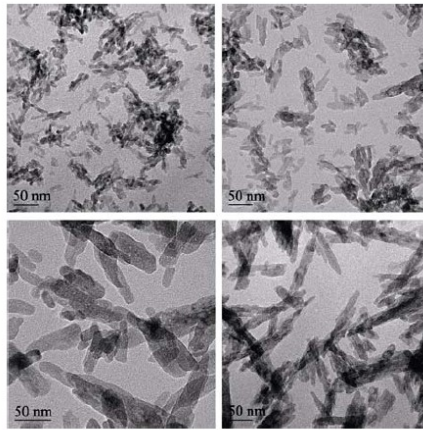


Fig. 2 TEM images of the FHAs prepared with different  $n(\text{F}^-)/n(\text{Ca}^{2+})$  ratios (pH=10,  $T=60^\circ\text{C}$ ) (a) 0.04; (b) 0.08; (c) 0.12; (d) 0.16

**Figure 2-11: Effect of initial F/Ca molar ratio on the morphology of FAP (73)**

Fulmer and Brown (76) synthesised fluorapatite in aqueous solution at room temperature by mixing  $\text{CaHPO}_4$  with  $\text{Ca}_4(\text{PO}_4)_2\text{O}$  and NaF, in a liquid to solid ratio of 1:200 by weight. The concentrations of reactants were gradually increased until the pH reached 11. In general, the pH first rose as precipitation occurred-likely due to the dissolution of  $\text{CaHPO}_4$  -then reached a steady state during apatite formation. A higher fluoride concentration accelerated the precipitation, and a low concentration retarded the precipitation. Initially  $\text{CaF}_2$  precipitated, and the fluoride concentration remained constant until apatite phases begin to precipitate. Once the apatite appeared, the fluoride ion substituted for the  $\text{OH}^-$  ion in the solid and the pH of the solution increased. This does not agree with the other research discussed in this section, who found that FAP could be formed at acidic pH, and Flora et al. (78) specifically found that

fluoroapatite formed preferentially to HAP. However, in all, the uptake of fluoride into the apatite increased with decreasing pH, but CaF<sub>2</sub> formed at low pH.

It is also possible to synthesise fluoroapatite from synthetic seawater solutions (77), as shown by Van Cappellen and Berner (77). The starting solution contained a mixture of NaCl, CaCl<sub>2</sub>, NaF and Na<sub>2</sub>HPO<sub>4</sub> at seawater concentrations of Ca<sup>2+</sup> and Cl<sup>-</sup> and seawater pH. The addition of magnesium hindered the growth of FAP. The growth of FAP decreased with increasing pH. However, this does not appropriately model growth in seawater due to the abundance of magnesium and the fact that N<sub>2</sub> was continuously bubbled into the system to avoid CO<sub>2</sub> contamination. The growth of FAP occurred mostly by growth on octacalcium phosphate precursor seeds.

Flora et al. (78) compared different methods of synthesis for FAP. Various reagents were mixed at room temperature or elevated to 100°C in an Erlenmeyer flask with a Bunsen valve to minimize any CO<sub>2</sub> contamination. The precipitates aged for varying durations and various pH values. The solids were vacuum filtered, then washed and dried at 125°C for 6 hours. Fluoroapatite was successfully synthesised under two conditions. The first involved mixing (NH<sub>4</sub>)<sub>2</sub>HPO<sub>4</sub> and Ca(OH)<sub>2</sub> at 80°C and pH 6. The second involved mixing Ca(C<sub>2</sub>H<sub>3</sub>O)<sub>2</sub> and NaH<sub>2</sub>PO<sub>4</sub> and Ca(OH)<sub>2</sub> at pH 5, and 75°C. Pure FAP was formed after only 2 hours, although samples aged for up to 24 hours. The higher temperature meant a more crystalline solid. Even at basic pH, fluoroapatite was preferentially formed to hydroxyapatite. Testing the effects of other ions in solution found that the inclusion of chlorine in solution did not yield chloroapatite, even when the chloride ion concentration was 10 times that of fluoride. However, a high concentration of fluoride yielded CaF<sub>2</sub> formation. The ease of formation of apatites of the form Ca<sub>5</sub>(PO<sub>4</sub>)<sub>3</sub>X followed this order: F>OH>Cl (78).

#### 2.4.2 Dissolution of Fluoroapatite

According to Stumm and Morgan (34), the K<sub>sp</sub> of HAP is 10<sup>-57</sup> and that of FAP is 10<sup>-59</sup>. Using PHREEQC, Zhu et al. calculated the K<sub>sp</sub> of HAP to be 10<sup>-53.28</sup>, and the K<sub>sp</sub> of FAP was 10<sup>-55.71</sup> (14). McCann found a K<sub>sp</sub> of 10<sup>-60.09</sup>

Zhu et al. (14), Bengtsson et al. (81), Chairat et al. (82), Wu et al. (83), Sandström et al. (84) all found that during dissolution fluoride was preferentially released, creating a calcium/phosphate rich surface layer. They hypothesized that this is due to OH<sup>-</sup>/F<sup>-</sup> ion exchange on surface sites. This is in accordance with the pH sensitivity of the surface. In low pH,

Bengtsson et al. found an accumulation of Ca and F in the surface, due to surface precipitation of  $\text{CaF}_2$  (74).

Groups report dissolution to be both non-stoichiometric (Zhu et al. (14) and Chairat (82)) and stoichiometric (Bengtsson (81), Harouiya (85), McCann (75)). The variation seems to be due to a difference in pH during dissolution, with incongruent dissolution occurring in basic solutions. Chairat et al. (82) also studied the impact of pH on the dissolution rate. In acidic conditions, the dissolution rate decreased with increasing pH, potentially due to the hydrolysis of the phosphate ions. In neutral/weakly alkaline conditions ( $7 < \text{pH} < 10$ ) the dissolution rate was independent of pH, and in basic conditions ( $\text{pH} > 10$ ), the dissolution rate decreased with increasing pH again. This three-section rate relationship is similar to that of carbonates and olivines. An increase in temperature leads to an increase in stability (73). The trend also seems to be that a higher pH will lead to less dissolution.

Bengtsson et al. (74) established a theoretical surface complexation model at  $25^\circ\text{C}$  and  $0.1\text{M}$  NaCl that was verified with experimental data. The complexation model included adsorption of  $\text{H}^+$  and  $\text{OH}^-$ , as well as the adsorption of dissolved fluoride, calcium or phosphate ions. The results of the model are illustrated in Figure 2-12. Chemical analysis revealed a surface layer composition of  $\text{Ca}_9(\text{HPO}_4)_2(\text{PO}_4)_4\text{F}_2$ , with a surface Ca/P molar ratio of 1.5, while the bulk solid had a molar ratio of 1.67 (81).

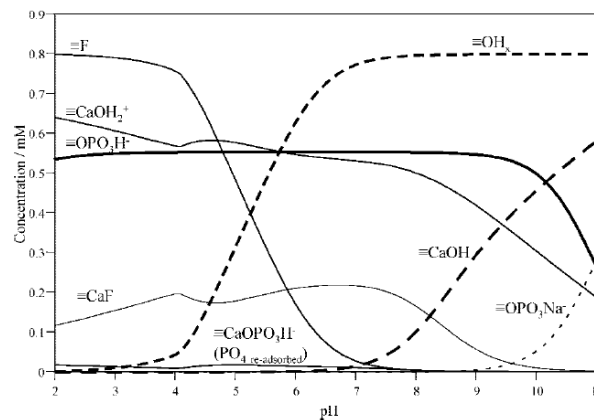


Figure 2-12: Surface complexation model of fluoroapatite (74)

Fluoroapatite substituted with carbonate ( $\text{Ca}_{10}(\text{PO}_4)_5(\text{CO}_3)(\text{F},\text{OH})_3$ ) was reported to have a solubility product of  $10^{-103}$  and dissolve congruently (86). At  $\text{pH} < 6$ , the dissolution included a high release of calcium, phosphate and fluoride. These results are significant as the presence of dissolved  $\text{CO}_2$  may lead to the substitution of carbonate species into the apatite matrix (87).

Carbonate groups are thought to replace phosphate in the apatite matrix, and are locally charge-compensated by fluoride ions (86).

Harouiya et al. studied the effects of temperature on the dissolution of FAP from 5 to 50°C and pH 1 to 6 by allowing the system to equilibrate for 180 days (85). Ca:P and Ca:F ratios in solution were close to stoichiometric. They found that the dissolution rate was independent of the solution composition or temperature but increased with decreasing solution pH in the acidic range, consistent with Chairat et al.'s finding in the same pH range (82).

## 2.5 Conclusion

The aqueous precipitation of insoluble compounds of arsenic (V) as a possible solution for the long-term storage of this toxic metalloid was reviewed. Previous work has included precipitation of various calcium arsenate compounds, with the most stable having an apatite structure. Johnbaumite ( $\text{Ca}_5(\text{AsO}_4)_3\text{OH}$ ) is the most studied arsenate apatite. In general, the aqueous precipitation of arsenate apatites is favored at a neutral or basic pH and a temperature greater than room temperature. The stability of the calcium arsenate compounds increases with increasing pH, but decreases with the dissolution of atmospheric  $\text{CO}_2$  in the solution.

In order to increase the stability of Ca- $\text{AsO}_4$  apatites, researchers have investigated the synthesis of mixed arsenate-phosphate compounds by the substitution of arsenate into calcium phosphate apatite structures, forming solid solutions. The replacement of phosphate with arsenates causes local distortions in the apatite structure if large fractions of arsenate is incorporated. The best stability was achieved with a phosphate to arsenate ratio greater than five in the case of hydroxy-apatites:  $\text{Ca}_5(\text{PO}_4)_{3-x}(\text{AsO}_4)_x\text{OH}$  ( $x \leq 0.5$ ).

Since the phosphate analogue of johnbaumite, hydroxyapatite, is less stable than fluorapatite ( $\text{Ca}_5(\text{PO}_4)_3\text{F}$ ), svabite, the arsenate analogue of fluorapatite is another potential compound for the long-term storage of arsenic. Some limited work in terms of synthesis and stability with this system has been reported. Svabite has been produced by either high-temperature sintering processes or by aqueous precipitation and long-term aging of one week. None of the studies examined the effect of different process parameters on the formation of crystalline svabite. In the meantime contradictory results have been reported when it comes to the solubility of svabite by the two groups who studied this system. The solubility data for svabite prepared by sintering as well as for natural svabite samples were one order of magnitude lower than the data for svabite

material synthesized by aqueous precipitation. This implies that aqueous precipitation of svabite requires further investigation to lead to svabite solids of better crystallinity/stability.

The mixed arsenate-phosphate fluoroapatite system needs to be investigated also as similarly to hydroxy-apatite system, should phosphate provide a more stable structure than that of svabite that contains only arsenate.



### 3 Objectives

This thesis investigates the precipitation of arsenic(V) from aqueous solution in the form of svabite ( $\text{Ca}_5(\text{AsO}_4)_3\text{F}$ ) as well as mixed fluoro-calcium phosphate/arsenate apatites by neutralization; the impact of different precipitation parameters on the phases formed; and the stability of these compounds in terms of arsenic release. The overall goal is to evaluate if aqueous precipitation of these compounds can lead to solids with good crystallinity and low solubility that potentially can find application in the mining industry as stable arsenate fixation media.

This is driven by the pressing need to develop new disposal technologies for arsenic-bearing metallurgical wastes that limit the release of arsenic to the environment within permitted levels under a wide range of conditions such as different pH, exposure to  $\text{CO}_2$  and oxidation-reduction regimes.

The main objectives of the work described in this thesis are as follows.

1. *Develop an aqueous precipitation process to synthesize crystalline svabite under atmospheric conditions.*

To date well crystalline svabite has been synthesized by sintering at high temperature (500-1300 °C) (58; 61; 62), a process that is not amenable to industrial application in the case of arsenic that has to be removed from aqueous solution. The sole reported aqueous precipitation method for svabite (63) yielded svabite of poor crystallinity. This method is not fully described, and involves one week of equilibration which results in a residence time that is unattractive for industrial applications. Therefore, no established or widely-accepted precipitation method exists for this compound.

The principal objective of this work is to determine the operational range for the successful precipitation of crystalline svabite via neutralization. The knowledge of this range can inform the design of an optimized process suitable for industrial application. The precipitation of multi-element compounds is influenced by the solution conditions (16). In this regard the effect of the following parameters on the production of svabite is investigated: precipitation pH, temperature, ageing time, initial concentration, and timing of fluoride addition to the solution. The testing of the different conditions was limited to determining whether a crystalline phase was formed. Any

other impacts of these parameters, such as particle morphology and growth, was not closely monitored.

*2. Demonstrate the application of the developed process to the precipitation of mixed svabite-fluoroapatite compounds (solid solutions)*

The inclusion of phosphate in arsenate-containing apatites yields solid solutions that are less susceptible to arsenic release through dissolution than apatites with arsenate alone (40). Since the ultimate application is the encapsulation of arsenic, it is worthwhile to investigate the leachability of svabite-fluoroapatite solid solutions. This requires a procedure to synthesize these compounds.

Much like svabite, limited work on the aqueous precipitation of solid solutions of svabite and fluoroapatite is available. A single procedure is reported in a foreign-language publication (64). In this thesis, the process developed for svabite as per Objective 1 is extended to the mixed arsenate/phosphate system to determine the effect of a variable PO<sub>4</sub>/AsO<sub>4</sub> ratio on the compounds formed.

*3. Evaluate the stability of the produced compound(s) via leachability testing under various aqueous conditions.*

The crystalline compounds formed by aqueous precipitation as per Objectives 1 & 2 will be subjected to leachability tests to determine their stability in terms of arsenic release. This will allow for an initial comparison of the compounds formed to previously reported stability results for svabite and svabite-fluoroapatite compounds, as well as to other compounds considered for the sequestration of arsenic. The stability tests presented in this thesis include leachability at a controlled pH, leachability under pH drifting (i.e. with no control), and leachability in the presence of dissolved CO<sub>2</sub> in the solution. The latter aspect is important as simple calcium arsenates are known to react with atmospheric CO<sub>2</sub>, converting to calcium carbonate with concomitant release of arsenic to water (52; 40). Apatite compounds resisting such conversion have potential as arsenic fixation media.

## 4 Experimental Methods

In this chapter the experimental procedures, the chemicals, and the characterization techniques used are described.

### 4.1 Chemical Reagents

All reagents used were supplied by Sigma-Aldrich.  $\text{As}_2\text{O}_5$  dissolved in de-ionized water (obtained using a Reverse Osmosis system) was used as the source of arsenic,  $\text{NaHPO}_4$  dissolved in de-ionized water was used as the source of phosphate. Fluoride was in the form of  $\text{NaF}$  dissolved in de-ionized water, and the source of calcium was  $\text{Ca}(\text{NO}_3)_2 \cdot 2\text{H}_2\text{O}$ . Stock solutions of each salt were made and used as needed during the synthesis experiments.  $\text{NaOH}$  and  $\text{HNO}_3$  were used for pH adjustments.

### 4.2 Procedure for Precipitation of Svabite and Svabite-Fluoroapatite Compounds

The development of the aqueous precipitation process for the synthesis of svabite and mixed compounds (“solid solutions”) of svabite and fluoroapatite as per Objectives 1 and 2 involved the following general experimental procedure.

This general procedure was conceived by studying-see Chapter 2- aqueous precipitation of the analogue apatites of johnbaumite (JBM) and fluorapatite (FAP). As per Table 2.4 and the references mentioned therein, aqueous precipitation of fluoroapatite is commonly done from solutions with stoichiometric composition (corresponding to  $\text{Ca}_5(\text{PO}_4)_3\text{F}$  formula) over the pH range 5-9 at temperatures 30-90 °C and finished with aging of the precipitated solids in the synthesis liquor over a period of time.

On the basis of this background, in a typical svabite precipitation test, a 0.5L solution was made by mixing stock solutions of Ca salt (1.5M) and As(V) (0.667M) of approximate pH ~2. To that an appropriate amount of  $\text{NaF}$  stock solution (1.0M) was added to give the final arsenic concentration desired with stoichiometric amounts corresponding to svabite of Ca and F. The solution was heated to the precipitation temperature while being agitated. Once the temperature was reached, the solution was neutralized to the precipitation pH by slowly adding 1M  $\text{NaOH}$  base drop-wise over 1.5 hours. After neutralization, the flasks were tightly sealed and the solution was maintained at an aging temperature for the duration of the aging time, for the

purpose of increasing the crystallinity of the precipitated solids via aging. The pH was not controlled or adjusted during the aging period.

Once aging was over, the precipitated slurries were allowed to reach room temperature before subjected to pressure filtration to recover the solids. The solids were then rinsed with de-ionized water, repulped and re-filtered three times, rinsing with de-ionized water between each filtration. This extensive washing procedure was adopted to ensure complete removal of any entrained soluble arsenic species hence ensuring reliable data during subsequent stability testing. The thoroughly washed solids were then collected, and dried in an oven at 60°C for 24 hours. Mild drying conditions were chosen rather than higher temperatures as precaution against undesirable phase changes that would have rendered the subsequent stability work not representative of the actual precipitated compounds.

A procedure successfully yielding svabite was used as the base case, and a single parameter was modified at a time. This section details the tested ranges of each parameter.

#### *Initial Concentrations in solution*

The majority of intentional syntheses of JBM, JBM-HAP, and FAP discussed in Chapter 2 concluded that a stoichiometric ratio in solution is required for the formation of the apatites. All initial concentrations for the syntheses presented in this work were at the apatite stoichiometric ratios.

Zhu et al. precipitated SVA and SVA/FAP solid solutions with an initial arsenic concentration of 0.167M (63) (64). The range of initial concentrations tested were centred around this value, and the following initial arsenate concentrations were used: 0.05M, 0.15M, 0.20M, and 0.35M.

#### *Precipitation Temperature*

A range of temperatures have been used to precipitate apatites. SVA has been precipitated at 70°C (63), but other apatites such as JBM and FAP have been precipitated in amorphous phases at ambient temperature (55), (12), (76), (77). Higher temperatures have also been shown to produce larger crystals of FAP (73) (14).

The variations in temperature included 70°C, which has been used to precipitate svabite, a synthesis at room temperature, and a synthesis closer to the boiling temperature of water (90°C).

### *Neutralization pH*

In general, the formation of SVA and JBM requires basic pH. FAP has been formed with a pH as low as 4.6 (75), while other groups have found that only non-apatitic compounds are formed at a pH < 8 (73). To investigate the effect of pH, syntheses with the following pH were tested: 4, 6, 7, 8, 9, 10, and 11.

### *Aging Time*

SVA and SVA-FAP solid solutions were reported to be formed after a week of precipitation. Research in johnbaumite synthesis and fluorapatite synthesis have shown that these can be formed with an aging time of 24 hours (73) (78).

No work has been reported about the precursors, if any, to the formation of svabite, or the kinetics of the precipitation reaction. A precursor to fluorapatite has been seen in the research by Amjad et al. (79). Looking at the phases formed after different aging times also allows for a better understanding of the system and the process of precipitation. The following aging times were tested: 1 hour, 4 hours, 24 hours. Longer aging times were not tested due to time constraints.

### *Timing of fluoride addition*

Although it is not discussed in the literature for the aqueous precipitation of SVA and SVA/FAP compounds, the timing of the addition of fluoride may impact the phase formed. Too much fluoride has been found to hinder the formation of fluorapatite (78) (76) due to the precipitation of CaF<sub>2</sub> and the removal of calcium from solution and resultant change in the ratio of As:Ca in solution. Fulmer and Brown (76) found that CaF<sub>2</sub> precipitated first before the apatite phase.

The results of the following syntheses are presented in this thesis:

- Adding the fluoride to the initial solution prior to adding the arsenate to the solution.
- Adding the fluoride into the initial solution once the calcium and arsenate solutions have already been mixed.
- Adding the fluoride to the solution after the solution has been heated and neutralized

### *Fluorapatite-Svabite Solid Precipitation*

For the synthesis of svabite-fluorapatite solid solutions, phosphate is added to the initial solution replacing some of the arsenate. The molar ratio of [Ca]:[As+P] was kept at 5:3, matching that of apatite, in all cases. The composition in the initial solution was varied so that

the initial combined concentration of phosphate and arsenate ranged from 0% to 75% arsenate. These compositions are within the range of arsenate content (0-90%) in the syntheses of SVA-FAP solid solution reported by Zhu et al. (64). Twidwell et al. (40) found that a ratio of  $\text{PO}_4:\text{AsO}_4 > 5$  was required for JBM-HAP compounds to be stable in the presence of  $\text{CO}_2$ , equivalent to a maximum of 17% arsenate content. A 15% arsenate content synthesis was included to compare the stability to that of the JBM-HAP solid solution in the presence of  $\text{CO}_2$ .

### 4.3 Characterization of Solids and Solutions

Once the precipitates were dry, they were ground using a mortar and pestle. The crystalline phases/compounds formed during each synthesis experiment were identified using X-Ray Diffraction (XRD). A Philips PW 1710 diffractometer with a copper target ( $\text{CuK}\alpha$  radiation,  $\lambda=1.54060 \text{ \AA}$ ), a crystal graphite monochromator and scintillation detector was used. The scan rate varied depending on the complexity of the sample and the number of phases detected by the XRD.

Select samples were characterized using scanning electron microscopy (SEM) with a Hitachi SU-3500 Variable Pressure SEM in terms of particle morphology, and in terms of their BET specific surface area using a Micromeritics Tristar 3000 Surface Area Analyzer. Only samples where the XRD pattern indicated the presence of svabite or svabite-fluorapatite were analysed. The same samples were digested in  $\text{HNO}_3$  and the resulting solution was analyzed as described below to determine their chemical composition.

Solution samples were first passed through a  $5 \mu\text{m}$  filter. Arsenic, calcium, and phosphorus concentrations in solution were analysed using Inductively Coupled Plasma Optical Emission Spectrometry (ICP-OES) performed with a Thermo Scientific iCAP 6000 series ICP-OES. Fluoride concentrations were measured using a Thermo Scientific Orion Fluoride Electrode.

The reproducibility of the developed synthesis procedure for svabite and mixed svabite/fluoroapatite compounds was confirmed with replicate tests and determination of the XRD patterns. However, no replicate stability tests (section 4.4) were performed due to lack of time.

### 4.4 Stability Evaluation Procedure

Representative samples of synthesized svabite and mixed fluorapatite/svabite compounds (with variable arsenic content) were subjected to leachability (=solids in contact with water) testing to evaluate their relative degree of stability in terms of released arsenic concentration in

water of certain pH. The adopted procedure was similar to the stability testing applied to other arsenate compounds such as yukonite and scorodite by the McGill HydroMET team (22) (26) (12).

More specifically the procedure consisted of the following steps: The selected dry powdered solids were first subjected to a series of washings. Each sample was placed in an HDPE container, which was tightly sealed. The solids were mixed with deionized water in a 20:1 solids to liquid weight ratio, this corresponded to 10 g of solids placed in 200 mL of water. The samples were agitated for 24 hours. The solids were then filtered using a pressure filter. Samples of the solution were collected and tested for pH and concentrations of arsenic, calcium, and phosphate. The filter cake was further rinsed three times with deionized water.

The filtered solids were then mixed with another 200 mL of deionized water. The washing procedure was repeated until the concentrations of arsenic and calcium stabilized. This is to remove any soluble salts that may have precipitated during the initial drying of the samples. The washing ensured that the solids tested for stability were free of entrained impurities. If not pre-washed out, any soluble impurities on the solids could be released into the leachability medium (water) and increase arsenate, calcium and phosphate concentrations, exaggerating the extent of dissolution of the solids.

Once the solids were washed, they were dried in an oven at 60°C until dry. The samples were then re-ground using a mortar and pestle and placed into fresh sealed HDPE containers with 200 mL of deionized water. The solution was brought to pH 9 by dropwise addition of 0.1M NaOH. The suspensions were kept at pH 9 for 3 days. The jars were agitated, and tightly sealed. No other precautions were taken to avoid carbon dioxide intrusion into the jars. Every 12 hours the pH was checked, and if within 0.5 pH units from 9, the pH was not adjusted. Otherwise, the pH was adjusted using 0.1M NaOH or 0.1M HNO<sub>3</sub>. 1 mL samples of the solution were removed for analysis using a 5 µm filter syringe. The liquid removed was not replaced with additional liquid.

A pH of 9 was chosen for the evaluation of the stability of svabite and its mixed compounds to allow for comparison to stability of scorodite and yukonite also done at pH 9 by the McGill HydroMET team (31) (9) (26). Furthermore, since apatites are less soluble in slightly basic solutions, it was assumed that at pH 9 the minimum dissolution would be measured. The test

would then demonstrate the “best case” scenario for the stability of the compounds determining if further research into these compounds is warranted.

After the first three days, pH adjustment ended and the agitated slurries were let to equilibrate for another three days to their ‘self-drifting’ pH values. Samples continued to be taken every 12 hours. After another three days (6 days in total), NaHCO<sub>3</sub> was added to the jars to simulate exposure to atmospheric CO<sub>2</sub>, albeit at a rather aggressive level. The carbonate was added to achieve a 1:1 Ca to CO<sub>3</sub> molar ratio. This was done to assess the effect of dissolved CO<sub>2</sub>/carbonate species on the stability of the arsenate apatite compounds synthesized, as there is a tendency for calcium to form CaCO<sub>3</sub> that at least in the case of simple calcium arsenates leads to their dissolution (88).



## 5 Results and Discussion

This chapter presents the results from the precipitation and the stability experiments.

### 5.1 Aqueous Precipitation of Svabite by Neutralization and Aging

As discussed in Chapter 2, only one group has reported the aqueous precipitation of svabite (63) and its solid solution with fluoroapatite (65) from arsenic(V)-containing solutions. In their studies Zhu et al. simply mixed individual solutions with the different precursor elements (Ca, As, F) at stoichiometric ratios ( $[Ca]/[As]=5/3$  and  $[As]/[F]=3$ ) and allowed the mixed solution (0.167M As(V)) to equilibrate at 70°C for one week. No information on pH or the effect of other precipitation parameters was reported. Moreover, their svabite and svabite/fluoroapatite solid solution products were deemed not to be fully crystallized releasing more arsenic during stability testing than another study involving natural svabite mineral (58). However, the same group in their parallel study on fluoroapatite (73), where they used the same precipitation approach indicate that the three precursor solutions were adjusted to pH 7-8 before mixed and heated/maintained at 70°C for one week. Such synthesis method though while feasible in a laboratory setting is not directly applicable to the treatment of industrial waste waters containing arsenic and other heavy metals.

#### 5.1.1 Neutralization-Based Process for the Precipitation of Svabite

The flowchart of the neutralization-based procedure developed for the synthesis of svabite is shown in Figure 5-1.

In this work a similar solution composition as per Zhu et al. (63) was used initially having 0.15M As(V) and stoichiometric amounts of calcium (added as  $Ca(NO_3)_2$ ) and fluoride (added as NaF). Fluoride was added last (further details in Section 5.1.6). The solution is heated to 70°C. Neutralization was performed using NaOH as a base.

As with the work of Zhu et al. ( (63), (64)) and other fluoroapatite synthesis methods summarized in Table 2.4, neutralization (1.5 hours at 70°C) was followed by aging to promote crystallization. This was done at 70°C for 24 hours.

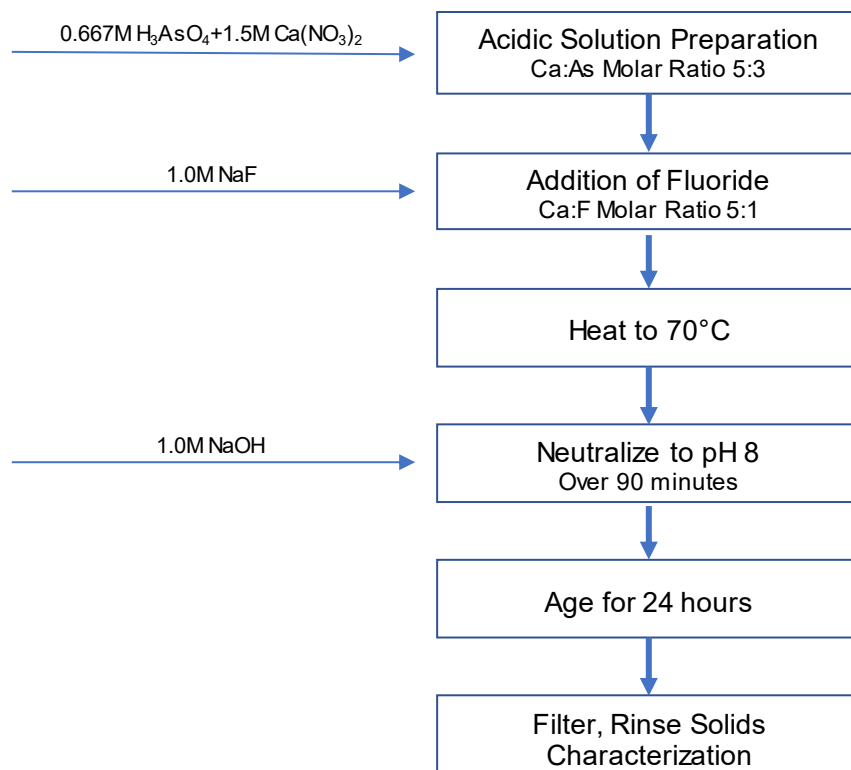


Figure 5-1: Flowchart of developed procedure for the precipitation of crystalline svabite by neutralization and aging

**Product Characterization:** The formation of crystalline svabite using the procedure presented in Figure 5-1 was confirmed by XRD analysis (Figure 5-2). The XRD pattern of the precipitated compound is compared to the reference pattern of svabite mineral. The reproducibility of the developed aqueous precipitation process in producing consistently crystalline svabite is shown by the XRD patterns of solids from duplicate tests (Figure 5-3, the codes refer to experiment codes used for internal data tracking).

Further to the XRD identification of svabite, chemical analysis of the precipitate following acid digestion determined that it had a Ca:As molar ratio of 1.65, nearly identical to the theoretical stoichiometric ratio of svabite of 1.67 suggesting a relatively pure compound. The surface area of the solids was measured using BET. The product obtained with the process of Figure 5-1 had a specific surface area of 13 m<sup>2</sup>/g that is close to that of aqueous synthesized fluoroapatite, 10.7 m<sup>2</sup>/g, measured by Bengtsson et al. (74).

The svabite precipitates were also examined by SEM to evaluate their particle morphological characteristics (Figure 5-4). These were found to be in the form of large (~30 microns) spherical aggregates of needle-like primary crystallites (a few microns long). The

needle morphology of the constituent primary crystallites was similar in appearance to johnbaumite crystallites but overall the aggregates seemed to be more compact than the latter when compared to the SEM images reproduced from Bothe et al. (see Figure 2-2 (19)). The needle morphology of the primary crystallites exhibited by the svabite produced in this work differs though from the dot-like crystallites of the svabite produced by Zhu et al. (63), apparently reflecting a different nucleation mechanism (16). The two procedures differed in method of neutralization and aging time –Zhu et al. neutralized the precursor solutions separately, letting them to react at the target pH only (suspected to be 7-8 (14)), while in the present work the precursor solutions were mixed in acidic pH and then neutralized slowly over 90 min period. By mixing the precursor solutions at high pH, it is postulated, that Zhu et al. induced fast homogeneous nucleation due to large supersaturation regime set up by the low solubility, resulting in the dot-like nanoparticle formation. By contrast, the slow increase in pH in the present work is believed to trigger nucleation at much lower supersaturation giving the opportunity to nuclei to grow into needles as pH increases. Such contrasting nucleation behaviour resulting in different size and morphology particles has been observed in the case of iron hydroxide precipitates obtained by neutralization as discussed elsewhere (16).

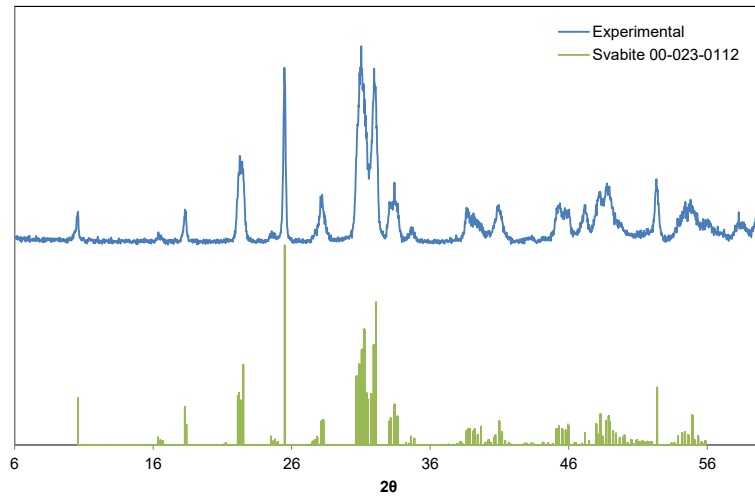


**Figure 5-2: XRD analysis of synthesized svabite compound**

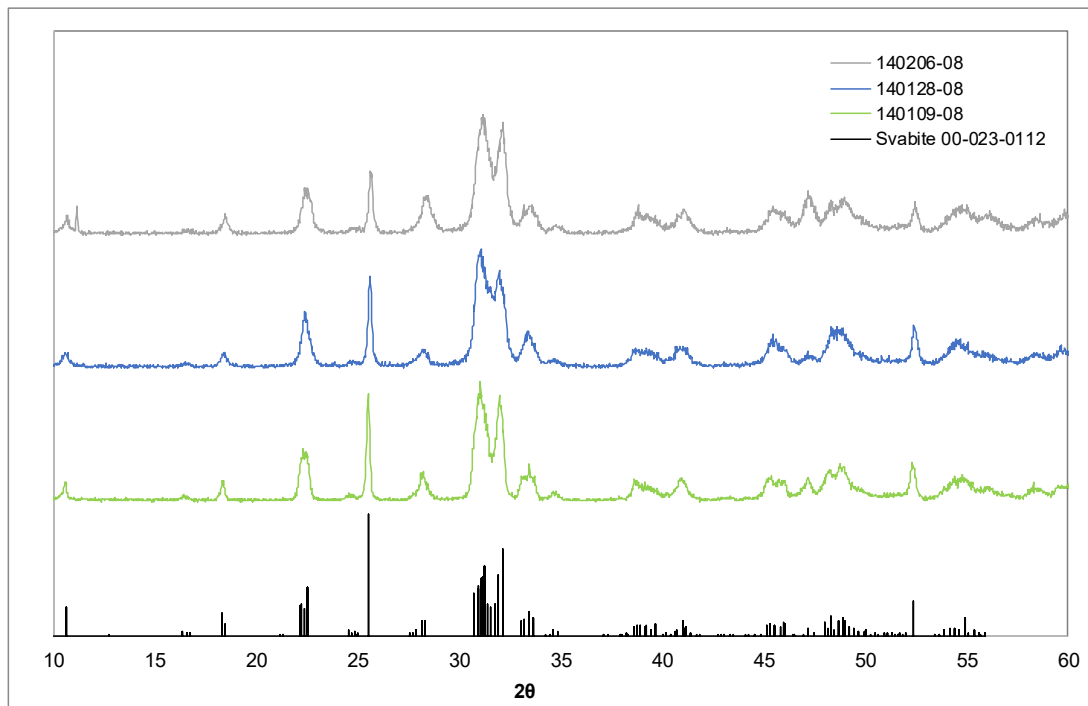


**Figure 5-3: XRD characterization of svabite precipitates obtained from replicate tests**

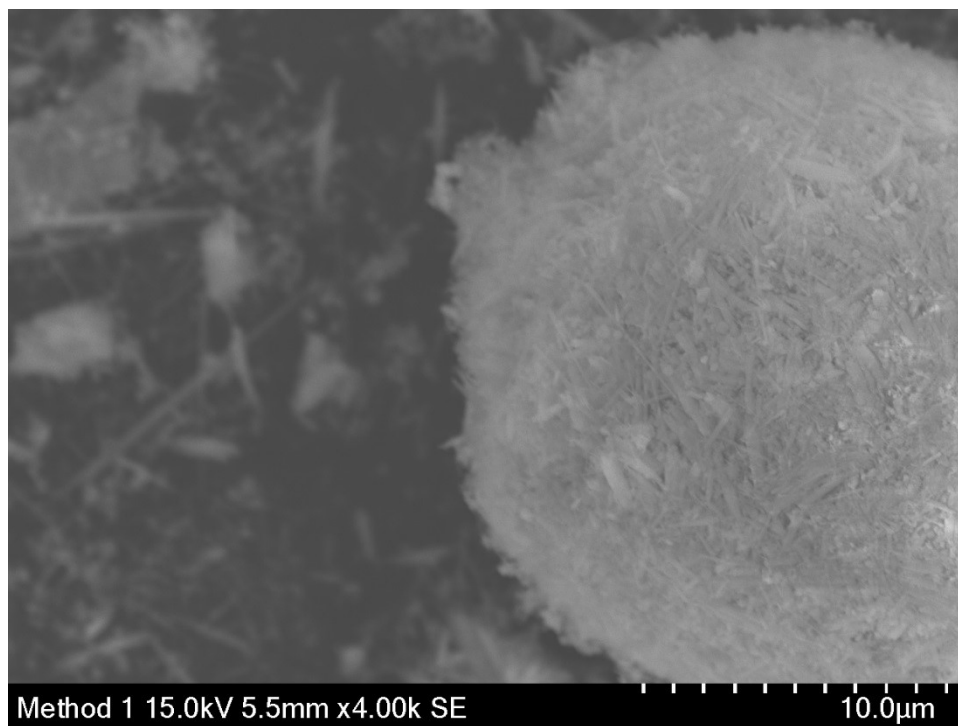


Figure 5-4: SEM image of svabite particles

### 5.1.2 Effect of Aging on Svabite Formation

Aging is a common step in the synthesis of apatite-like compounds by aqueous precipitation. Research in johnbaumite synthesis and fluorapatite synthesis have shown that these compounds can be formed with an aging time of 24 hours (78). The method described with the flowchart of Figure 5-1 involved 24 aging of the neutralization precipitate at 70°C to form svabite, which is much shorter than the week of aging under the same conditions employed by Zhu et al. (63). A shorter aging time is desirable from a practical industrial standpoint. Investigating the solids formed after shorter aging times could provide interesting insight as to the kinetics and mechanism of svabite crystallization over time, and whether svabite is formed via transformation of a precursor precipitate like fluorapatite (79). In this context solution and solid samples were taken after 1-hour, 4-hour, and 10-hour aging at 70°C after a neutralization to pH 8 and analysed for dissolved calcium, arsenate, phosphate, and fluoride and phase formation/crystallinity. Longer aging times than 24 hours were not tested due to time constraints.

Figure 5-5 presents the experimental XRD patterns after different times of aging, as well as the reference XRD patterns for svabite ( $\text{Ca}_5(\text{AsO}_4)_3\text{F}$ ) and haideringite ( $\text{CaHAsO}_4$ ). The solid formed after only one hour aging is mostly haideringite (peaks 11°, 30°), but peaks corresponding

to svabite are clearly evident. After four hours of aging at 70°C, the XRD pattern has changed. Haideringite seems to be present in trace amounts judging from the tiny peaks at around 28° and 33.5° 2θ . This remains the case after 10 hours of aging. A fully developed svabite pattern is seen after 24 hours. Haideringite is the stable calcium arsenate phase at a slight acidic pH (35), and in general is more stable than johnbaumite in acidic solutions. It seems that with the gradual increase of pH, haideringite is first formed in the early stages of the neutralization while the pH is low. As the pH increases different phases dominate (Figure 2-1) triggering the formation of svabite at the expense of haideringite. The observed delay in obtaining fully crystallized svabite indicates that it takes some time for the dissolution of haideringite and the nucleation-growth of svabite .

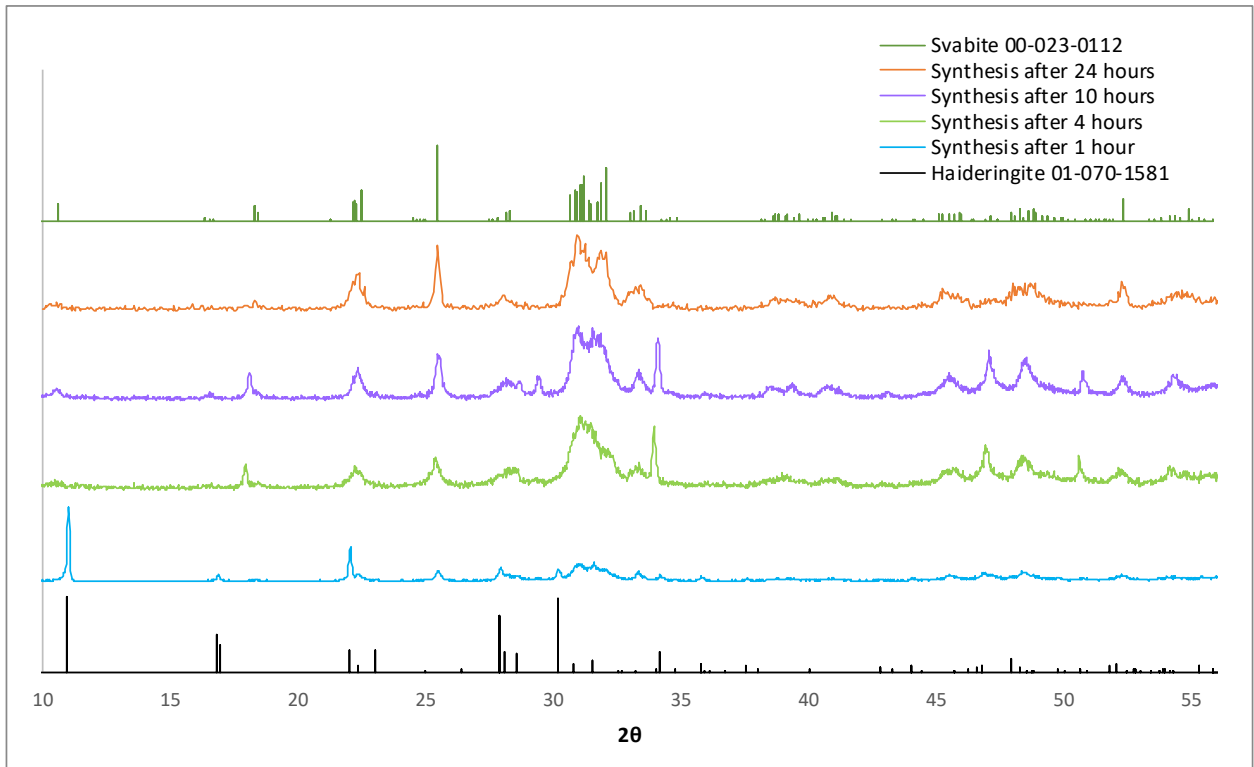


**Figure 5-5: XRD patterns of precipitates after 1 hour, 4 hours, 10 hours, and 24 hours of aging**

In addition to characterizing the solids the variation of calcium, arsenic, and fluoride concentrations in solution with aging time was monitored and reported in Figure 5-6 (fluoride concentrations are on a different axis than the other elements). Time “0” on this graph is when the neutralization was complete. The flasks were agitated and maintained at 70°C. Most of the elements have precipitated out of solution (89% As, 94% Ca and >99.97% F). As XRD analysis

showed after 1-hr aging the presence mostly of haideringite that contains no F ( $\text{CaHAsO}_4$ ) and the latter is a 1:1 calcium arsenate compound, it may be deduced that the excess Ca and F are present in some non-XRD detectable form like amorphous/poorly crystalline svabite and  $\text{CaF}_2$ . Similar observations of initial  $\text{CaF}_2$  precipitation during the fluorapatite synthesis were reported by Fulmer & Brown (76), while a metastable calcium phosphate phase has been observed to form prior to fluoroapatite precipitation (79). With the progress of aging the concentrations of As and Ca (although the data point at 4-hr may be an analytical overestimation) are seen to increase (Figure 5-6) and this may be attributed to dissolution of haideringite and the formation of poorly crystalline svabite as evident by the broad peaks (Figure 5-5). But after 24 hours aging the Ca and As concentrations decrease reflecting the complete crystallization of svabite. Such variation of solubility of a compound with degree of crystallization is in agreement with the Gibbs-Thomson law that relates solubility to nanosize of crystals. This was discussed by Demopoulos for the case of ferric arsenate compounds (16). The findings here show that aging times shorter than a week are sufficient to lead to crystallization of svabite, but that the crystal formation mechanism goes through phase evolution with haideringite ( $\text{CaHAsO}_4$ ) nucleating first at low pH that subsequently transforms gradually to crystalline svabite ( $\text{Ca}_5(\text{AsO}_4)_3\text{F}$ ) during aging.

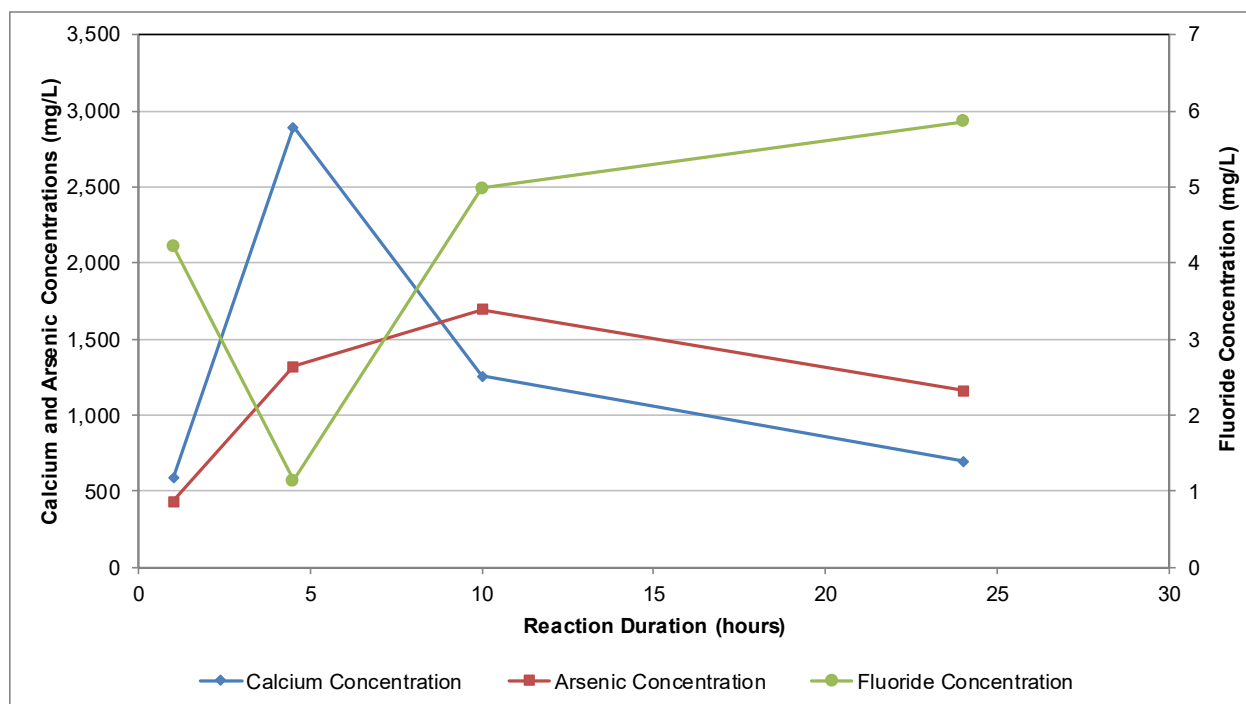


Figure 5-6: Solution concentration profiles during aging-at pH 8, 70°C, initial As concentration of 0.15M

### 5.1.3 Effect of Neutralization pH on Svabite Formation

The previous work by Zhu et al. did not report the pH used to synthesise svabite (63). Their parallel study of fluoroapatite (73) used a neutralization to pH 7-8 so it is assumed they used a similar pH range for their svabite experiments. Fluorapatite synthesis has been reported over a wider pH range (refer to Table 2.4), with a pH as low as 4.6 (75) so it is of interest to establish the effect of pH on svabite crystallization. To this end the neutralization pH was investigated by performing experiments at 70°C over the pH range 4 to 11. All aging was done without pH control. The XRD patterns of the solids formed are presented in Figure 5-7.

At pH 4, the only solid formed was CaF<sub>2</sub>. This is attributed in part to speciation of arsenic acid in solution as well as to solubility compound differences - CaF<sub>2</sub> is known to be less soluble than fluoroapatite in the acidic region (75). At pH 4, arsenic is mostly in the form of H<sub>2</sub>AsO<sub>4</sub><sup>1-</sup> (34) and the activity of AsO<sub>4</sub><sup>3-</sup> is possibly too low for the supersaturation of svabite. This seems to differ from fluoroapatite (which does not have arsenate), which has been precipitated at a pH as low as 4.6 (75).



Increasing the neutralization pH to 6 yielded an arsenate phase identified by XRD as haideringite ( $\text{CaHAsO}_4 \cdot x\text{H}_2\text{O}$ ) (see Figure 5-7). Duplicate syntheses under these conditions are presented in Appendix A and all resulted in the formation of this phase. Other groups, such as Nishimura and Robins (52) and Mahapatra et al. (54), also precipitated haideringite in this range, but did not have fluoride present in the solution.

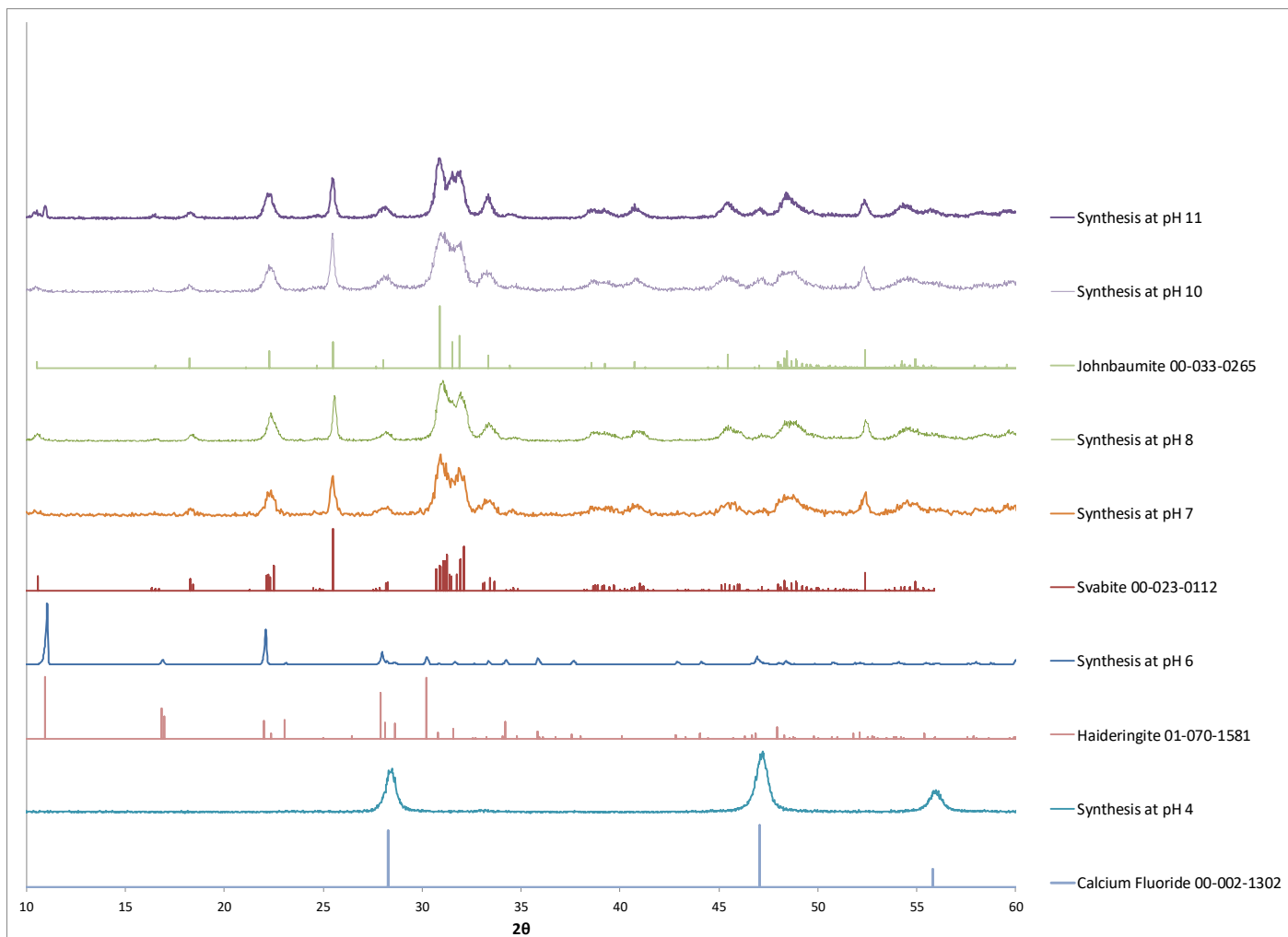


**Figure 5-7: XRD patterns of solids precipitated by neutralization at different pH endpoints at 70°C**

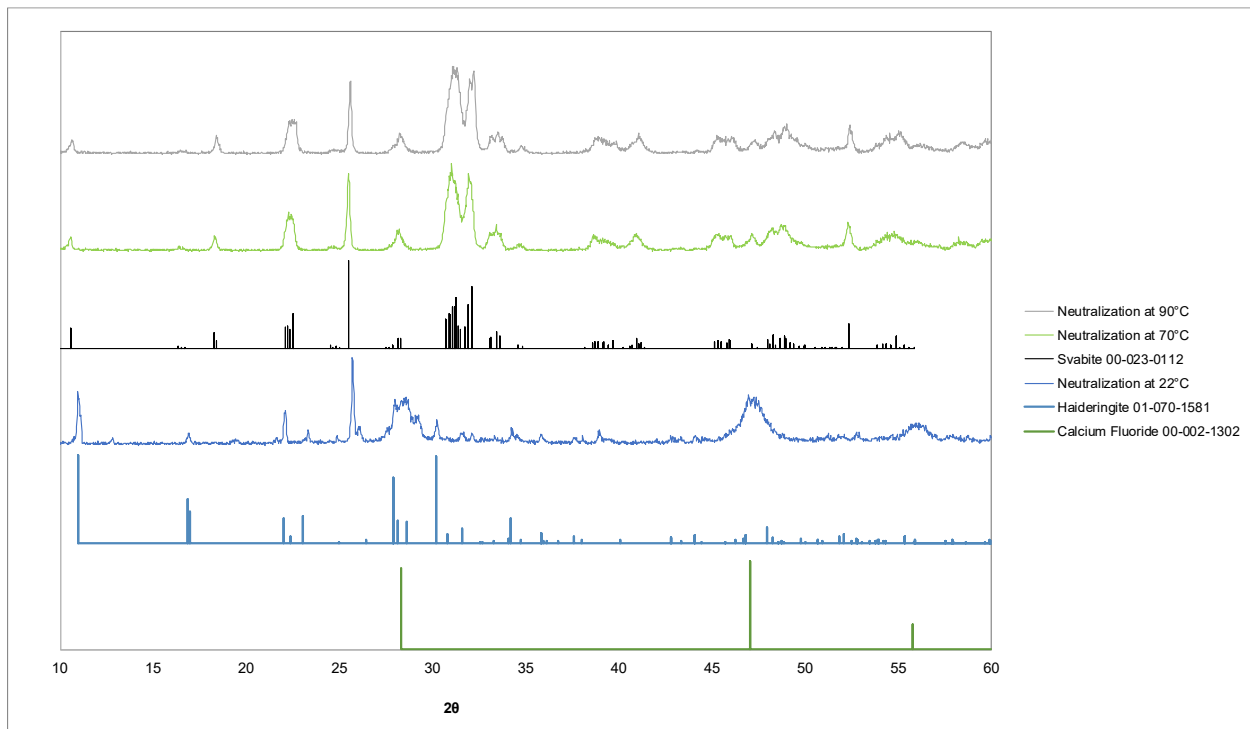
It was by increasing the neutralization pH to 7 that svabite did form. As already discussed, pH 8 also yielded svabite (Figure 5-2 and 5-3). At pH 10 svabite is formed, however some minor presence of johnbaumite cannot be ruled out (see overlapping lines at  $\sim 10^\circ$  and  $28^\circ$ ) as it is known to start forming at that pH—refer to Table 2.1. A neutralization to pH 11 only yielded johnbaumite. At higher pH, the prevalence of hydroxide ions in solution causes johnbaumite ( $\text{Ca}_5(\text{AsO}_4)_3\text{OH}$ ) to compete favorably against svabite ( $\text{Ca}_5(\text{AsO}_4)_3\text{F}$ ). This series of tests

demonstrated that the formation of svabite is favored within the pH window pH 7 to pH 10, when aging is done at 70°C.

#### 5.1.4 Effect of Neutralization Temperature on Svabite Formation

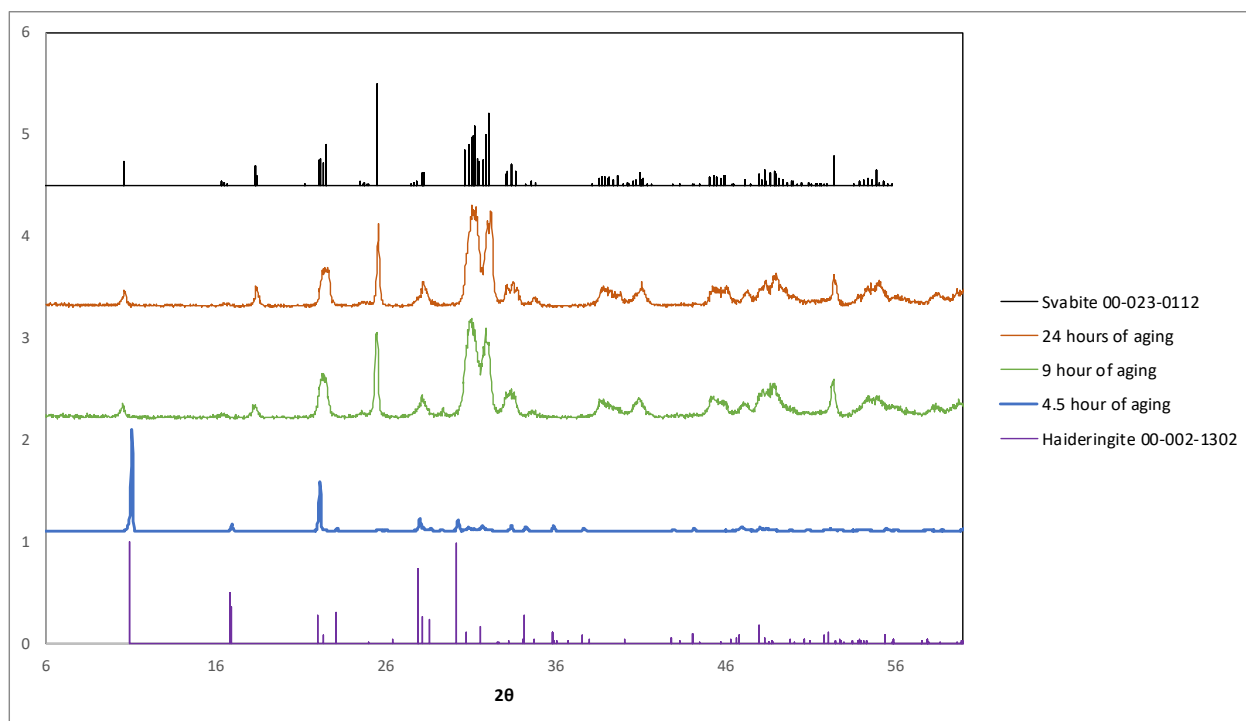
A range of temperatures have been used to precipitate apatites (refer to Tables 2.1 and 2.4). The only previous study on precipitation of svabite was performed at 70°C (63). The precipitation temperature has an impact on the formation of solids. For instance, a higher temperature will usually increase the speed of crystallization (16). Apatites tend to be less soluble at higher temperatures (75) (34), and a higher temperature usually results in greater precipitation yield (16). In addition to the tests done at 70°C and described above, neutralization tests (to pH 8) were done at 22°C and at 90°C for 90 min followed by aging at 70°C for 24 hours.

Figure 5-8 shows the XRD patterns of the solids produced by aging at 70°C after neutralization at different temperatures. The neutralization at 22°C (room temperature) followed by aging at 70°C did not yield svabite but a mixture of partially crystalline haideringite and CaF<sub>2</sub>. Raising the precipitation temperature to 90°C (followed by aging at 70°C) seems to give a more crystalline svabite product as evident by the sharper XRD peaks.



**Figure 5-8: XRD patterns of solids produced at different precipitation temperature by neutralization to pH 8 and aging at 70° C for 24 hours**

The above presented data on the effect of precipitation temperature on svabite formation corresponded to aging at 70°C for 24 hours. A test was done at 90°C involving only 4.5 hours of aging at 70°C. However, this aging time was not sufficient to produce svabite. Instead the phase formed was haideringite, as identified by XRD analysis (Figure 5-8). This result was unexpected as the results presented in Figure 5-5 showed the formation of svabite (albeit not fully crystalline) after 4 hours aging when precipitation was carried out at 70°C. It is postulated that at 90°C the intermediate that precipitates, i.e. haideringite due to its enhanced crystallinity and possible grain growth undergoes slower transformation to svabite negating otherwise the positive effect of elevated temperature. Further work is required to better understand the system. Aging 9 hours yielded svabite as identified by XRD.



**Figure 5-8: XRD pattern for solids precipitated at 90°C after varying aging times at 70°C**

### 5.1.5 Effect of Initial As Concentration on Svabite Formation

The process developed above (see flowchart in Figure 5-1) was demonstrated for an initial arsenic concentration of 0.15M, which is similar to the concentration of 0.167M used by Zhu et al. (63). At this concentration, it was determined that a neutralization to the pH range 7-9 is required to promote crystallization of svabite at 70°C. As concentration determines the supersaturation of the solution which is the driving force of the crystallization process (12) it was decided to perform a limited number of tests at different As(V) concentrations, namely at 0.05M, 0.15M (base), 0.20M, and 0.35M to determine their effect on svabite formation (Figure 5-9). Precipitation tests at pH 8 with initial concentrations of 0.05M and 0.20M were found to yield svabite, while an initial concentration of 0.35M did not. At an initial concentration of 0.35M there were visual observations of a precipitate to immediately forming, hypothesized to be CaF<sub>2</sub>. CaF<sub>2</sub> has been shown to form first in fluoroapatite precipitation (76) and as such can be assumed that interfered with the formation of svabite.

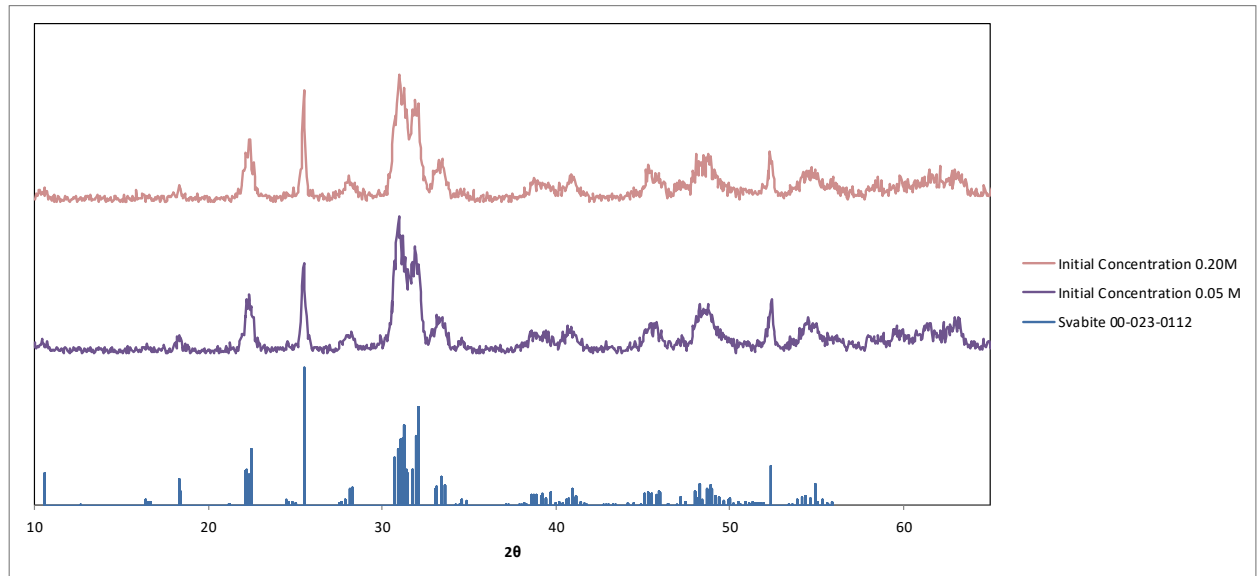


**Figure 5-9: XRD patterns for solids precipitated at different arsenic concentrations at pH 8, 70°C, aging for 24 hours**

In the meantime a repeat of the concentration tests at pH 6 gave the results reported in Figure 5-10. According to these results, lowering the arsenic concentration to 0.05M As and performing precipitation at pH 6/70°C and aging for 24 hours, yielded svabite. A similar trend has been reported for johnbaumite, which was observed to form at lower pH as the concentration was reduced (80). The same pH and temperature conditions at 0.15M and 0.35M of arsenic yielded haideringite as the final solid phase (as identified by XRD, see Figure 5-9). This seems to indicate that the pH range for the precipitation for svabite does shift with arsenic concentration. Since there is an initial solid forming immediately at higher concentration, it is possible that there is a maximum concentration for the precipitation, but this work has not confirmed this maximum. These results are in general agreement with crystallization theory that predicts at low supersaturation, i.e. low concentration, the formation of a stable (least soluble) compound is favored while at high supersaturation metastable compounds are favored (12). In the context of the present study compounds like  $\text{CaF}_2$  and haideringite are the metastable phases formed at high concentration, which subsequently slowly transform to final form of svabite as the pH and aging time increase.

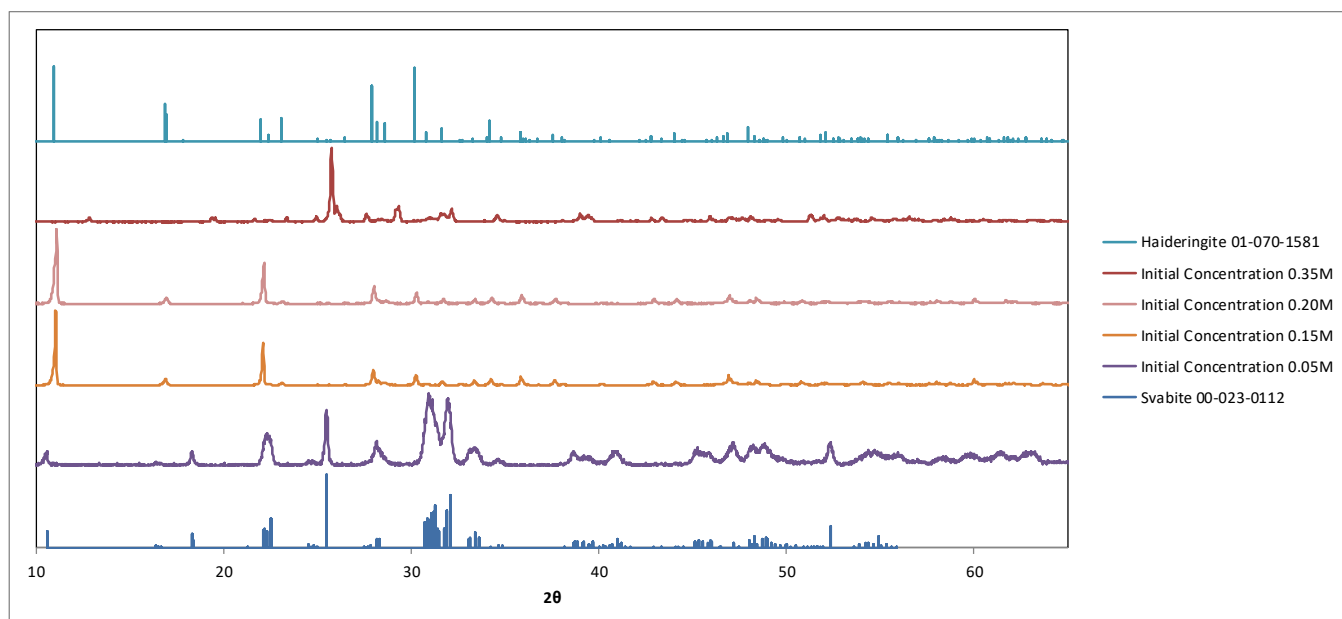


Figure 5-10: XRD patterns for solids precipitated at different arsenic concentrations at pH 6

#### 5.1.6 Effect of Timing of Fluoride Addition to the Solution

Although it is not discussed explicitly in the literature of aqueous precipitation of SVA and SVA/FAP compounds, the timing of the addition of fluoride may impact the phase formed. Too much fluoride has been found to hinder the formation of fluoroapatite (78) (76) due to the precipitation of  $\text{CaF}_2$  and the removal of calcium from solution and resultant change in the ratio of As:Ca in solution. Fulmer and Brown (76) found that  $\text{CaF}_2$  precipitated first before the apatite phase.

All the synthesis results presented so far were obtained using starting solutions in which fluoride (as a solution of NaF) was added after calcium and arsenate precursor chemicals had been dissolved into it. After that the acidic mixed solution was heated ( $70^\circ\text{C}$ ) and neutralized to pH 8 and aged for 24 hours yielding crystalline svabite. However, when the starting solution was prepared by dissolving first NaF and after adding the calcium and arsenate chemicals no svabite formed despite using the same otherwise process sequence: heating – neutralization – aging as in flowchart in Figure 5-1. The XRD pattern from this test is presented in Figure 5-11 along the XRD patterns of precipitates obtained from starting solution in which fluoride was added last (i.e. as per flowchart of Figure 5-1) or from a test in which fluoride was added after neutralization but before aging. As demonstrated by these patterns, the synthesis where the fluoride was added first did not yield svabite. In this case it appears that precipitation of some

intermediate took place that despite subsequent neutralization to pH 8 and aging did not convert to svabite—refer to discussion in sections 5.1.2 and 5.1.3. The XRD pattern for this synthesis (Figure 5-11) shows the formation of haideringite and potentially some  $\text{CaF}_2$ . The precipitation of  $\text{CaF}_2$  as observed with fluoroapatite studies fluoroapatite (78) (76) seems therefore to have impacted the molar ratio of Ca:As, impeding the formation of svabite. A synthesis with fluoride added after the neutralization, did form svabite. The sequence in this case was: preparation of Ca-As solution (0.15M As) – heating ( $70^\circ\text{C}$ ) – neutralization (to pH 8) – fluoride addition – aging. Comparing the XRD patterns (Figure 5-10), it seems the svabite obtained with the alternative method to be more crystalline as evident by the sharper peaks. Duplicate tests involving fluoride addition after neutralization confirmed the production of svabite as it can be verified with the XRD patterns presented in Appendix A.

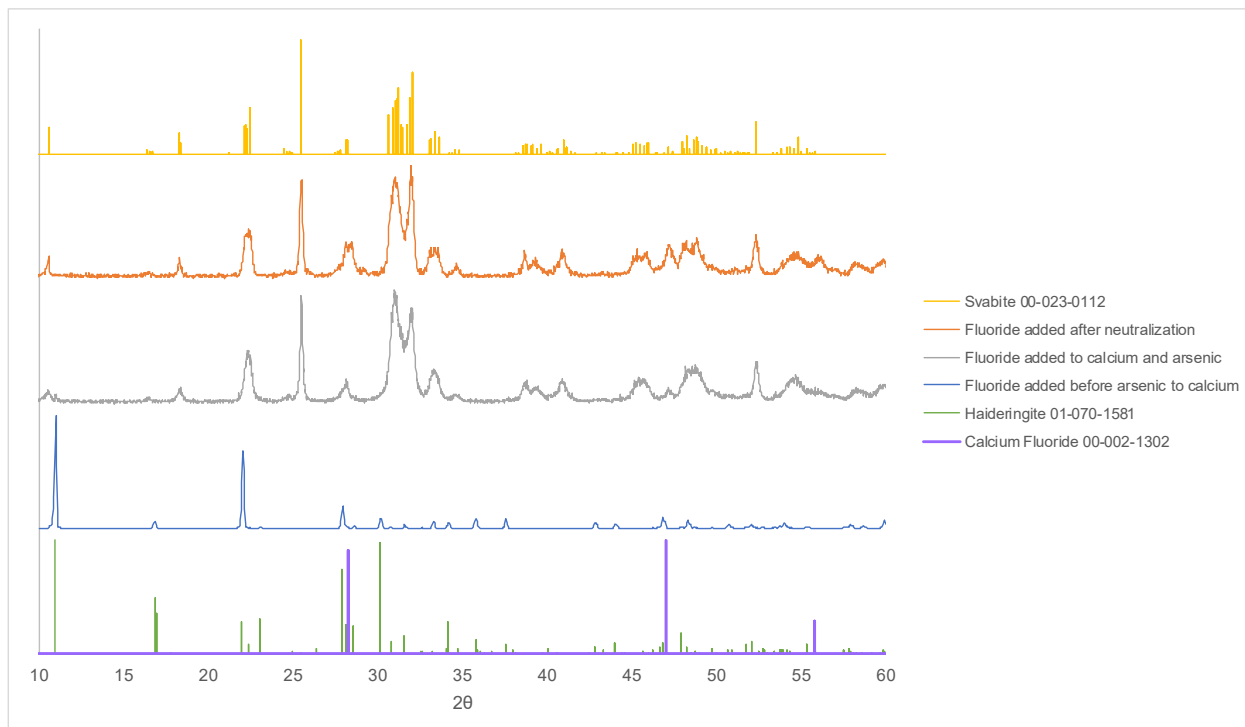
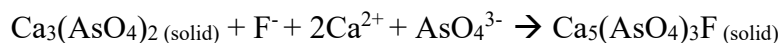


**Figure 5-11: XRD patterns of precipitated compounds obtained by varying timing of fluoride addition at pH 8/70°C/24 hr aging**

Interestingly, adding fluoride after neutralization and before aging yielded svabite even when neutralization was done at pH 6—refer to XRD patterns in Figure 5-12. By contrast the flowchart of Figure 5-1 in which fluoride is added to the Ca-As solution, i.e. prior to neutralization did not yield svabite but haideringite ( $\text{CaHAsO}_4$ , Ca:As=1.0)—refer to section 5.1.3. The absence of fluoride in solution during the neutralization avoids the formation of  $\text{CaF}_2$ , hence

by extension the stoichiometric Ca:As molar ratio (5:3=1.67) required for the precipitation of svabite is preserved. It is hypothesized that as such neutralization in the absence of fluoride most likely has led to an intermediate calcium arsenate phase with composition closer to that of svabite, for example:  $\text{Ca}_3(\text{AsO}_4)_2$  with Ca:As=1.5 (refer to Figure 2-1 in Chapter 2). Subsequently upon fluoride addition and aging the intermediate converts to svabite via  $\text{F}^-$  incorporation and reorganization. Such process may be represented by the following simple reaction:



Further research is necessary to substantiate-elucidate the underlying mechanism.

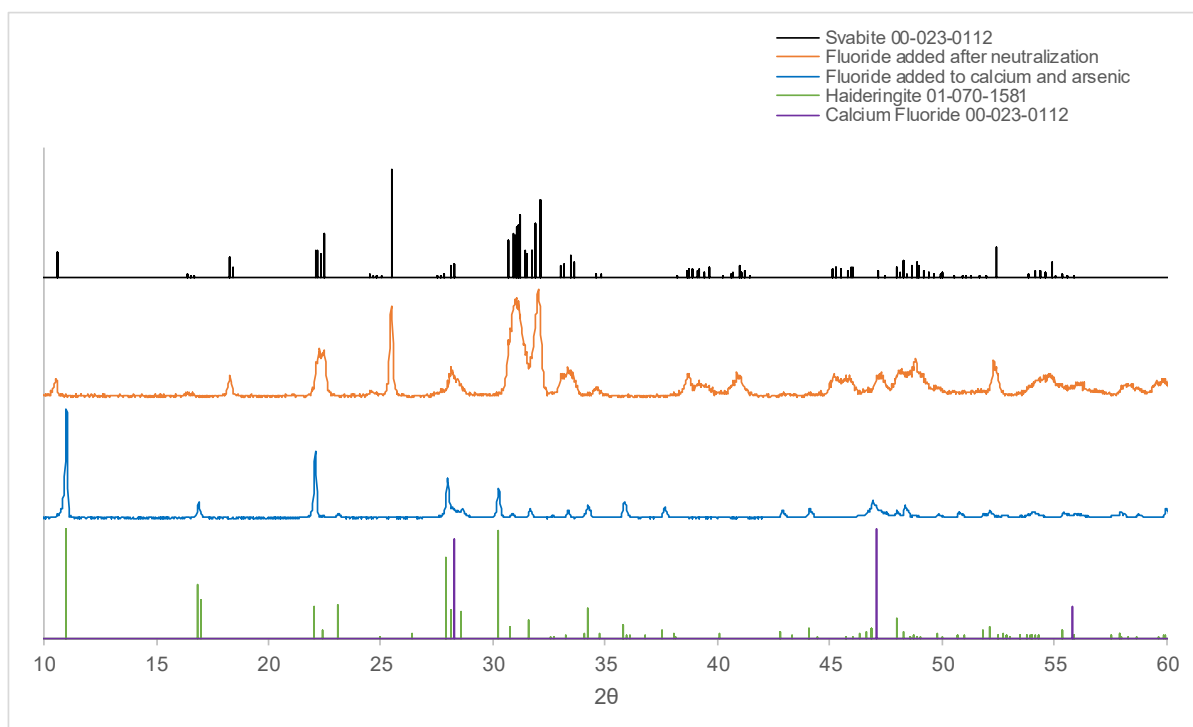


**Figure 5-12: XRD patterns of precipitated compounds obtained by varying timing of fluoride addition at pH 6**

The svabite solids formed using this alternative method were further characterized in terms of morphology (SEM images in Figure 5-13), specific surface area and chemical stoichiometry (Table 5.3). Both solids appear to be in the form of aggregated particles comprising primary needle-like crystallites, with the base case product seeming to be more compact than that of the alternative method. The difference in compactness between the two svabite products was confirmed by the BET surface area measurements. The base case product had a specific surface



area of 13 m<sup>2</sup>/g, while the solid formed using the alternative method had a surface area of 44 m<sup>2</sup>/g; i.e. the former is less porous than the latter. The surface area of the base case svabite was closer to the value 10.7 m<sup>2</sup>/g of fluoroapatite measured by Bengtsson et al. (74). Finally, both solids have Ca:As molar ratios close to the theoretical svabite stoichiometric ratio of 1.67.

In conclusion, other than the flowchart in Figure 5-1, it was determined that svabite can be produced by adding fluoride after neutralization; this very interesting result –not reported previously – opens an alternative process pathway to produce svabite from arsenate-containing solutions. However, much more work is required to optimize the whole svabite crystallization process.

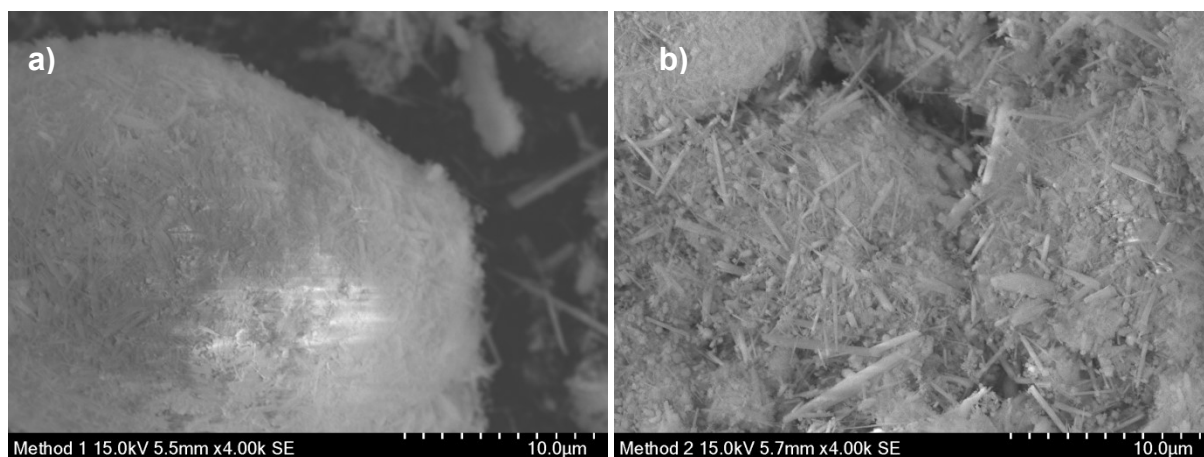


Figure 5-13: SEM images of svabite particles formed using different methods of fluoride addition: a) prior to neutralization (base case) and b) after neutralization (alternative case)

Table 5.1: Chemical composition and BET area of solids formed at pH 8/70°C/24-hr

Method	Arsenic (mmol)	Calcium (mmol)	Molar Ratio	BET (m <sup>2</sup> /g)
Base Case: Flowchart of Fig. 5.1	57	91	1.65	13
Alternative: F added after Neutralization	83	144	1.73	44

## 5.2 Synthesis of Mixed Fluoroapatite/Svabite

Analogous to the work at Montana Tech (40), which showed mixed phosphate/arsenate hydroxyapatites to be more stable than johnbaumite alone, the stabilization of svabite via incorporation of phosphate was investigated. The present work builds on the study by Zhu et al.

(64), who synthesized mixed arsenate/phosphate fluoroapatite compounds and studied the release of arsenic as function of the arsenate content (varied from 0 to 90% of the arsenate/phosphate total) of the mixed compounds. As mentioned earlier Zhu et al. did not report details on the synthesis of svabite or mixed arsenate-phosphate apatites, hence the need for revisiting this system. In the present work the same procedure developed for the synthesis of svabite as described with the flowchart of Figure 5-1 was used, with part of the arsenate substituted with phosphate. The total initial molar concentration of arsenate+phosphate used was kept constant at 0.15M. The percentage of arsenate (moles of arsenate relative to the moles of arsenate and phosphate) in the solution was varied from 0% (to form fluoroapatite) to 75%, with variations of arsenic content within this range. Fluoride was added last to avoid the complication of CaF<sub>2</sub> formation. The solution was heated at 70°C, neutralized with dropwise addition of 1M NaOH for 90 min to different pH from 5 to 9, and aged for 24 hours.

The XRD patterns of the resulting solids by neutralization and aging at pH 8 and 70°C are presented in Figure 5-14. Duplicate syntheses under these conditions are presented in Figures A.7-A.9 in Appendix A. The reference XRD patterns for svabite and fluoroapatite are also shown on the figure. As it can be seen there is a transition from fluoroapatite to svabite structures as the arsenate portion increased. At 15% and 25% As content the XRD patterns match that of fluoroapatite (absence of shoulder at 31-32°). At 75% As the XRD pattern resembles the svabite pattern. It is tentatively concluded that at low arsenate content, arsenate-substituted fluoroapatite solid solution forms (As-FAP; Ca<sub>5</sub>(PO<sub>4</sub>)<sub>3-x</sub>(AsO<sub>4</sub>)<sub>x</sub>F, x<50%) while at high arsenate content, phosphate-substituted svabite solid solution forms (P-SVA; Ca<sub>5</sub>(AsO<sub>4</sub>)<sub>3-x</sub>(PO<sub>4</sub>)<sub>x</sub>F, x>50%). At intermediate composition range (~50%) peaks for both fluoroapatite and svabite patterns are present hence it is uncertain whether truly solid solutions were formed or simply had a mixture of separately nucleated svabite and fluoroapatite microcrystallites, which assembled together into heterogeneous aggregates. Further detailed characterization work is required to clarify the true identity of this intermediate range mixed arsenate-phosphate product.

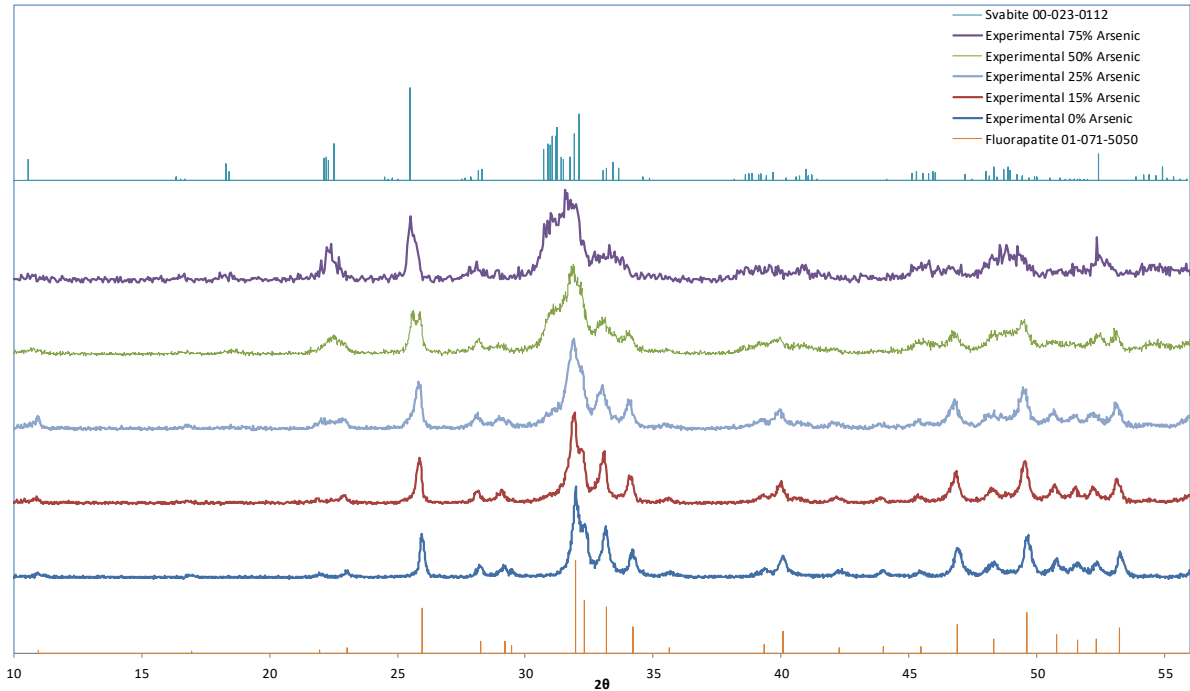


**Figure 5-14: XRD patterns of mixed arsenate-phosphate fluoroapatite solids formed with varying arsenate content**

Results from mixed phosphate/arsenate solid syntheses completed with different pH endpoints from 5 to 9 are presented in the Appendix (Figures A-10-A-12). A sample of the data corresponding to the 50% As system are shown in Figure 5.14. It is interesting that in all cases even at pH 5 (refer to Figures A-11 and A-12) mixed crystalline phases of svabite/fluoroapatite formed while in the absence of phosphate (section 5.2) svabite was observed to form only at  $\text{pH} \geq 7$  (refer to Figure 5-7). Carefully examining the XRD peaks at  $25\text{-}26^\circ$  and  $31\text{-}32^\circ$  where svabite and fluoroapatite exhibit differences it can be seen the apatite formed at pH to have clearly the FAP structure only. Svabite appears as minor structure judging from the peak at  $25\text{-}26^\circ$  and the shoulder at  $31\text{-}32^\circ$ . At higher pH 7-9 the broadening of the peaks at  $31\text{-}34^\circ$ , where svabite and fluoroapatite peaks overlap, points to co-existence of both phases or the formation of solid solutions with both host structures. Similar trends were observed with the 25% As-apatite (Figure A-10 in Appendix) but also the 75% As product (Figure A-12 in Appendix). Again more detailed characterization studies will be useful in future to further elucidate the crystal structure of these mixed arsenate-phosphate apatites. Nevertheless the formation of crystalline apatite structure at pH 5 when phosphate is present, it suggests that the fluoroapatite (phosphate-containing) apatite crystal structure that acts as host for partially substituted arsenate to have a

larger domain of stability than svabite (formed only at  $\text{pH} \geq 7$ ). This observation was confirmed with the solution analysis results reported in Figure 5-15 as well as the subsequent stability testing section.

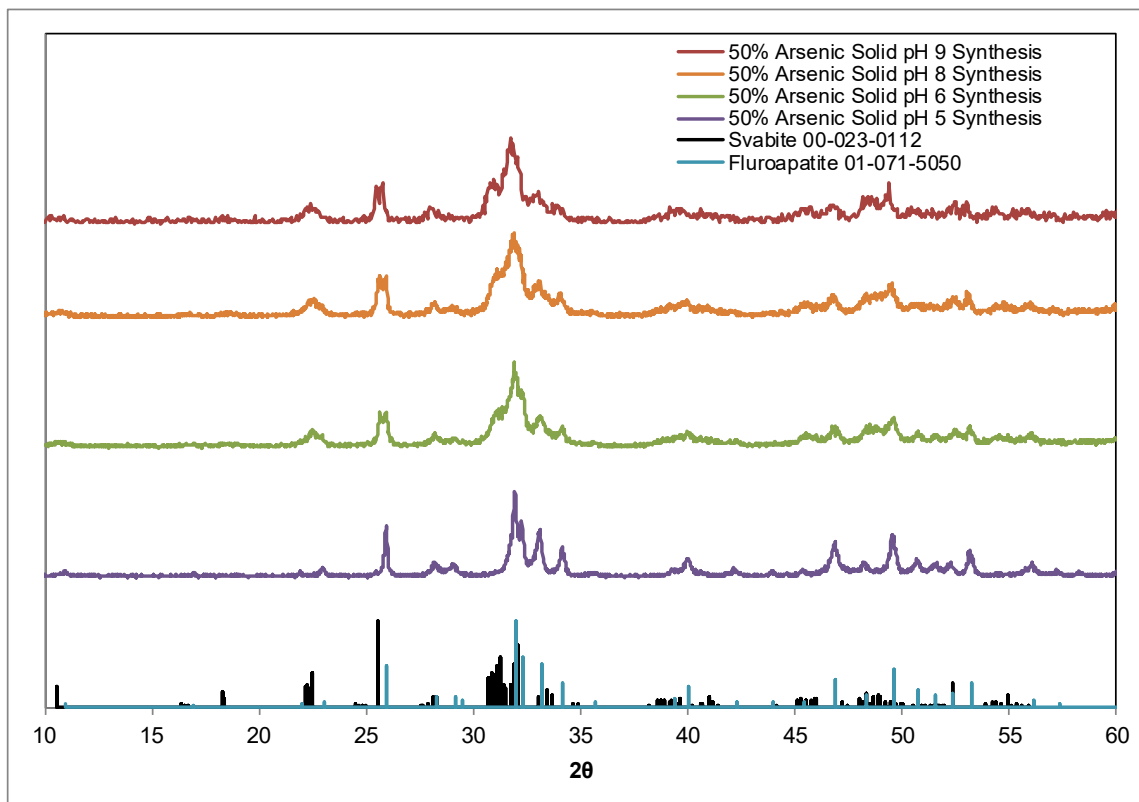


**Figure 5-15: XRD patterns of mixed arsenate-phosphate fluoroapatite solids formed with 50% arsenate content at different pH**

The evolution of calcium, fluoride, and As+P concentrations during aging at  $70^\circ\text{C}$  is presented in Figure 5-15. The solution calcium concentration tends to increase as the arsenic fraction decreases. The lowest calcium concentration is found in the 75% arsenate sample. The differences in calcium concentrations may be due to differences in solubility of different composition apatite solids being formed in the solution like-calcium-deficient apatites by incorporating Na (89). Further detailed characterization of the different phases as well estimation of solubilities using aqueous chemistry modeling software, such as PHREEQC (90), may aid in determining the solution chemistry during the precipitation and the corresponding crystal composition but time constraints did not allow for their application in this system.

No trend can be seen for F concentration with either time or arsenic content of the solution (Figure 5-16b). In general the F concentration was low around  $1 \pm 0.5$  mg/L pointing to nearly

100% incorporation in the precipitated apatite compound(s). The outlier point at 7.5 hours for the 25% As-apatite is suspected to be an experimental error. Unfortunately time constraints did not permit replicate tests to perform.

The sum of concentrations of arsenate and phosphate (As + P) were much lower than calcium, and much lower than the arsenate concentrations measured during svabite syntheses. This is attributed to a difference in stability between fluorapatite and svabite - the  $pK_{sp}$  of svabite has experimentally been shown to be 39 (63), while the  $pK_{sp}$  of fluorapatite is 59 (60). The difference in concentration magnitudes for the calcium and the arsenate could be due to the formation of calcium-deficient apatite compounds as mentioned earlier, with a Ca:As molar ratio less than 1.67 or possibly some poorly crystalline co-precipitated minor phases not detected by XRD.

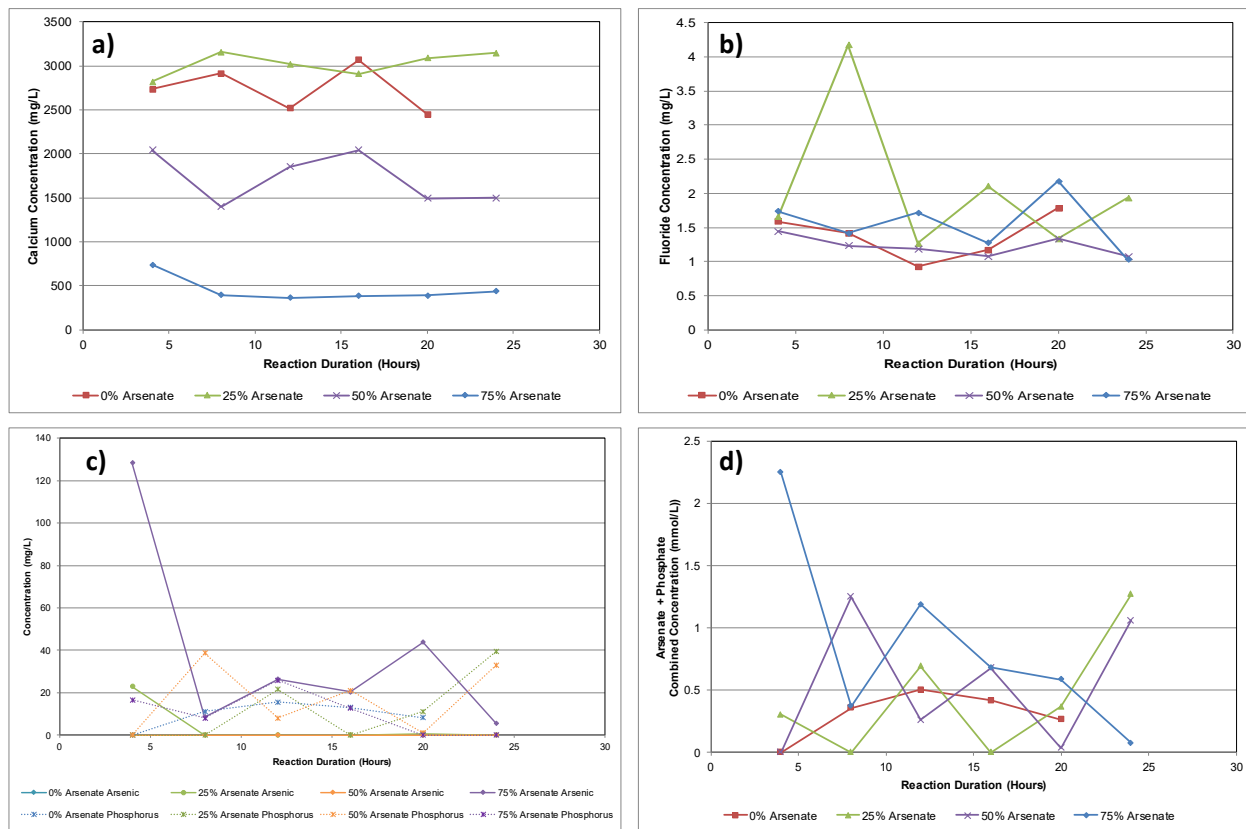


**Figure 5-16: Solution concentration profiles of Ca (a), F (b), and As/P (c), and As + P (d) during aging of arsenate-phosphate fluoroapatites with different arsenate content -at pH 8, 70°C, total initial [As+P] = 0.15M**

The produced mixed arsenate-phosphate apatite solids were submitted to SEM examination and surface area (BET) measurements. All solids formed were microcrystalline. The morphology

of arsenate-containing solids (Figure 5-17) differs from that of fluoroapatite but otherwise is similar to that of svabite (highly aggregated particles). It is interesting to note that the morphology of the fluoroapatite produced in this work (elongated crystals) differs from the tabular-like crystals precipitated by Zhu et al. (64), potentially due to the different method of neutralization employed here-refer to section 5.1 and the decreased aging time (1 day vs. 1 week).

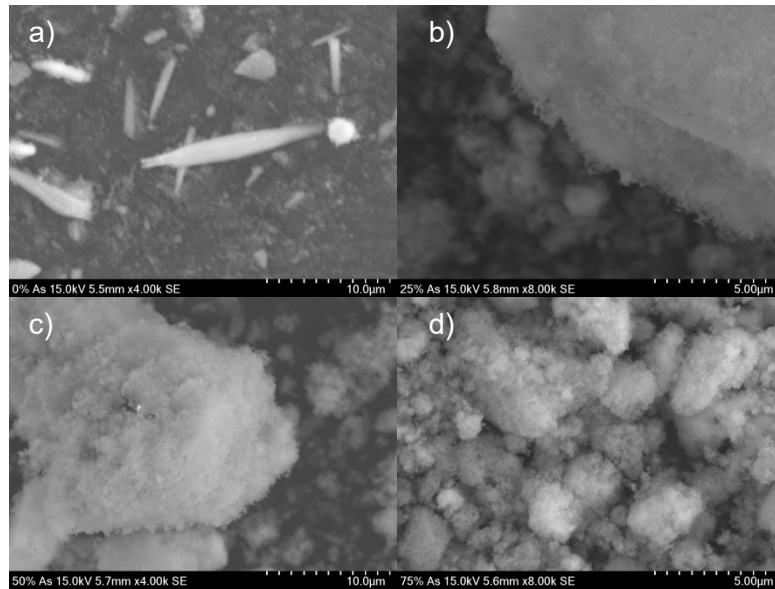


**Figure 5-17: SEM images of phosphate-arsenate solids with varying arsenate fraction: a) 0%, b) 25%, c) 50% and d) 75%.**

The different mixed apatite solids were found to have surface areas varying from 33 to 41  $\text{m}^2/\text{g}$  (BET results in Table 5.2). The specific surface area of the mixed solids formed with arsenic and phosphate is higher than the area of the pure svabite solids formed by the base case method (13  $\text{m}^2/\text{g}$ ), but approximately the same with that of svabite produced by adding the fluoride after neutralization (the alternative method) (44  $\text{m}^2/\text{g}$ )-refer to Table 4.3 in section 5.1.6. By comparison the surface area reported by Bengtsson et al. (74) for fluorapatite was 10.7 $\text{m}^2/\text{g}$  where fluorapatite was formed at a near-boiling temperature and was aged longer. It is tentatively concluded that the method of precipitation and presence of phosphate alters the nucleation-growth mechanism hence the observed differences. The differences in morphology and crystal sizes with increasing arsenate content has also been seen in other research with arsenate/phosphate apatite solid solutions (57) (64) and with fluoroapatite precipitation (75). It has also been shown that phosphate content impacts the rate of crystallization in the JBM/HAP

system, further impacting the morphology of the solids formed (49). Further research is required for a better understanding of the underlying crystallization phenomena.

**Table 5.2: BET surface area for mixed fluoroapatite solids with varying arsenic content**

Fluoroapatites with variable arsenic content	Surface Area
	m <sup>2</sup> /g
15%	33
25%	41
50%	48
100%	44

### 5.3 Stability Evaluation

Five different solids where XRD had identified apatite phases with varying arsenic content were selected for leachability testing to test the stability of the compounds. Four of the samples were mixed phosphate/arsenate solids (solid solutions or mixtures of fluoroapatite and svabite). The initial arsenate content of the samples was 15%, 25%, 50%, and 75%. Previous works involving hydroxyapatite (40) and fluoroapatite (65) have observed mixed arsenate-phosphate apatites to release less arsenic when equilibrated in water than arsenate-only compounds hence the selection of these samples for stability evaluation. The svabite product selected for stability evaluation was the one synthesized using the alternative method where fluoride was added after the neutralization. This product was chosen since it was hypothesized to be of better quality and was easier to synthesize: the XRD peaks from the synthesis were sharper, it allowed synthesis at a lower pH, lessening the chance of the formation of johnbaumite due to a lower pH, and it avoids residual CaF<sub>2</sub> in the product. Arsenic, calcium, and phosphorus concentrations were determined using ICP, while fluoride was measured using an ion-specific electrode.

#### 5.3.1 Effect of Washing

As mentioned in section 4.4, prior to stability evaluation, the selected samples were washed in multiple contacts with de-ionized water to remove any entrained soluble-or coprecipitated amorphous- material that could have given erroneous results as per previous established protocols (5; 28). This series of tests showed that the solids required 5 cycles of washing until the constituent concentrations and pH became constant. The concentrations of released species after each wash cycle are presented in Figure 5-18.

The pH of the final wash solution ranged from pH 8.8 (the 15% arsenic sample) to pH 9.0 (the 100% arsenic-svabite sample). A similar trend in increasing pH upon contact of svabite with water of different pH was observed by Kucharski et al. (58)-refer to Table 2.3 in Chapter 2.

The stabilized concentrations of arsenic ranged from 5.17 mg/L (15% arsenic) to 13.3 mg/L (svabite). Arsenic release into solution increased with increasing arsenic content, with the exception of the 25% and 50% samples, which are reversed for the majority of the cycles. With each wash cycle, the spread of concentrations of the samples decreased. After the first wash, arsenic concentrations ranged from 12.7 mg/L (15% arsenic) to 124 mg/L (svabite).

Calcium concentrations after the final wash cycle ranged from 5.9 mg/L (15% arsenic) to 19.6 mg/L (svabite) and increased with increased arsenic content. Phosphate concentrations after the final wash cycle range from 0.034 mg/L as P (15% arsenic) to 0.78 mg/L as P (75% arsenic). Concentrations were much lower than the concentrations of arsenic or calcium. This behaviour is consistent with the earlier observation made in section 5.2 that the fluoroapatite (100% phosphate) is more stable than svabite (100% arsenate) judging from their published  $pK_{sp}$  solubility product constants: the  $pK_{sp}$  of svabite = 39 (63) vs.  $pK_{sp}$  of fluorapatite = 59 (60).

No clear trend with increasing arsenic fractions was seen during the last four wash cycles, although there is certain data scattering due to apparent analytical error given the low concentration range.

Theoretically,  $Ca_5(AsO_4)_x(PO_4)_{3-x}F$  apatite solids have a Calcium:[Arsenate+Phosphate] molar ratio of 1.67. Analysis of the wash waters showed a gradually increasing Ca/[As+P] ratio with progressing washing from anywhere between 0.9-2.3 to 1.7-2.7. The biggest increase was shown by svabite (from 0.9 to 2.7). By far the 25% arsenic and 75% arsenic samples gave the closest to stoichiometry (1.67) molar ratio, namely from 1.4 to ~1.7. The 50% arsenic and 15% arsenic samples appeared to be reaching a ratio of 2.2 and 2.1 respectively at the end of the fifth washing cycle. The contrasting difference in molar ratio change between svabite and the arsenate-substituted fluoroapatite samples could be due to inherent differences in stability between svabite and fluorapatite that was already mentioned above.



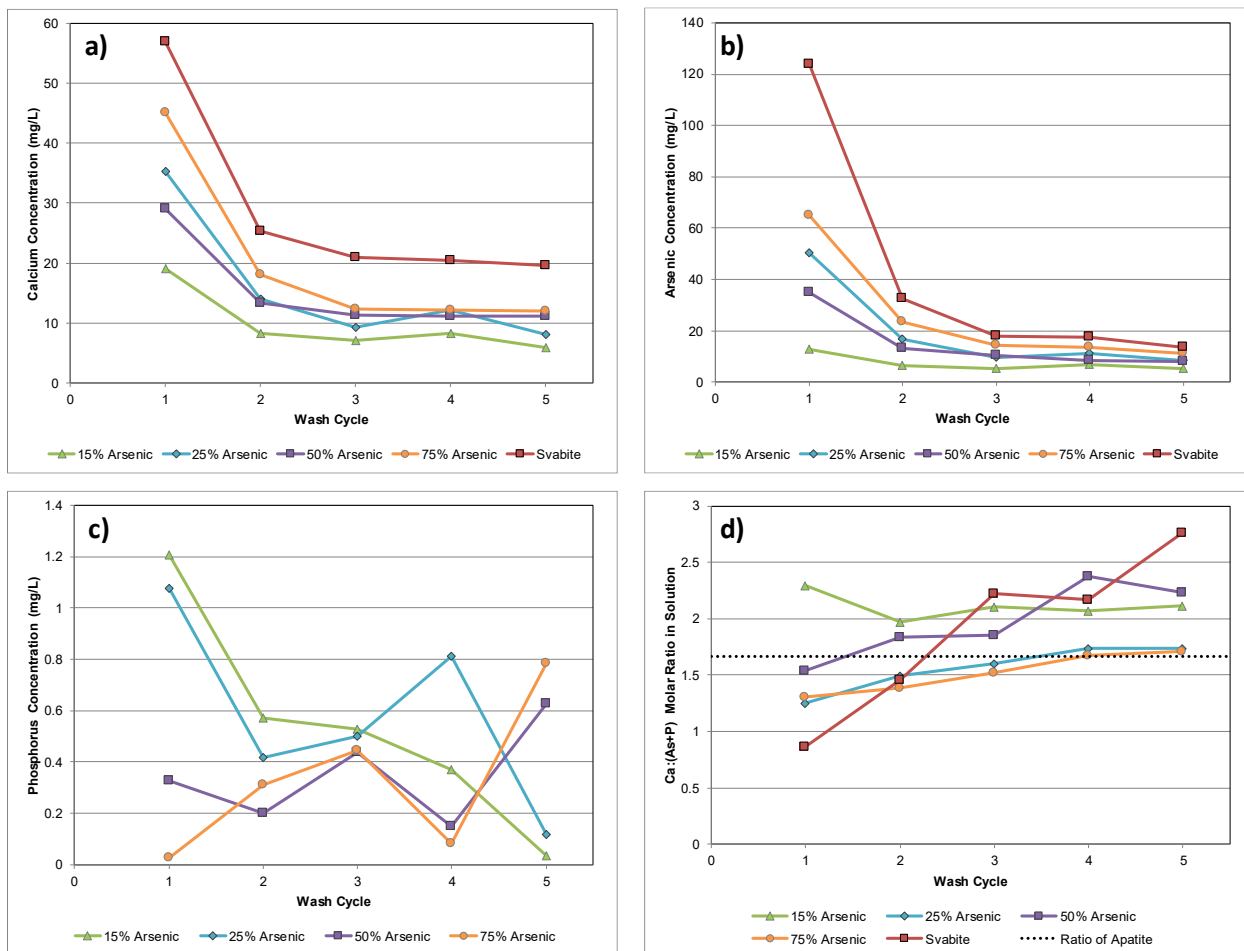


**Figure 5-18: Evolution of concentrations of constituent elements and molar ratio of Ca: [P+As] during successive washing cycles**

### 5.3.2 Stability at pH 9

Previous studies of the stability of calcium apatites - refer to Chapter 2 - have shown that stability increases with pH ( (54), (47), (40), (63)). The stability of the synthesized apatite samples was tested at pH 9 to establish the minimum concentration that will be released by the solids, and to determine the solids' potential as arsenic fixation media.

The initial leachability tests lasting three days at pH 9 and room temperature (22°C) showed a steady increase in arsenic, phosphorus and calcium concentrations (data presented in Figure 5-19). Fluoride concentrations (Figure 5-19(d)) remained relatively constant after the first 1.5 days at a rather low level varying from 0.2 to 0.8 mg/L with increasing arsenic content. Phosphorus (Figure 5-19(c)) stabilized at very low level (<0.1 mg/L) for all phosphate-containing samples

independent of arsenate content. Calcium concentrations (Figure 5-19(a)) were higher initially gradually decreasing after 1 day or so towards quasi-stable level. Like with fluoride the highest calcium was released by the svabite sample. It is interesting to comment here on the initial rapid increase in concentrations of Ca, P, and F and the following decrease and stabilization at lower level. Similar behaviour has been observed by other investigators studying the dissolution of fluoroapatite. It is hypothesized this to be due to small crystals dissolving and then re-precipitating/re-crystallizing into bigger ones with lower solubility (47) (14).

In contrast to the rising and subsequently decreasing and stabilizing profiles seen with Ca, P, and F, the arsenic release shows a steady increase with time for all phosphate/arsenate samples except the one with the lowest %As content (15%As). This may suggest that there was a svabite component in all samples (except the 15%As one) that was not fully crystallized and its dissolution and recrystallization is rather slow, resulting in a continued arsenic release. In other words, a solid solution has not been achieved in the mixed arsenate/phosphate apatite samples. Alternatively, the mixed arsenate/phosphate particles may not be homogeneous in composition and rather have arsenic-rich surface zones, resulting in the preferential release of arsenic. Clarification of this point will require additional detailed characterizations that go beyond the scope of this time-limited study.

None of the samples stabilised to a steady concentration, indicating that equilibrium was not reached.

Arsenic concentrations in solution did not trend with the arsenic content in the solids. It was hypothesized a smaller ratio of arsenate:phosphate would lead to lower concentrations in solution, as was seen with previous works (40) (64) (54). The same trend was not observed in this series of preliminary stability tests. Release of arsenic ranged from 16.4 mg/L to 23 mg/L with the former corresponding to the 15% arsenate apatite sample and the latter to 100% arsenate sample, i.e. svabite.

The released arsenic from the svabite sample (23 mg/L) was greater than the arsenic released during the experiments conducted by Kucharski et al. (total arsenic concentrations reached 5.5 mg/L at pH 9.47 for synthesised svabite), but was less than the arsenic released by the aqueously precipitated/aged svabite studied by Zhu et al. (64) (arsenic concentration ~70 mg/L at pH 9/25°C). Xu et al. (65) further found the release arsenic at pH 9 to decrease with decreasing arsenate content in the mixed apatite samples varying from 4.8 mg/L (sample with

9%As content) to ~30 mg/L (with 50% As content) and to ~65 mg/L (for 90%As content)-refer to Table 2-3. The observed differences between the present data and the concentrations reported by Xu et al. (the only other group that studied the stability of mixed FAP/SVA solids) may well reflect differences in crystallinity and/or purity of synthesized compounds or the attainment (in the case Xu et al.) and non-attainment (present work) of equilibrium (3 days equilibration this work vs. 125 days in Zhu’s work).

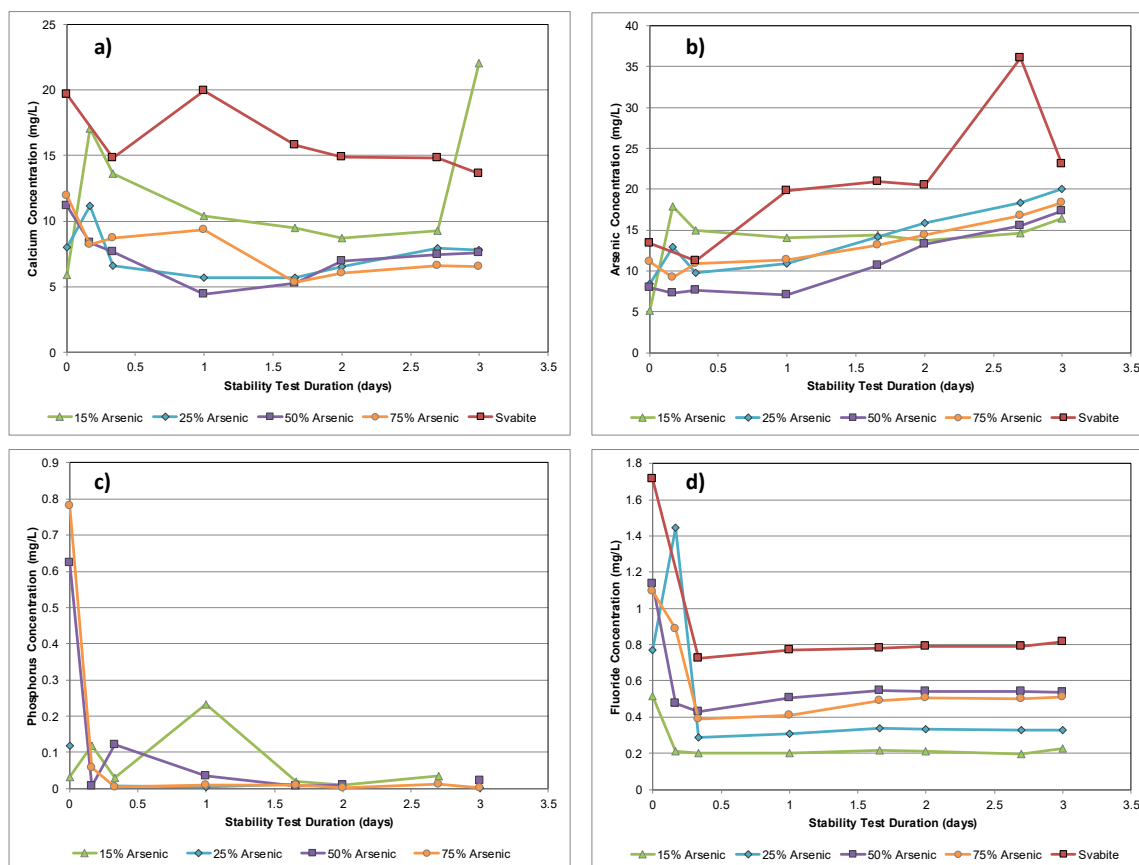


**Figure 5-19: Stability testing of svabite and arsenate-substituted fluoroapatite samples: Ca(a), As(b), P(c), and F(d) release at pH 9**

The molar ratios in solution during the stability tests at pH 9 are presented in Figure 5-20. All samples had a ratio that decreased throughout the stability test<sup>1</sup> tending to stabilize around 1 after two days. All the samples had a ratio much lower than the molar ratio of calcium apatites of 1.67. The low ratios could be explained by the observed preferential release of arsenic (Figure 5-

<sup>1</sup> The ratio for the 15% arsenic sample spiked on the third day of the stability test to 2.5 that was taken to be an outlier due to experimental error and not included with the other data.

19 (b)) possibly arising from the presence of arsenic-rich surface layer on the particles. Further leachability tests that will include replicate measurements are required in association with detailed characterizations to fully clarify the true underlying dissolution mechanism.

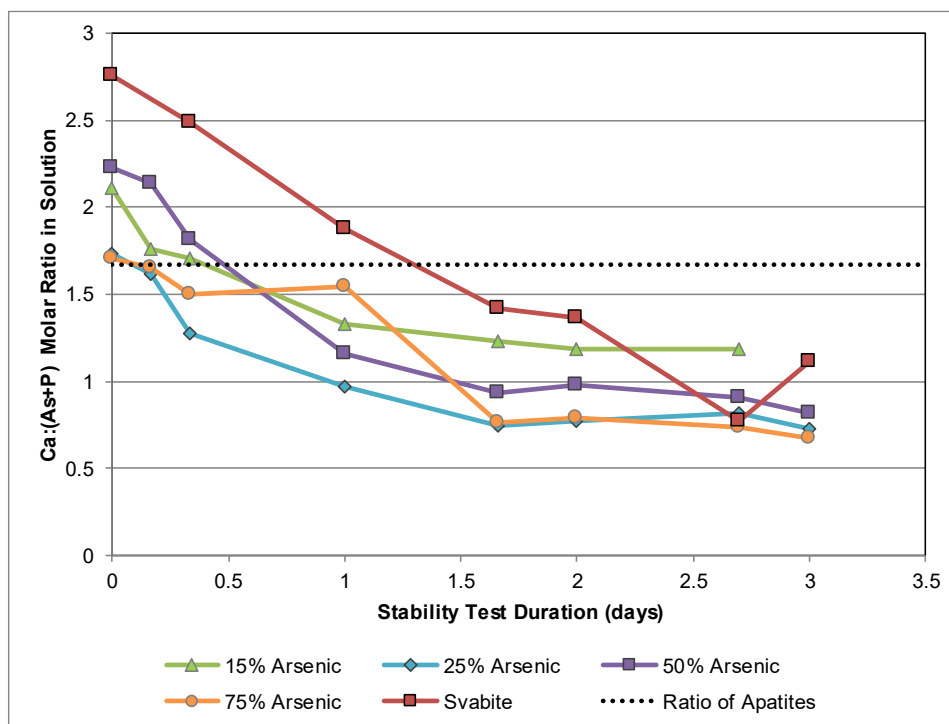


Figure 5-20: Molar ratio of Ca:(P+As) concentrations during stability tests at pH 9

### 5.3.3 Stability Evaluation Without pH Control

The pH of the solution in the series of stability tests presented in the previous section was controlled at pH 9 by addition of base (refer to methodology in section 4.4). Each sample showed a decreasing pH trend. This may indicate that the optimal equilibrium pH for the solids tested is lower than pH 9. A potential mechanism to explain this tendency is the exchange of fluoride ions on the surface of the solids for hydroxide ions, releasing hydrogen and decreasing the pH as per following reaction:



The pH drift during this extended equilibration period is presented in Figure 5-21. The pH for all samples dropped, reaching a range of 8.3 (for svabite) to 8.7 (for the 15% arsenate sample). The final pH of the solutions varied according to arsenate content. Due to the short duration of the test, it is possible that the pH of each solution had not stabilised completely and

would continue dropping over time. The observed pH drift direction agrees with the work of Zhu et al. (63) but differs from that reported by Kucharski et al. (58) where all solutions reached a final pH greater than 9.5 (even for solutions with an initial pH less than 9) (refer to Table 2.3). The apparent discrepancy with the work of Kucharski et al. may be due to the difference in sample purity. It is suspected that Kucharski's samples contained residual CaO (a strong base) as this reagent had been used in their synthesis hence the increase in pH.

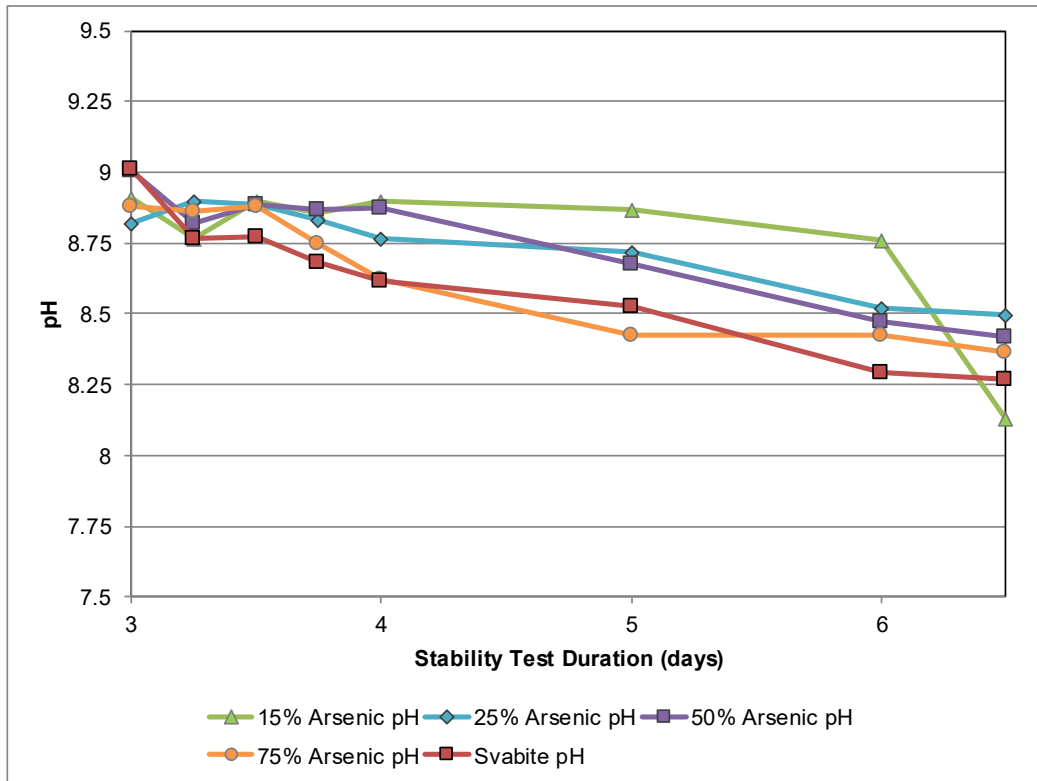


Figure 5-21: pH drift during the uncontrolled equilibration tests

Concentration vs. time data are presented in Figure 5-22. The concentrations (arsenic, calcium, and fluoride) initially spiked after the pH was no longer controlled. The magnitude of the increase in arsenic concentration ranged from 10 to 20 mg/L. After the initial response to the lack of pH control, which lasted for only one day, the concentrations dropped over the next three days. The final concentrations ranged from 15 mg/L arsenic (with the solid made up of 15% arsenic), to 25 mg/L arsenic in solution (for svabite).

For the solid with 100% arsenic, the arsenic concentration released from the svabite sample was greater than the concentrations reported by Kucharski et al. (~5 mg/L), and less than the

value reported by Zhu et al. (63) (after 120 days they had approximately 62 mg/L arsenic; see Table 2.3) under similar conditions (pH~8.5).

For the mixed arsenate-phosphate apatite samples the 15 mg/L As concentration recorded after 3 days with the 15% As sample is between the values 4.8 mg/L (sample with 9%As content) and 22 mg/L As (sample with 20%As) of Xu et al. (65)-see Table 2.3. The 50% As sample released around 35 mg/L As, close to the value of ~30 mg/L reported by Zhu et al. for their 50% As sample (Table 2.3). The decreasing concentration trend seen during this period (Figure 5-19), indicates that the systems had not reached equilibrium while Zhu et al. used 120 days of equilibration. Therefore it may be tentatively concluded that svabite and mixed arsenate-phosphate apatite compounds synthesized in the present work are at least as stable, if not more stable, than the equivalent compounds synthesized by Zhu et al. even if only one day aging was employed instead one week by the other group.

It is interesting to comment on the initial spike of concentrations of Ca, As, and F before starting decreasing. It is noted this spike to be associated with the drop in pH (Figure 5-21). As Zhu et al. (63) discussed, the dissolution of svabite proceeds with the sorption of protons on the surface and concomitant release of  $\text{Ca}^{2+}$ ,  $\text{AsO}_4^{3-}$ , and  $\text{F}^-$ . Phosphate ( $\text{PO}_4^{3-}$ ) release is almost nil (the data point at 3.5 days-Figure 5.22(c) is most likely in error as it does not match any other trends in other samples nor the other elements in solution) reflecting the higher stability of fluorapatite crystal structure that was previously mentioned. With the build-up of Ca, As, and F as pH decreases, re-crystallization leading to their incorporation into the solid seems to take place. Zhu et al. also hypothesized that cations (such as calcium) return to sorb to the surface of the solid after being in solution – which would mean that the concentrations would decrease. Calcium and arsenate dissolution trend differently with increasing arsenic content – where arsenate solubility increases with arsenate content (also seen in other group’s research in johnbaumite/hydroxyapatite systems (64) (49) (54)), and the calcium solubility does not.

Other than considering the concentration of released arsenic in solution that has to meet environmental standards, another issue from the standpoint of long term storage for arsenic, is the relative amount of arsenic contained in mass of disposed solids. In the “15% arsenic”<sup>2</sup> solids,

---

<sup>2</sup> The “15% As” in the labeling of the sample refers to 15% on molar basis of P+As of the mixed calcium arsenate-substituted fluoroapatite.

the material contains 6.4 wt.% of arsenic on mass basis. Svabite contains a fraction greater by a factor of 5, with 35 wt.% of arsenic. Svabite can accommodate a larger quantity of arsenic per mass unit while the arsenate-substituted fluoroapatite is more stable. Further work is required to evaluate quantitatively the relative stability of the different compounds that will include replicate tests at longer equilibration times.

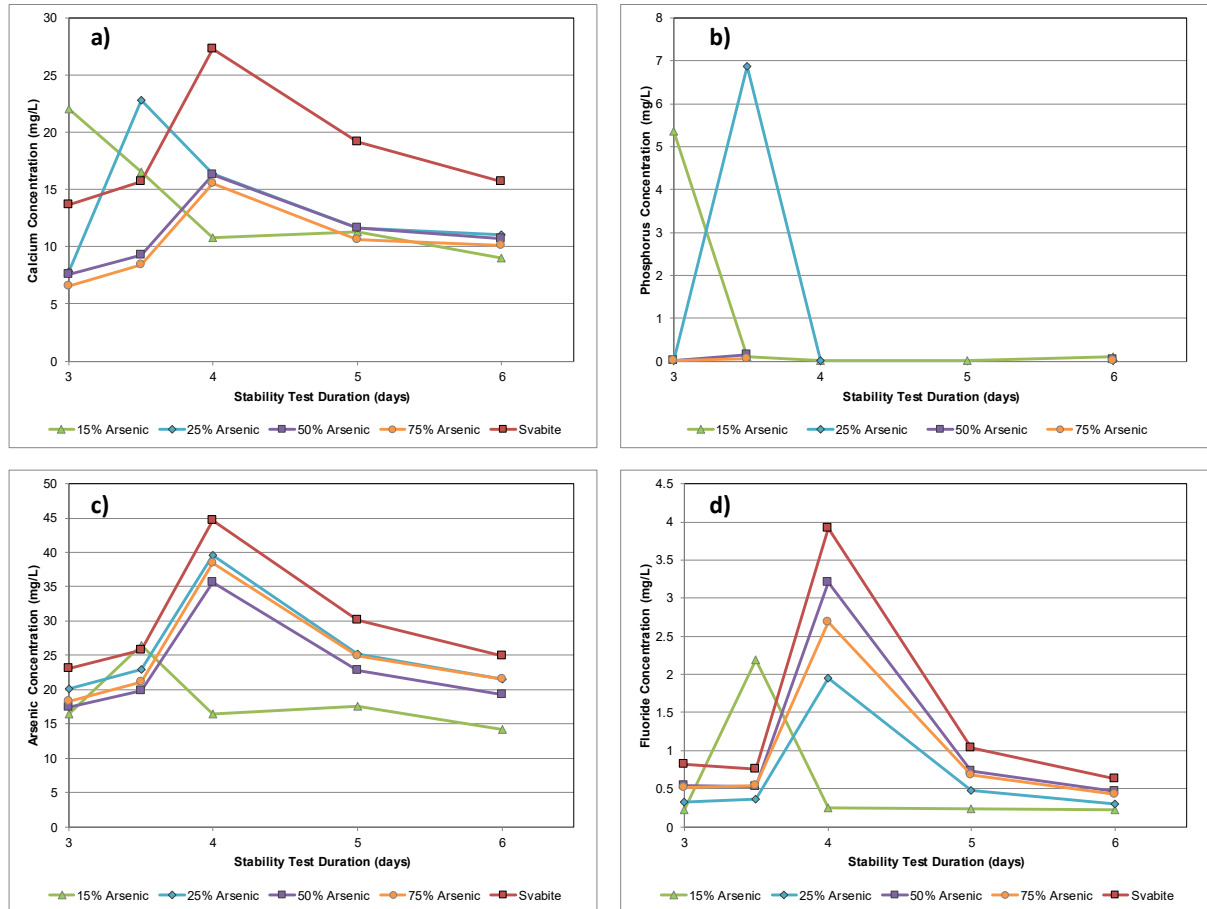


**Figure 5-22: Stability testing of svabite and arsenate-substituted fluoroapatite samples: Ca(a), As(b), P(c), and F(d) release during pH drift period**

The molar ratios of calcium to phosphate and arsenate are presented in Figure 5-23. There is no correlation between the ratios and arsenic or calcium release. The ratios also show that the solutions did not reach equilibrium during this test, but were changing at a slower rate than in the constant pH 9 tests. The ratios are still lower than the apatite molar ratios, and could be explained by the formation of a calcium-rich surface layer on the solids, if not due to experimental error. Further tests are required to determine whether the solids would dissolve

congruously, as the solutions during the uncontrolled stability tests were not changed after the stability tests at pH 9, and already contained some dissolved constituents.

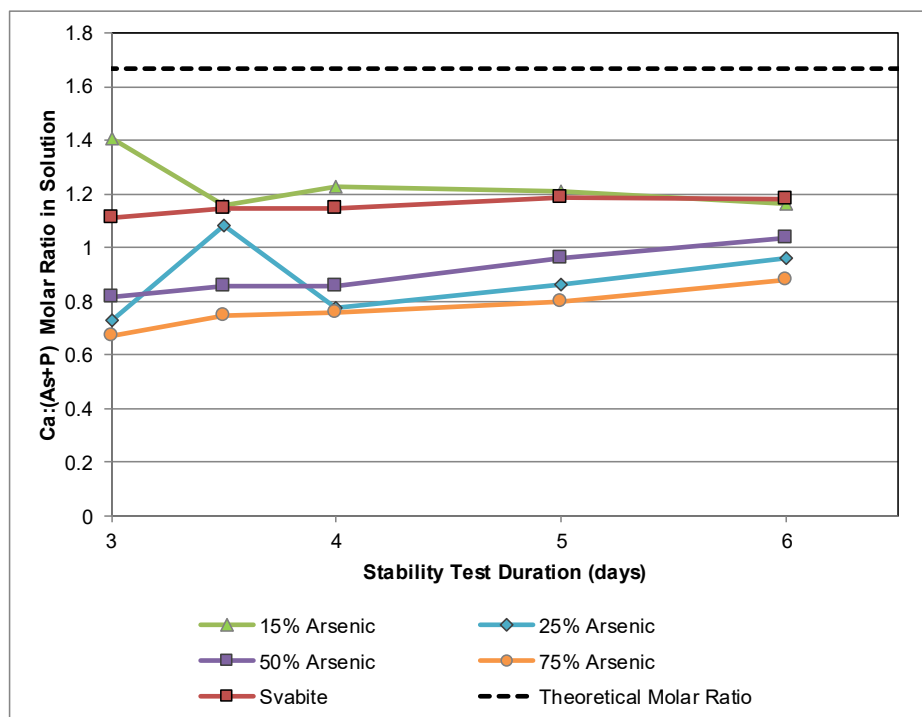


Figure 5-23: Solution molar ratios of Ca: (As+P) evolution during pH drift stability tests

### 5.3.4 Stability Evaluation in the Presence of Carbonate in Solution

As discussed in Chapter 2, calcium arsenates are vulnerable to destabilization by reaction with dissolved atmospheric CO<sub>2</sub>, leading to calcium carbonate formation and the release of arsenate into solution. Twidwell et al. (40) found that mixed arsenate-phosphate of hydroxyapatite composition are considerably more resistant to such destabilization than simple calcium arsenates. These investigators reported that mixed arsenate (johnbaumatite-JBM)-phosphate (hydroxyapatite-HAP) compounds with ratio of PO<sub>4</sub>:AsO<sub>4</sub> >5 to be stable in the presence of CO<sub>2</sub>; this PO<sub>4</sub>:AsO<sub>4</sub> ratio is equivalent to a maximum of 17% arsenate content, hence the inclusion in the present stability study of a 15% arsenate SVA-FAP sample. In order to evaluate the stability of the fluoro-calcium arsenate/phosphate solids when exposed to atmospheric CO<sub>2</sub> of carbonate-saturated waters, NaHCO<sub>3</sub> was added to each of the stability series flasks at the end of the 3-day pH drifting period, i.e. end of day 6. The use of NaHCO<sub>3</sub> as opposed to sparged CO<sub>2</sub> was selected as a means of accelerating any likely reaction for quickly detecting the reaction products given the time limitations the present study was confronted with. The addition of NaHCO<sub>3</sub> had a great impact on the solution composition and pH profiles. The



pH of the solution, as illustrated in Figure 5-24, initially dropped slightly, but then increased to reach a quasi-stable range of 8.2 to 8.5. The pH did not correlate to initial arsenic content, or to the final recorded calcium concentration. Despite the relatively slight pH alteration caused by the addition of  $\text{NaHCO}_3$  there was significant release of apatite constituents, in particular arsenate, pointing to a reaction with the introduced carbonate anions.

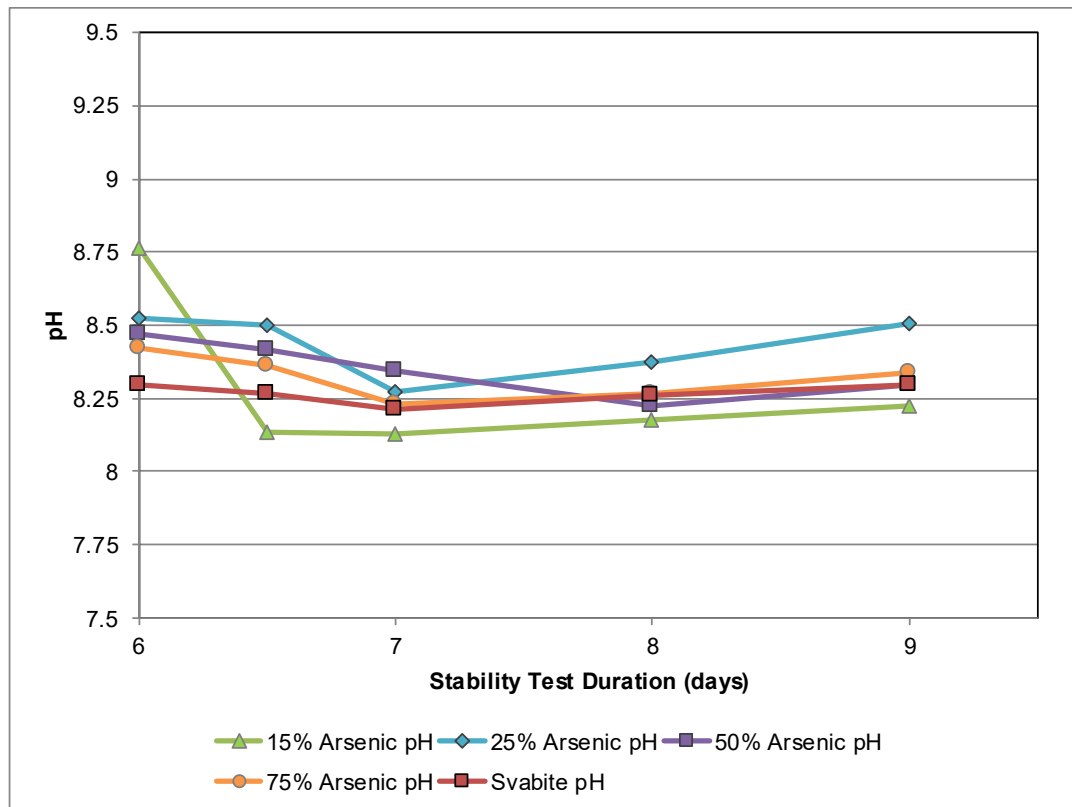


Figure 5-24: pH evolution after addition of  $\text{NaHCO}_3$

Figure 5-25 presents the release of arsenic, calcium, phosphate, and fluoride in solution as result of reaction with  $\text{NaHCO}_3$ . Arsenic concentrations immediately increased after the addition of the carbonate salt (Figure 5-25(b)). Concentrations went from 15-25 mg/L of arsenic to a range of 750 mg/L to almost 2,000 mg/L. Concentrations continued to increase until the end of the tests. Final concentrations did not correlate with initial arsenic content. Nor did they correlate to the arsenic concentrations at the end of the other tests. Of all the samples tested, the svabite sample yielded the lowest concentration in solution, followed by the 25% arsenic sample, with the 50% arsenic sample dissociating the most. This could potentially be due to varying degrees of heterogeneity within each sample. Irrespective of the origin of this variability, the data clearly

demonstrate the fluoro-calcium arsenate/phosphate solids to be vulnerable to aggressive carbonate attack.

The release of phosphate paralleled that of arsenate but it was 3 orders of magnitude lower indicating that the phosphate structure is more stable than the arsenate structure, apparently having different bond strength in these solids. Fluoride (Figure 5-25(d)) was also released initially but tended to plateau after day 8. Similarly calcium concentration seemed to stabilize after an initial spike (Figure 5-25(a)). Final Ca concentrations did not correlate to initial arsenic content.

Due to time and material constraints, no duplicates were run, and the final solids after the stability tests were not analysed to identify the formation of  $\text{CaCO}_3$ .

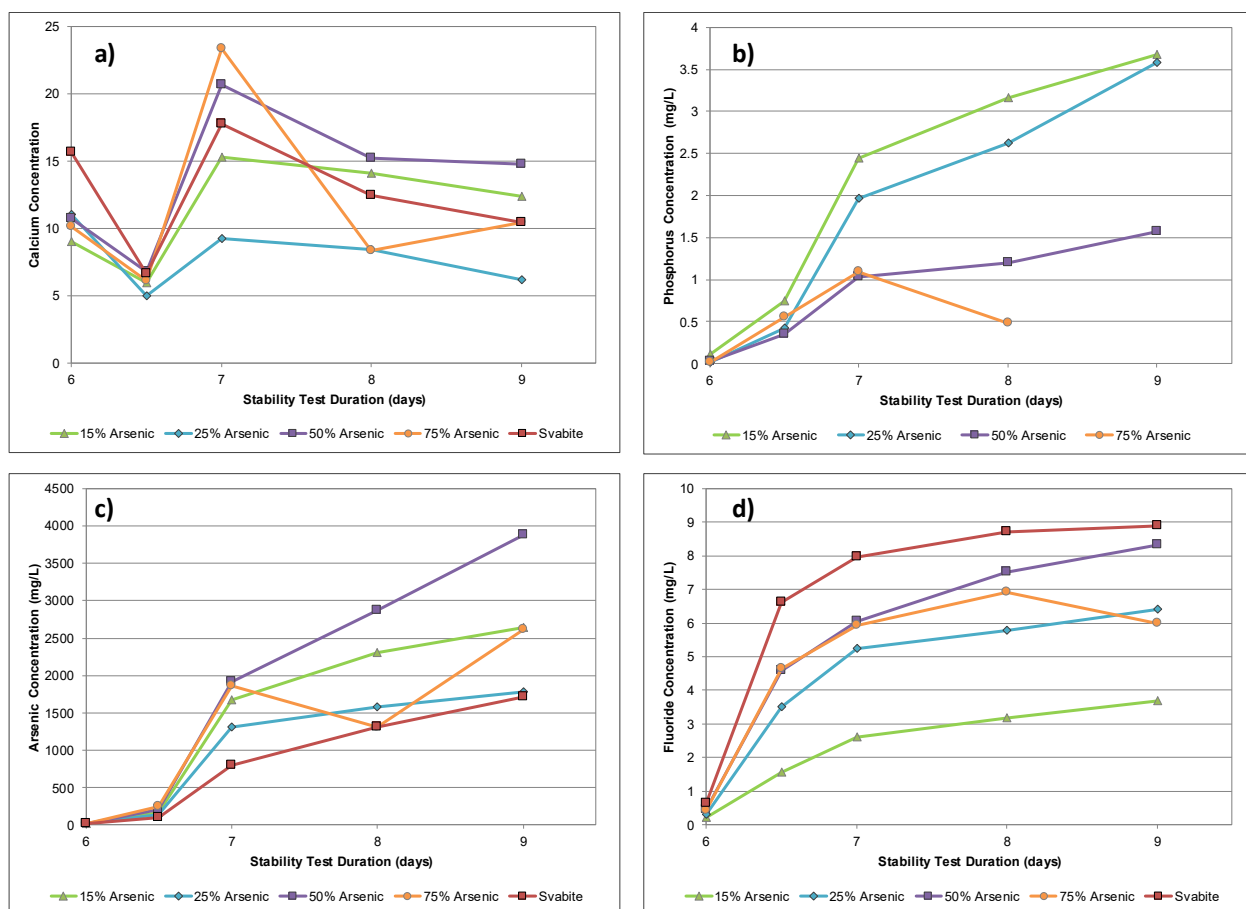


Figure 5-25: Stability testing of svabite and arsenate-substituted fluoroapatite samples: Ca(a), As(b), P(c), and F(d) release after addition of  $\text{NaHCO}_3$

### 5.3.5 Comparison of Stability Data

As per the work of Twidwell et al. (40) with arsenate-substituted hydroxyapatite solids, there was a hypothesis that the arsenate content of the arsenate-substituted fluoroapatite solids prepared in this work would have an impact on the stability and subsequent arsenic release from the solids. Increased arsenate content was expected to result in increased arsenic release due to larger distortion of the fluoroapatite host structure (33). This trend was only in part observed. As seen in Table 5.3, the 15% arsenic and the svabite samples had the minimum and maximum concentrations of arsenic respectively for the stability tests prior to  $\text{NaHCO}_3$  addition. The other three samples had concentrations that were very similar, and no continuous trend can be established between stability and arsenic content between 25% and 75% for the tests prior to addition of  $\text{NaHCO}_3$ .

This discontinuous trend could be due to multiple factors. It is possible that not all solids were synthesised to the same degree of crystallinity or purity. To reduce this error and uncertainty further tests are required, preferably with duplicate samples.

Another potential reason for this discontinuity is if a solid solution of fluoroapatite and svabite was formed, it is possible that certain ratios of arsenate to phosphate form an immiscibility zone, where the two compounds are present as heterogeneous pockets of each compound. Since the sample with 100% arsenate dissolved the most, it follows that if there are “pockets” of compounds with no phosphate, that these would release more arsenic. Further tests are necessary to fully characterize the stability of svabite/fluoroapatite solid solutions (mixed arsenate/phosphate compounds).

Since fluoroapatite is more stable than hydroxyapatite (60), it was hypothesized that svabite would be more stable than johnbaumite. The release of arsenic from the sample of svabite at pH 9 (23 mg/L As) is indeed less than the release from the johnbaumite precipitated by Mahapatra et al. (54), who achieved an arsenic concentration of 45.75 mg/L after 10 hours of dissolution at pH 8. The arsenic release reported by Twidwell et al. (40) without air sparging at pH 10.2 after 10 days was 23 mg/L, very close to the arsenic concentration after svabite dissolution at pH 9 after 3 days. Zhu et al. (47) achieved a concentration of 2.04 mg/L at pH 13.4 after 100 days of dissolution, a much longer time but a much higher pH. It would appear that the arsenic release seen with svabite in this work does not conclusively show that svabite is more stable than johnbaumite.

Twidwell et al. (40) also found that concentrations of arsenic in solution were below 3 mg/L at pH 8 for dissolutions of johnbaumite-hydroxyapatite solids containing less than 17% arsenate (relative to arsenate+phosphate) in the solid solution. The results found in this thesis had concentrations of 16 mg/L for a solid that was 15% arsenate, an order of magnitude greater than the concentrations reported by Twidwell and his group. This does not support the hypothesis that svabite is more stable than johnbaumite, although there is the possibility that a more crystalline svabite-fluoroapatite product would release less arsenic. Further work is required to determine the true solubility of svabite.

**Table 5.3: Summary of released arsenic concentrations after each phase of the stability tests**

Arsenic Content of F-apatite solids (% molar basis)	Fifth Washing	pH 9/3 days	pH Drifting (+3 days)	NaHCO <sub>3</sub> Addition (+3 days)
	mg/L	mg/L	mg/L	mg/L
15%	5	16	14	2,640
25%	8	20	22	1,779
50%	8	17	19	3,874
75%	11	18	22	2,622
100%/Svabite	13	23	25	1,711

The destabilizing effect of carbonate species that is seen to cause at least 100-fold increase in arsenic release deserves to be further studied under conditions more realistic from a waste disposal standpoint, such as exposure to atmospheric CO<sub>2</sub>, rather than the high concentration carbonate salt that was employed under necessity in the present work. To avoid exposure to CO<sub>2</sub>, calcium fluoro-arsenate-phosphate solids should be considered for disposal under anaerobic conditions.

## 6 Conclusions

The research described in this thesis has shown that it is possible to form svabite and svabite-fluorapatite solids from solutions containing arsenic(V) via precipitation promoted by neutralization and subsequent aging at 70-90°C. The successful formation of these compounds was confirmed by XRD analysis (part of Objective 1 of this thesis).

Due to the complexity of the calcium-arsenate-fluoride aqueous system and the potential formation of competing phases, different precipitation conditions were studied. It was found that it is important that the fluoride is added in a manner to avoid the precipitation of CaF<sub>2</sub>. This meant that the method developed included adding the fluoride last in the initial solution or after neutralization. The ideal pH for precipitation with an initial solution with an arsenate concentration of 0.15M is a moderately basic pH (greater than 7), but not too basic (should not be > pH 9), otherwise johnbaumite solids will also be formed. If the fluoride is added after the precipitation, svabite can be formed over a wider pH range down to pH 6. This pH range is specific to the initial concentration in solution.

Tests with different aging times revealed that an initial intermediate phase is formed during neutralization, which transforms to crystalline svabite upon aging. Aging is promoted as temperature is elevated above ambient conditions. It was determined 24-hour aging to be adequate to produce crystalline svabite.

The svabite precipitation method developed was successfully employed to produce mixed arsenate-phosphate apatite solids with different degrees of arsenate incorporation within the crystal matrix as confirmed by XRD analysis (Objective 2 of this thesis). This could indicate that at low ( $\leq 25\%$ ) level of substitution (low or high arsenic content) solid solution forms (fluoroapatite at low arsenic or svabite at low phosphate) rather than co-precipitated apatites. The morphology of the precipitated svabite solids was in the form of aggregated particles comprising primary needle-shaped crystallites resembling johnbaumite particle morphology.

Preliminary stability tests involving equilibration of produced solids for 3 days at pH 9 and another three days under drifting pH (8.2-8.5) conditions yielded the lowest dissolution for calcium arsenate fluoride compounds that have been previously precipitated from solution. This is attributed to the better crystallinity of the compounds synthesized in the present work. Nevertheless, the level of arsenic release (anywhere between 15 and 25 mg/L depending on the apatite composition, i.e. % As content) makes them questionable as fixation media for the long-

term disposal of arsenic. This is particularly so if no precaution is taken to avoid their exposure to carbonate-saturated waters as the fluoroapatite/svabite precipitates were found to react releasing prohibitive levels of arsenic ( $>1,000$  mg/L). It is remarked however that the quantity of carbonate used in these stability tests was excessive. It is possible that introducing carbonate at a lower rate – for instance by bubbling air or carbon dioxide throughout the solution – that the rate of arsenic release is manageable especially if further development of synthesis methods results in more crystalline solids. These tests and conclusions fulfilled Objective 3 of this thesis.

### *Limitations of Work Conducted*

The work presented achieved the main objective that was to produce crystalline svabite by aqueous precipitation involving neutralization and a short aging time. However, early complications from fluoride causing the formation of interfering  $\text{CaF}_2$  did not allow for comprehensive study of the precipitation process and the compounds formed. The mechanism of svabite crystallization was therefore only superficially established in terms of intermediate phase precipitating during neutralization and converting to svabite during aging. No information on nucleation and growth kinetics was derived.

The work is further limited by varying a single parameter at time ignoring possible parameter interaction effects. For instance, the concentration in solution impacts the pH where svabite will form, and the temperature of the solution impacts the kinetics of precipitation and the aging time required.

The present work also only identified the phases formed, rather than the degree of crystallinity or the purity of the phases. More detailed characterization of the solid compounds formed after various syntheses could lead to optimization of synthesis parameters yielding more reliable stability data.

The stability tests also have some limitations. No duplicate samples were run. The short duration also means that equilibrium was not reached by the end of the experiments. Also, the tests were run continuously in immediate succession in a single container for each sample. This may not be representative of the behaviour of the compounds if they were placed in these conditions until they reached equilibrium. Stability tests were not completed for all of the syntheses, and for an unrefined product – it may not be indicative of the actual stability possible with aqueously precipitated svabite.

### *Potential Future Work*

Further study is required to fully understand the system involved in the formation of svabite-fluorapatite. The solubility of both solids and the equilibrium between the solids and solutions are not well known. The crystallization of either solid could also be optimized for the formation of solids with greater crystallinity. Supersaturation control (12) has been used to precipitate fluorapatite from aqueous solution. Similar techniques may be possible, incorporating the formation of svabite into the crystals formed from fluorapatite supersaturation – allowing for secondary nucleation and the formation of more crystalline solids.

Further study would also allow the determination of whether the solids formed are a true solid solution, or whether the formation of fluoroapatite just helps with the formation of svabite. Further laboratory work, aided by modeling software such as PHREEQC (90) could determine the ultimate limits of stability of these type of arsenate-containing fluoroapatites. Further stability tests could be optimized by increasing testing time, and testing the stability of the solids under a single set of conditions, rather than multiple sets of conditions applied to the same solution, as was the case in this work because of time constraints. Any further work should include more quality assurance checks, such as duplicate samples from solution, in place.

## 7 Works Cited

- [1] World Health Organization, "Guidelines for drinking-water quality," WHO, 2011.
- [2] Government of Canada, Schedule 4, Metal Mining Effluent Regulations, 2014.
- [3] C. Sullivan, M. Tyrer, C. R. Cheeseman and N. J. Graham, "Disposal of water treatment wastes containing arsenic - A review," *Science of the total environment*, vol. 408, 2010.
- [4] R. J. De Klerk, Y. Jia, R. Daenzer, M. A. Gomez and G. P. Demopoulos, "Continuous circuit coprecipitation of arsenic (V) with ferric iron by lime neutralization: Process parameter effects on arsenic removal and precipitate quality," *Hydrometallurgy*, Volumes 111-112, pp 65-72, 2012.
- [5] D. Filippou and G. P. Demopoulos, "Arsenic immobilization by controlled scorodite precipitation," *JOM*, vol. 49, no. 12, pp 52-55, 1997.
- [6] M. Gomez, L. Becze, R. Blyth, J. Cutler and G. Demopoulos, "Molecular and structural investigation of yukonite (synthetic & natural) and its relation to arseniosiderite", *Geochimica et Cosmochimica Acta*, vol. 74, no. 20, pp 5835-5851, 2010.
- [7] Ecometales, "Codelco and Ecometales inaugurate arsenic stabilization plant," 10 August 2012. [Online]. Available: <http://www.ecometales.cl/codelco-and-ecometales-inaugurate-arsenic-stabilization-plant-2?lang=en>.
- [8] H. Kubo, M. Bumiya and M. Matsumoto, "Dowa Mining scorodite process - Application to Copper Hydrometallurgy," *Copper 2010*, no. 7, pp 2947-2958, 2010.
- [9] M.-C. Bluteau and G. P. Demopoulos, "The Incongruent Dissolution of Scorodite: Solubility, Kinetics and Mechanism," *Hydrometallurgy*, vol. 87, pp 163-177, 2007.
- [10] C. Verdugo, G. Lagos, L. Becze, M. Gomez and G. Demopoulos, "Study of arsenic release of atmospheric scorodite in reductive environments," *HydroProcess 2012 – 4<sup>th</sup> International Seminar on Process Metallurgy*, Santiago, Chile, pp 86-94, 2012.
- [11] P. Yuanming and M. E. Fleet, "Compositions of the Apatite-Group Minerals: Substitution Mechanisms and Controlling Factors," vol. 48, no. 1, 2002.
- [12] L. Katsarou, "Synthesis and application of hydroxyapatite and fluoroapatite to scorodite encapsulation," *McGill University Master's Thesis*, Montreal, 2011.
- [13] Mineralogical Society of America, "Svabite," *Handbook of Mineralogy*, Accessed 7/1/2017. [Online].



- [14] Y. Zhu, X. Zhang, Y. Chen, Q. Xie, J. Lan, M. Qian and N. He, "A comparative study on the dissolution and solubility of hydroxylapatite and fluorapatite at 25 degC and 45 degC," *Chemical Geology*, vol. 268, pp 89-96, 2009.
- [15] O. Sohnle and J. Garside, Precipitation: Basic principles and industrial applications, Oxford: Butterworth Heinemann, 1992.
- [16] G. Demopoulos, "Aqueous precipitation and crystallization for the production of particulate solids with desired properties," *Hydrometallurgy*, vol. 96, pp 199-214, 2009.
- [17] P. Drahota and M. Filippi, "Secondary arsenic minerals in the environment: A review," *Environment International*, vol. 35, 2009.
- [18] M. C. F. Magalhaes, "Arsenic. An environmental problem limited by solubility," *Pure Applied Chemistry*, vol. 74, no. 10, pp 1843-1850, 2002.
- [19] J. V. Bothe and P. W. Brown, "Arsenic immobilization by calcium arsenate formation," *Environmental Science and Technology*, vol. 33, pp 3806-3811, 1999.
- [20] P. Riveros, J. Dutrizac and P. Spencer, "Arsenic Disposal Practices in the Metallurgical Industry," *Canadian Metallurgical Quarterly*, vol. 40, no. 4, 2001.
- [21] L. Twidwell and J. McCloskey, "Removing arsenic from aqueous solution and long-term product storage," *JOM* vol. 63, no. 8, pp 94-100, 2011.
- [22] Montana Tech of the University of Montana, "Final Report-Arsenic Stabilization Research Project: Mine Waste Technology Program Activity IV, Project 5," Report MWTP-82 for the US Environmental Protection Agency, Butte, Montana, 1998.
- [23] G. P. Demopoulos, "On the preparation and stability of scorodite," *Arsenic Metallurgy*, TMS (The Minerals, Metals & Materials Society), pp 25-50, 2005.
- [24] United States Environmental Protection Agency, Test methods for evaluating solid waste, physical/chemical methods. SW-846 Test Method 1311: Toxicity Characteristic Leaching Procedure, EPA-902-B-94-001, 1994.
- [25] S. Singhania, Q. Wang, D. Phillipou and G. Demopoulos, "Temperature and Seeding Effects on the Precipitation of Scorodite from Sulphat Solutions under Atmospheric Pressure Conditions," *Metall. Materi. Trans. B.*, vol. 46B, pp 327-333, 2005.
- [26] G. Demopoulos, F. Lagno, Q. Wang and S. Singhania, "The atmospheric scorodite process," *Copper 2003*, pp 597-616, 2003.
- [27] G. P. Demopoulos, "Arsenic immobilization research advances: past, present and future," *Conference of Metallurgists*, Vancouver, 2014.

- [28] E. Rochette, G. Li and S. Fendorf, "Stability of arsenate minerals in soil under biotically generated reducing conditions," *Soil Science Society American Journal*, vol. 62, pp 1530-1537, 1998.
- [29] M.-C. Bluteau, L. Becze and D. GP, "The dissolution of scorodite in gypsum-saturated waters: Evidence of Ca-Fe-AsO<sub>4</sub> mineral formation and its impact on arsenic retention.," *Hydrometallurgy*, vol. 97, pp 3-4, 2009.
- [30] F. Lagno, "Encapsulation of scorodite particles with phosphate coatings," *McGill University Doctorate Thesis*, Montreal 2005.
- [31] K. Leetmaa, "Scorodite stabilization with aluminum hydroxy-gels," *McGill University Master's Thesis*, Montreal, 2009.
- [32] J. Adelman, "Investigation of sodium silicate derived gels as encapsulating materials for scorodite," *McGill University Master's Thesis*, Montreal 2013.
- [33] F. Lagno, S. Rocha, S. Chryssoulis and G. Demopoulos, "Scorodite Encapsulation by Controlled Deposition of Aluminum Phosphate Coatings," *Journal of Hazardous Materials*, vol. 181, pp 526-534, 2010.
- [34] T. Baikie, P. H. Mercier, M. M. Elcombe, J. Y. Kim, Y. Le Page, L. D. Mitchell, T. White and W. P. S, "Triclinic Apatites," *Acta Crystallographica*, vol. 8, no. B63, pp 251-256, 2007.
- [35] W. Stumm and J. J. Morgan, *Aquatic Chemistry*, 3rd edition, New York: Wiley and Sons, 1996.
- [36] M. C. F. Magalhaes and P. A. Williams, "Apatite group minerals: Solubility and environmental remediation," in *Thermodynamics, Solubility and Environmental Issues*, Elsevier B. V., 2007.
- [37] S. Cazalbou, C. Combes, D. Eichert and C. Rey, "Adaptive physico-chemistry of bio-related calcium phosphates," *Journal of Materials Chemistry*, vol. 14, pp 2148-2153, 2004.
- [38] T. Dordevic, S. Sutovic, J. Stojanovic and L. Karanovic, "Sr, Ba and Cd arsenates with the apatite-type structure," *Acta Crystallographica Section C: Crystal Structure Communications*, vol. 64, no. 9, pp 182-186, 2008.
- [39] C. P. Y. Z. Y. Wei, Z. Zhang, H. Liu and Z. Zhu, "Synthesis and characterization of the Ba<sub>5</sub>(P<sub>x</sub>)As<sub>(1-x)</sub>O<sub>4</sub>(3)Cl solid solutions," in *Advanced manufacturing technology Pts 1,2*, Advanced Materials Research, 2011, pp 232-236.
- [40] C. Johnson, J. Feldmann, D. Macphee, F. Worrall and J. Skakle, "Synthesis and proposed crystal structure of a disordered cadmium arsenate apatite Cd-5(AsO<sub>4</sub>)(3)Cl<sub>1-2x-y</sub>O<sub>x</sub> rectangle gOH<sub>y</sub>," *Dalton Transactions*, no. 21, pp 3611-3615, 2004.
- [41] F. Juillot, P. Ildefonse, G. Morin, G. Calas, A. de Kersabiec and M. Benedetti, "Remobilization of arsenic from buried wastes at an industrial site: mineralogical and geochemical control," *Applied Geochemistry*, vol. 14, pp 1031-1048, 1999.

- [42] P. J. Dunn, D. R. Peacor and N. Newberry, "Johnbaumite, a new member of the apatite group from Franklin, New Jersey," *American Mineralogist*, vol. 65, pp 1143-1145, 1980.
- [43] S. Hendricks, A. Bascot and H. Young, "The relative toxicity of the arsenates of calcium," *Industrial and Engineering Chemistry*, vol. 18, no. 1, 1926.
- [44] T. Itakura, R. Sasai and H. Itoh, "Arsenic recovery from water containing arsenite and arsenate ions by hydrothermal mineralization," *Journal of Hazardous Materials*, vol. 146, pp328-333, 2007.
- [45] V. Dutre and C. Vandecasteele, "Solidification/stabilisation of hazardous arsenic containing waste from a copper refining process," *Journal of Hazardous Materials*, vol. 40, pp 55-68, 1995.
- [46] G. Neupane and R. J. Donahoe, "Calcium-phosphate treatment of contaminated soil for arsenic immobilization," *Applied geochemistry*, vol. 28, pp 145-154, 2013.
- [47] C. M. Magalhaes and P. A. Williams, "Apatite Group Minerals: Solubility and Environmental Remediation," in *Thermodynamics, Solubility and Environmental Issues*, Elsevier B.V., 2007.
- [48] Y. Zhu, X. Zhang, Q. Xie, D. Wang and G. Cheng, "Solubility and stability of calcium arsenates at 25degC," *Water, Air, and Solid Pollution*, vol. 169, pp 221-238, 2006.
- [49] D. H. Moon, D. Dermatas and N. Menounou, "Arsenic immobilization by calcium-arsenic precipitates in lime treated soils," *Science of the Total Environment*, vol. 330, pp 171-185, 2004.
- [50] L. G. Twidwell, J. McCloskey, M. G. Lee and J. Saran, "Arsenic removal from mine and process waters by lime/phosphate precipitation," in *Arsenic Metallurgy: Fundamentals and Applications*, The Minerals, Metals & Materials Society, 2005.
- [51] O. Nelson and H. MM, "Calcium arsenates. An investigation into the three-component system calcium oxide-arsenic oxide-water," *Journal of the American Chemical Society*, vol. 59, 1937.
- [52] M. E. Taboada, P. C. Hernandez, E. K. Flores, H. R. Galleguillos and T. A. Graber, "Equilibria of aqueous system phases containing arsenic+iron and arsenic+calcium at (323.15 and 343.15)K," *Journal of Chemical & Engineering Data*, vol. 54, pp 3059-3068, 2009.
- [53] T. Nishimura and R. Robins, "A re-evaluation of the solubility and stability regions of calcium arsenites and calcium arsenates in aqueous solution at 25 degC," *Mineral Processing and Extractive Metallurgy Review: An International Journal*, vol. 18, no. 3-4, 1998.
- [54] J. C. Raposo, O. Zuloaga, M. A. Olazabal and J. M. Madariaga, "Study of the precipitation equilibria of arsenate anion with calcium and magnesium in sodium perchlorate at 25 degrees C," *Applied Geochemistry*, vol. 19, pp 855-862, 2004.
- [55] P. Mahapatra, L. Mahapatra and B. Mishra, "Arsenate hydroxyapatite: a physico-chemical and thermodynamic investigation," *Polyhedron*, vol. 6, no. 5, pp 1049-1052, 1987.

- [56] Y. J. Lee, P. W. Stephens, Y. Tang, W. Li, B. L. Phillips, J. B. Parise and R. J. Reeder, "Arsenate substitution in hydroxylapatite: Structural characterization of the  $\text{Ca}_5(\text{P}_x\text{As}_{(1-x)}\text{O}_4)_3\text{OH}$  solid solution," *American Mineralogist*, vol. 94, pp 666-675, 2009.
- [57] G. Neupane and R. J. Donahoe, "Calcium-phosphate treatment of contaminated soil for arsenic immobilization," vol. 28, 2013.
- [58] Y. J. Lee, "Spectroscopic investigation of arsenate and selenate incorporation into hydroxylapatite," *Current Applied Physics*, vol. 10, 2010.
- [59] Y. Zhu, X. Zhang, F. Long, H. Liu, M. Qian and N. He, "Synthesis and characterization of arsenate/phosphate hydroxyapatite solid solution," *Material Letters*, vol. 63, pp 1185-1188, 2009.
- [60] M. Kucharski, W. Mroz, J. Kowalczyk, B. Szafiriska and M. Gluzinska, "Leachability and thermal stability of synthesised and natural svabite," *Archives of Metallurgy*, vol. 47, no. 1, 2002.
- [61] S. Mazziotti-Tagliani, M. Angelone, G. Armiento, R. Pacifico, C. Cremisini and A. Gianfagna, "Arsenic and fluorine in the Etnean volcanics from Biancavilla, Sicily, Italy: environmental implications," *Environmental Earth Sciences*, vol. 66, no. 2, pp 561-572, 2012.
- [62] W. Stumm and J. J. Morgan, Aquatic Chemistry: Chemical Equilibria and Rates in Natural Waters, 3rd Edition, 1995.
- [63] T. White, G. Poniatowski, N. Kawashima, F. Lincoln, B. Rodier, G. Eaton and J. Kyle, "Xtaltite ceramics for toxic metal immobilization," Conference on Mining and the Environment, Sudbury, 1995.
- [64] T. White and I. Toor, "Stabilizing toxic metal concentrates by using SMITE," *JOM*, pp 54-58, 1996.
- [65] Y. Zhu, X. Zhang, H. Eng, H. Liu, N. He and M. Qian, "Characterization, dissolution and solubility of synthetic svabite  $[\text{Ca}_5(\text{AsO}_4)_3\text{F}]$  at 25-45 °C," *Environmental Chemistry Letters*, vol. 9, pp 339-345, 2011.
- [66] Y. Zhu, Y. Chen, F. Long, J. Lan, N. He and M. Qian, "Synthesis and Characterization of arsenate/phosphate fluorapatite solid solution," *Metallurgical and Materials Transactions A*, vol. 40A, pp 2659-2663, 2009.
- [67] L. Xu, Y. Zhu, M. Liang, N. He and T. Long, "Study on the solubility and stability of the arsenate/phosphate fluorapatite solid solution at 25 degC," *Acta Chimica Sinica*, vol. 69, no. 4, pp 418-424, 2011.
- [68] M. Manecki, P. A. Maurice and S. J. Traina, "Uptake of aqueous Pb by Cl-, F- and OH- apatites: Mineralogic evidence for nucleation mechanisms," *American Mineralogist*, vol. 85, pp 932-942, 2000.
- [69] M. Slijivic, I. Smiciklas, I. Plecas and M. Mitric, "The influence of equilibration conditions and hydroxyapatite physico-chemical properties onto retention of Cu 2+ ions," *Chemical Engineering Journal*, vol. 148, pp 80-88, 2009.

- [70] K. Viipsi, S. Sjoberg, K. Tonsuaadu and A. Schukarev, "Hydroxy- and fluorapatite as sorbents in Cd(II)-Zn(II) multi-component solutions in the absence/presence of EDTA," *Journal of Hazardous Materials*, vol. 252, pp 91-98, 2013.
- [71] E.-A. Perseil, P. Blanc and D. Ohnenstetter, "As-bearing fluorapatite in manganiferous deposits from St. Marcel-Praborna, Val D'Aosta, Italy," *The Canadian Mineralogist*, vol. 38, no. 1, pp 101-117, 2000.
- [72] K. A. Gross and K. A. Bhadang, "Sintered hydroxyfluorapatites. Part III: Sintering and resultant mechanical properties of sintered blends of hydroxyapatite and fluorapatite," *Biomaterials*, vol. 25, pp 1395-1405, 2004.
- [73] K. A. Gross and Rodriguez-Lorenzo, "Sintered hydroxyfluorapatites. Part I: Sintering ability of precipitated solid solution powders," *Biomaterials*, vol. 25, pp 1375-1384, 2004.
- [74] H. Ye, X. Liu and H. Hong, "Fabrication of titanium/fluorapatite composites and in vitro behavior in simulated body fluids," *Journal of Materials Science and Technology*, vol. 29, no. 6, pp 523-532, 2013.
- [75] Q.-X. Zhu, W.-H. Jiang, H.-D. Wang and C. Shao, "Investigation on preparation factors for fluorhydroxyapatite by an aqueous precipitation method," *Journal of Inorganic Materials*, vol. 26, no. 12, 2011.
- [76] A. Bengtsson, A. Shchukarev, P. Persson and S. Sjoberg, "Phase transformations, ion-exchange, adsorption, and dissolution processes in aquatic fluorapatite systems," *Langmuir*, vol. 25, pp 2355-2362, 2009.
- [77] H. McCann, "The solubility of fluorapatite and its relationship to that of calcium fluoride," *Archs oral Biology*, vol. 13, pp 987-1001, 1968.
- [78] M. Fulmer and P. W. Brown, "Low-temperature formation of fluorapatite in aqueous solution," *Journal of the American Ceramics Society*, vol. 75, no. 12, pp 3401-3407, 1992.
- [79] P. Van Cappellen and R. A. Berner, "Fluorapatite crystal growth from modified seawater solutions," *Geochimica et Cosmochimica Acta*, vol. 55, pp 1219-1234, 1991.
- [80] N. J. Flora, K. W. Hamilton, R. W. Schaeffer and C. H. Yoder, "A comparative study of the synthesis of calcium, strontium, barium, cadmium, and lead apatites in aqueous solution," *Synthesis and reactivity in Inorganic and Metal-Organic Chemistry* vol. 34, no. 3, pp 503-521, 2004.
- [81] Z. Amjad, P. Koutsoukos and G. Nancollas, "The crystallization of fluoroapatite. A constant composition study," *Journal of Colloid and Interface Science*, vol. 82, no. 2, 1981.
- [82] J. V. J. Bothe and P. W. Brown, "CaO-As<sub>2</sub>O<sub>5</sub>-H<sub>2</sub>O System at 23degC +/- 1degC," *Journal of the American Ceramic Society*, vol. 85, no. 1, pp 221-224, 2002.

- [83] A. Bengtsson and S. Sjöberg, "Surface complexation and proton-promoted dissolution in aqueous apatite systems," *Pure applied Chemistry*, vol. 81, no. 9, pp 5901-5912, 2009.
- [84] C. Chairat, J. Schott, E. H. Oelkers, J.-E. Lartique and N. Harouiya, "Kinetics and mechanism of natural fluorapatite dissolution at 25 °C and pH from 3 to 12," *Geochimica et Cosmochimica Acta*, vol. 71, pp 5901-5912, 2007.
- [85] L. Wu and W. S. P. W. Forsling, "Surface complexation of calcium minerals in aqueous solution: 1. Surface protonation at fluorapatite - water interfaces," *Journal of Colloid and Interface Science*, vol. 147, no. 1, pp 178-185, 1991.
- [86] D. E. Sandstrom, M. Jarlbring, O. E. Antzugin and F. Willis, "A spectroscopic study of calcium surface sites and adsorbed iron species at aqueous fluorapatite by means of <sup>1</sup>H and <sup>31</sup>P MAS NMR," *Langmuir*, vol. 26, no. 22, pp 11060-11064, 2006.
- [87] N. Harouiya, C. Chairat, S. J. Kohler, R. Gout and E. H. Oelkers, "The dissolution kinetics and apparent solubility of natural apatite in closed reactors at temperatures from 5 to 50 °C and pH 1 to 6," *Chemical Geology*, vol. 244, pp 554-568, 2007.
- [88] H. Yi, E. Balan, C. Gervais, L. Segalen, F. Fayon, D. Roche, A. Person, G. Morin, M. Guillaumet, M. Blanchard, M. Lazzeri and F. Babonneau, "A carbonate-fluoride defect model for carbonate-rich fluorapatite," *American Mineralogist*, vol. 98, no. 5-6, pp 1066-1069, 2013.
- [89] J. Perrone, B. Fourest and E. Giffaut, "Surface characterization of synthetic and mineral carbonate fluoroapatites," *Journal of Colloid and Interface Science*, vol. 249, pp 441-452, 2002.
- [90] R. Robins, "The solubility of metal arsenates," *Metallurgical Transactions B*, vol. 12, no. 1, pp 103-109, 1981.
- [91] M. Vallet-Reg, L. Rodriguez-Lorenzo and A. Salinas, "Synthesis and characterisation of calcium deficient apatite," *Solid State Ionics*, Vols. 101-103, no. Part 2, pp 1279-1285, 1997.
- [92] D. Parkhurst and C. Appelo, "Description of input and examples for PHREEQC version 3- A computer program for speciation, batch-reaction, one-dimensional transport, and inverse geochemical calculations," Chapter A43 in US Geological Survey Techniques and Methods, Book 6, 2013.
- [93] I. Sneddon, H. Garelick and E. Valsami-Jones, "An investigation into arsenic (V) removal from aqueous solutions by hydroxylapatite and bone-char," *Mineralogical Magazine*, vol. 69, no. 5, pp 769-780, 2005.

## Appendix A: Duplicates of Synthesis Procedures

This appendix presents the duplicate syntheses for various procedures. The labels for each series are synthesis codes assigned by the researcher.

*Repeated syntheses: pH 8, Arsenate Concentration 0.15M, 70°C Neutralization and Aging, 24 Hours Aging, Fluoride in Initial Solution*

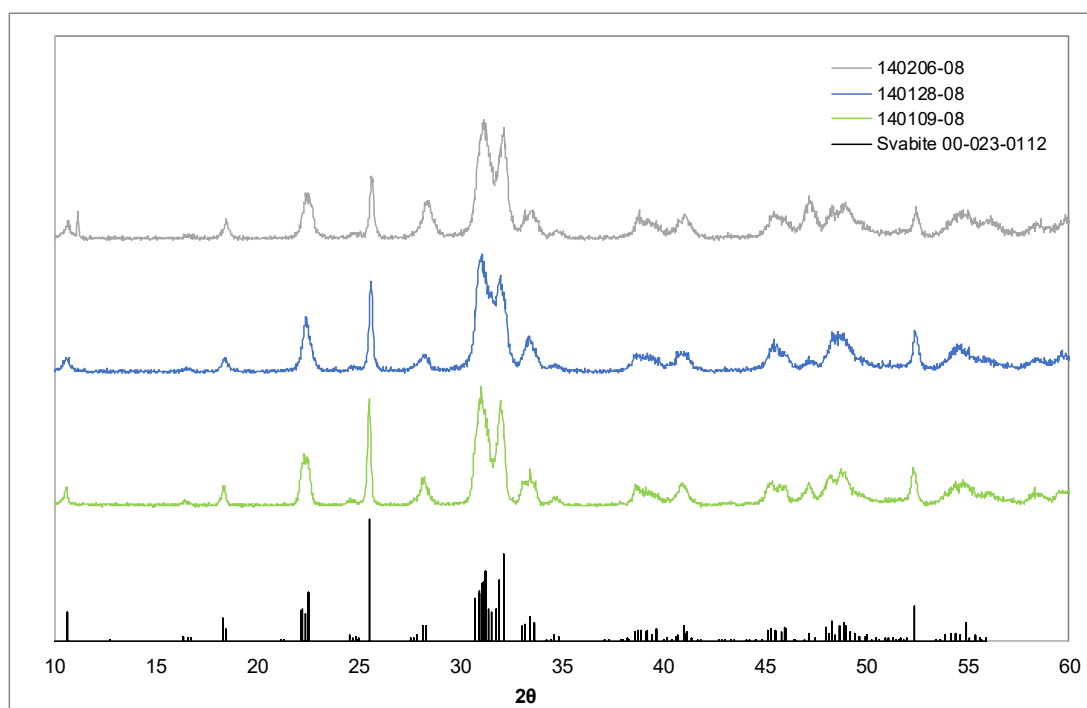


**Figure A-1: Svabite precipitation duplicates using synthesis at pH 8, 0.15M initial concentration, fluoride in initial solution, neutralization and aging at 70°C**

*Repeated Syntheses : pH 6, Arsenate Concentration 0.15M, 70°C Neutralization and Aging, 24 Hours Aging, Fluoride in Initial Solution*

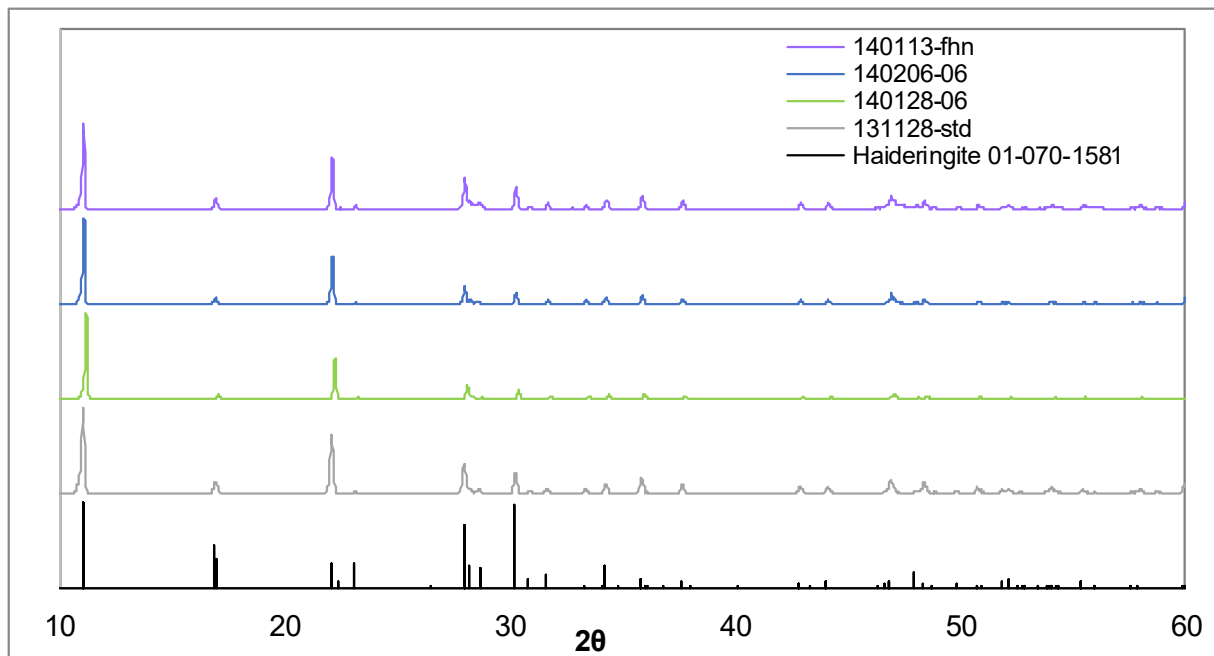


**Figure A-2: Haideringite precipitation duplicates using synthesis at pH 6, 0.15M initial concentration, fluoride in initial solution, neutralization and aging at 70°C**



*Repeated Syntheses : pH 4, Arsenate Concentration 0.15M, 70°C Neutralization and Aging, 24 Hours Aging, Fluoride in Initial Solution*

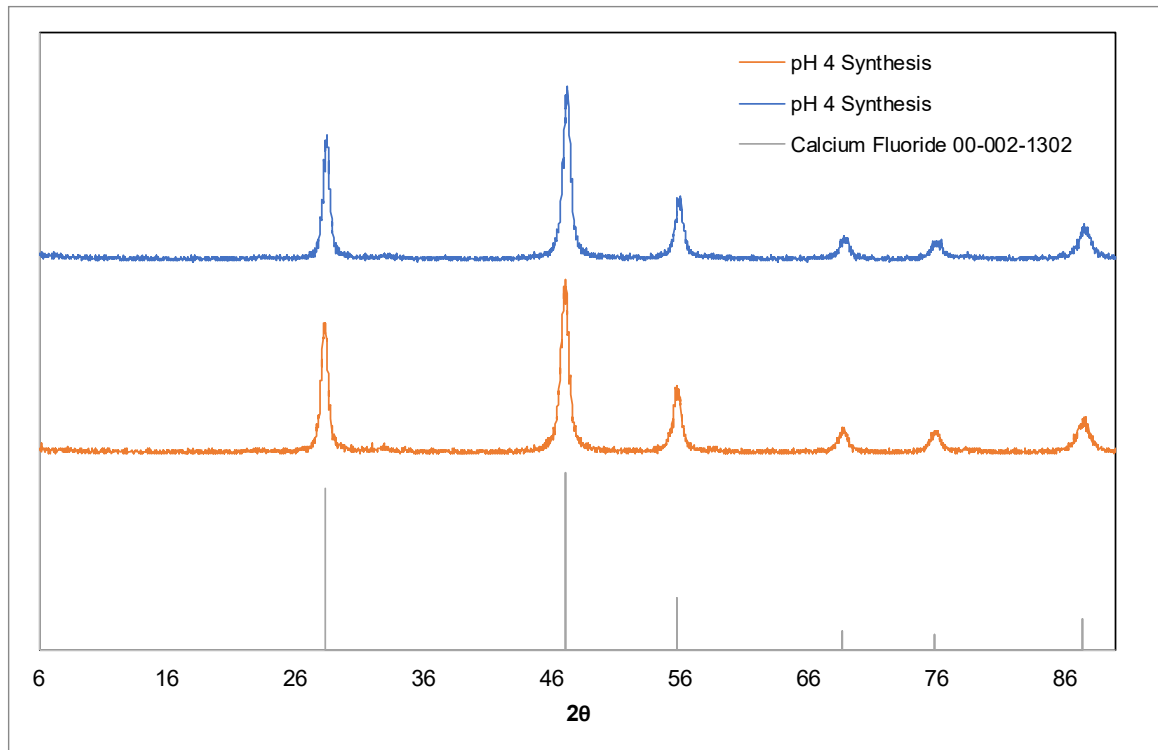


**Figure A-3: CaF<sub>2</sub> precipitation duplicates using synthesis at pH 4, 0.15M initial concentration, fluoride in initial solution, neutralization and aging at 70°C**

*Repeated Syntheses : pH 10, Arsenate Concentration 0.15M, 70°C Neutralization and Aging, 24 Hours Aging, Fluoride in Initial Solution*

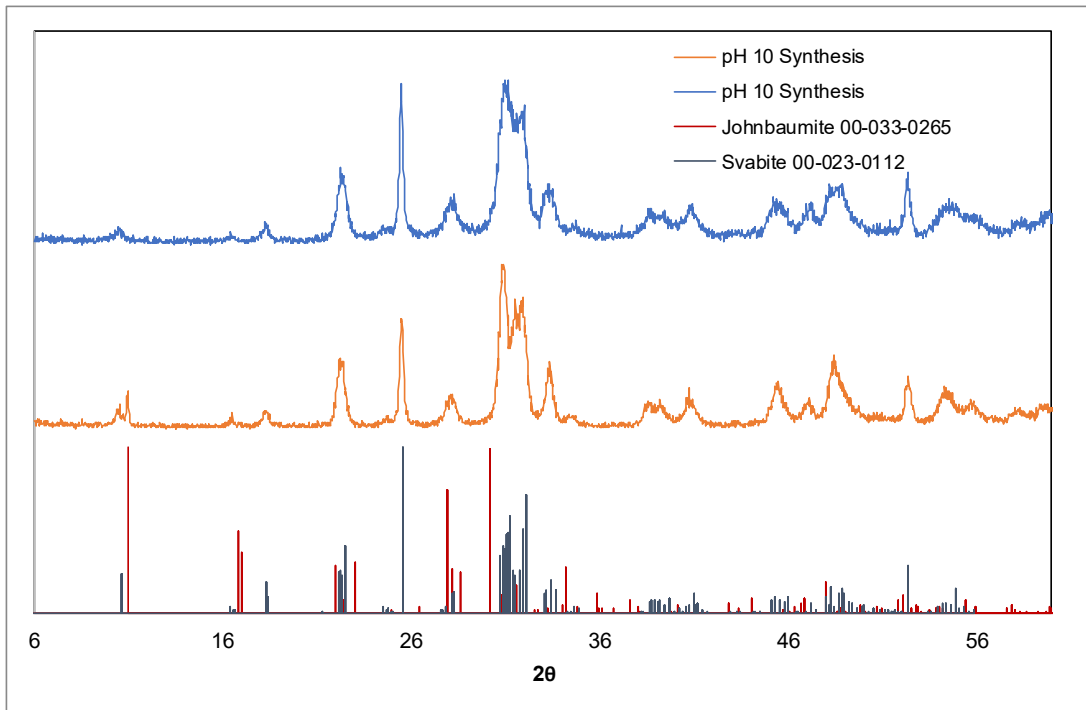


**Figure A-4: Duplicates using synthesis at pH 10, 0.15M initial concentration, fluoride in initial solution, neutralization and aging at 70°C**

*Repeated syntheses: pH 8, Arsenate Concentration 0.15M, 70°C Neutralization and Aging, 24 Hours Aging, Fluoride Added After Neutralization*

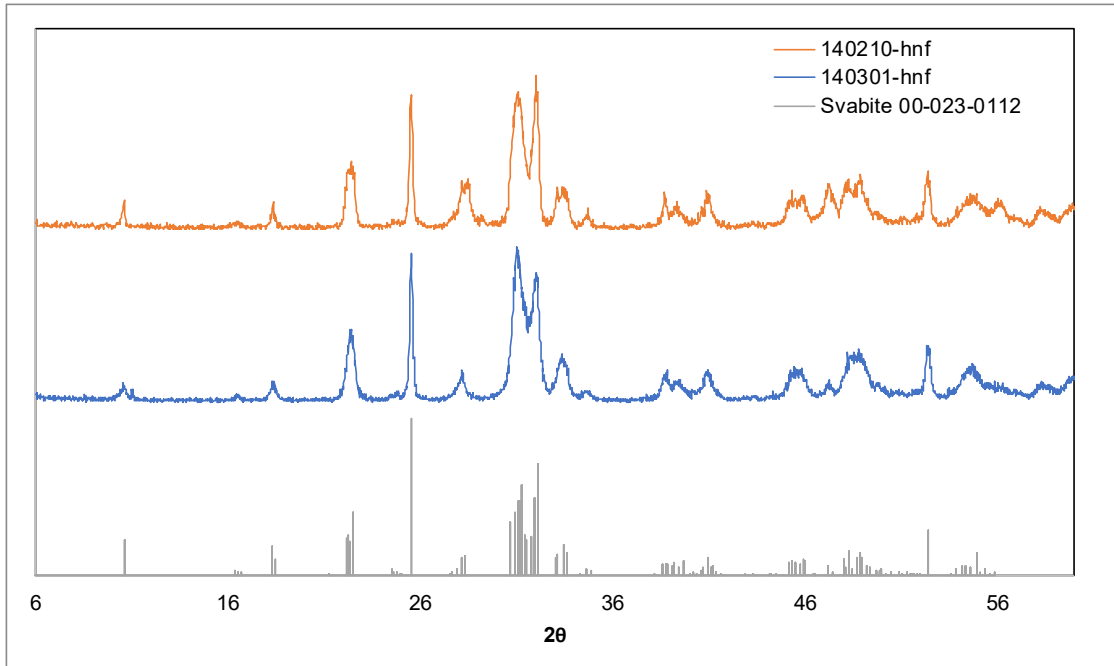


**Figure A-5: Svabite precipitation duplicates using synthesis at pH 8, 0.15M initial concentration, fluoride added after neutralization, neutralization and aging at 70°C**

*Repeated syntheses: pH 8, Arsenate and Phosphate Concentration 0.15M, 70°C Neutralization and Aging, 24 hours Aging, Fluoride Added After Neutralization*

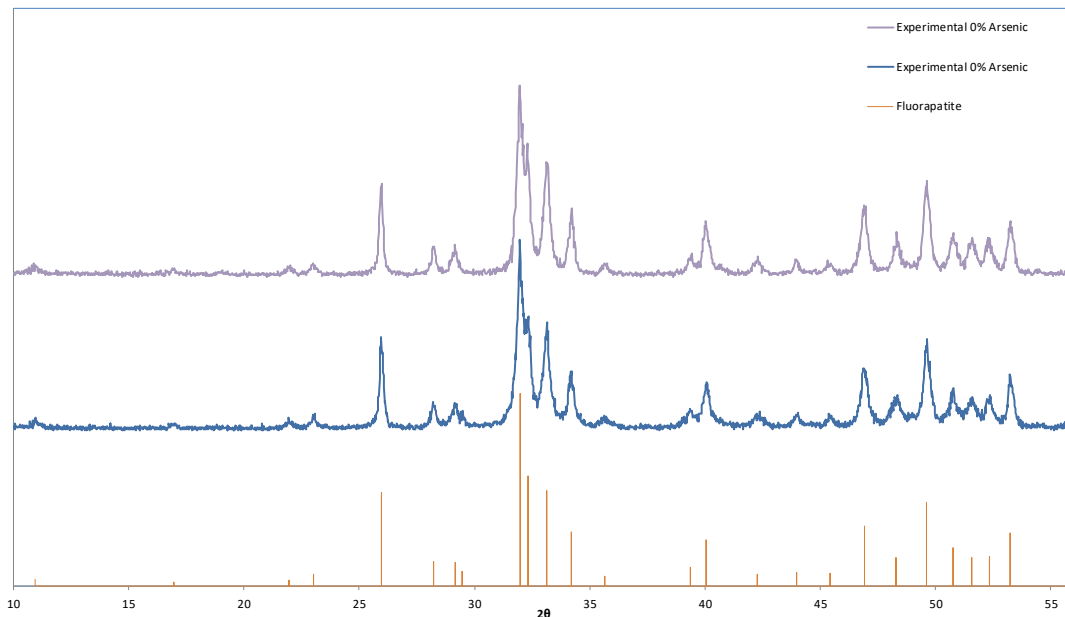


**Figure A-6: Duplicates of fluorapatite synthesis at pH 8**

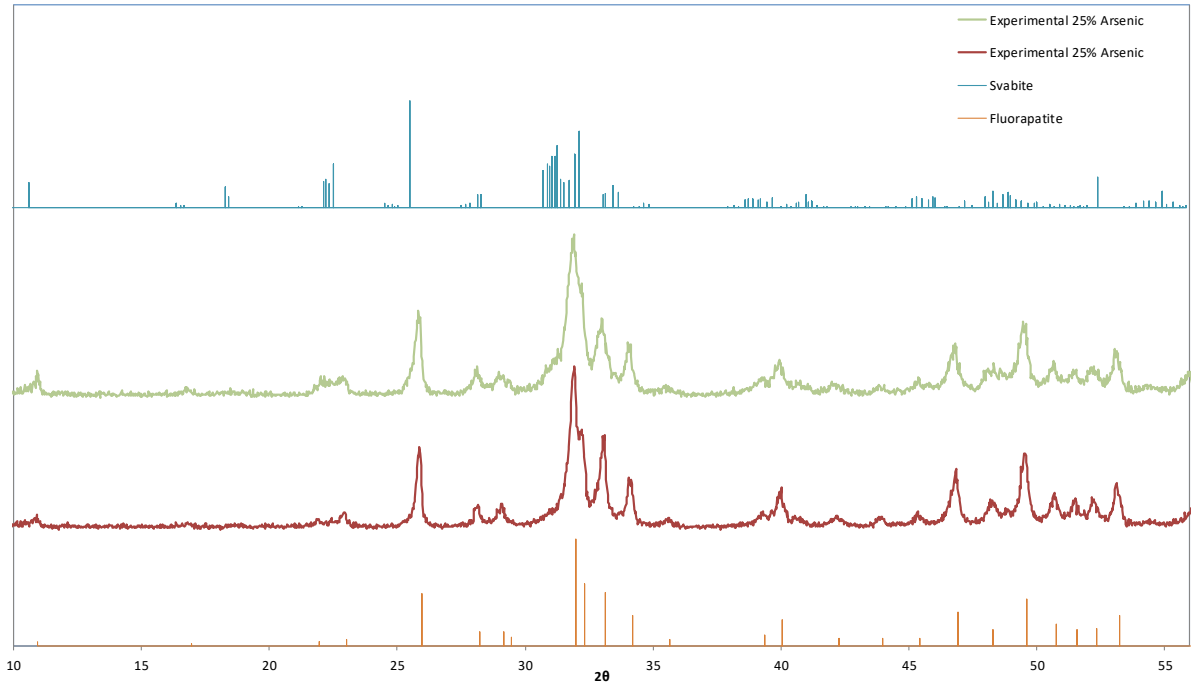


**Figure A-7: Duplicates of 25% Arsenate Svabite-Fluorapatite Synthesis at pH 8**

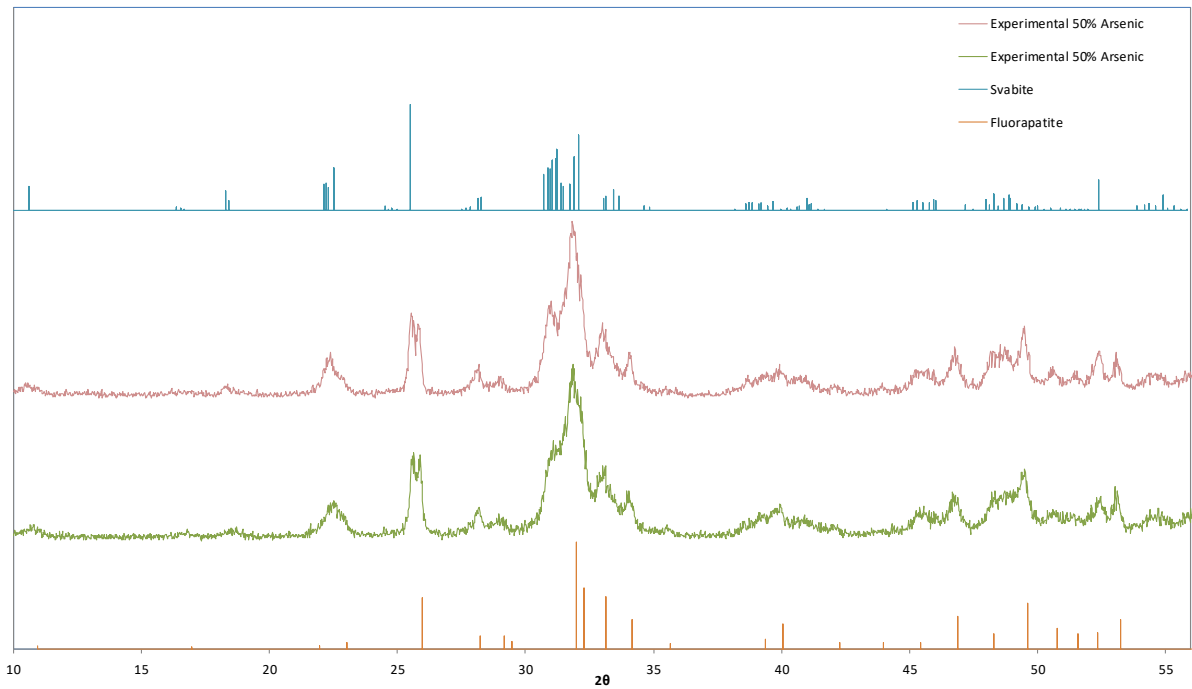


**Figure A-8: Duplicates of 50% arsenate svabite-fluorapatite synthesis at pH 8**

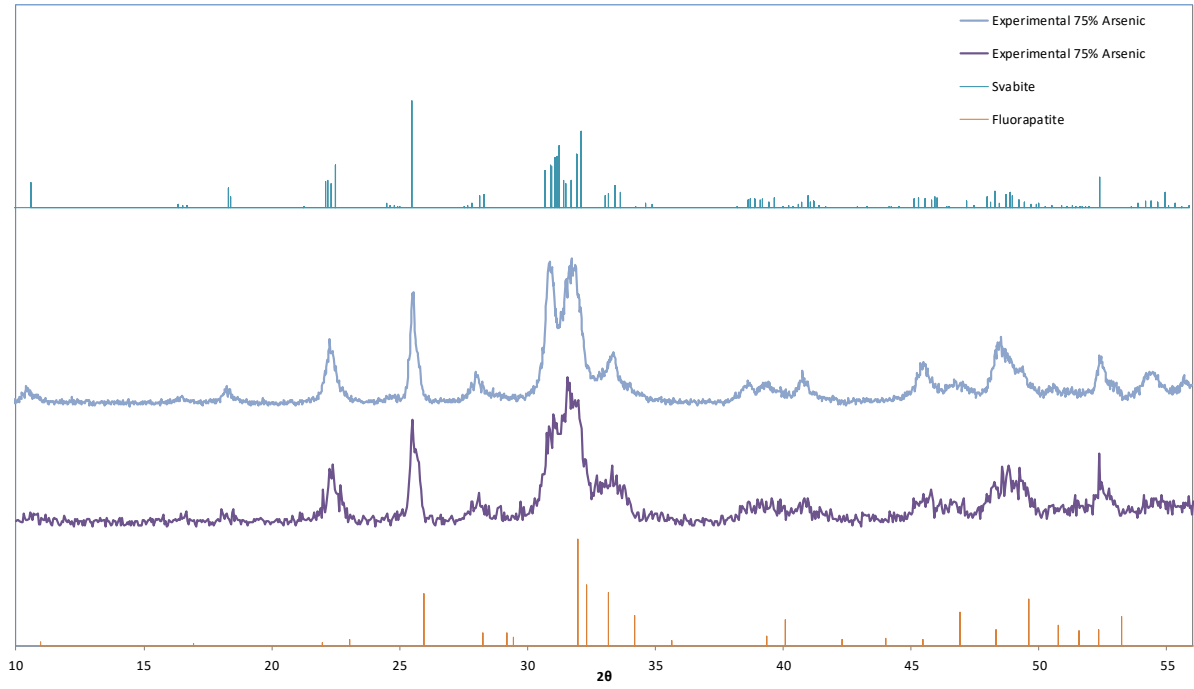


**Figure A-9: Duplicates of 75% arsenate svabite-fluorapatite synthesis at pH 8**

## Appendix B: Synthesis of Mixed Arsenate/Phosphate Apatites at Different Neutralization pH

This section presents synthesis of additional mixed arsenate/phosphate solids at different neutralization pH.

In addition to the results presented in section 5.2 involving synthesis of mixed compounds at 70°C and pH 8, synthesis tests were also carried out by neutralizing to different pH endpoints, before being allowed to age without pH control. Samples with 0% arsenic were neutralized to pH 6, 8, and 9. All three syntheses resulted in the formation of fluoroapatite, as identified by XRD (see Figure B-1). Syntheses with 25% arsenic are presented in Figure B-20. Peaks for svabite appear in syntheses at a pH greater than pH 6.

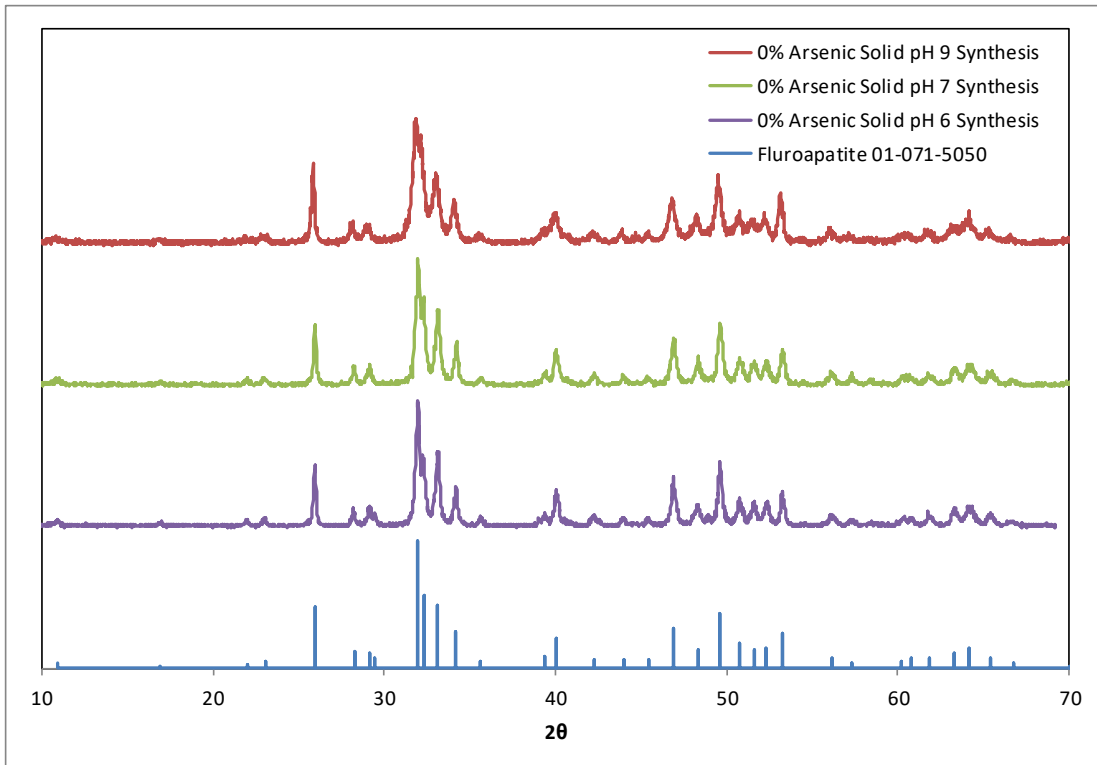
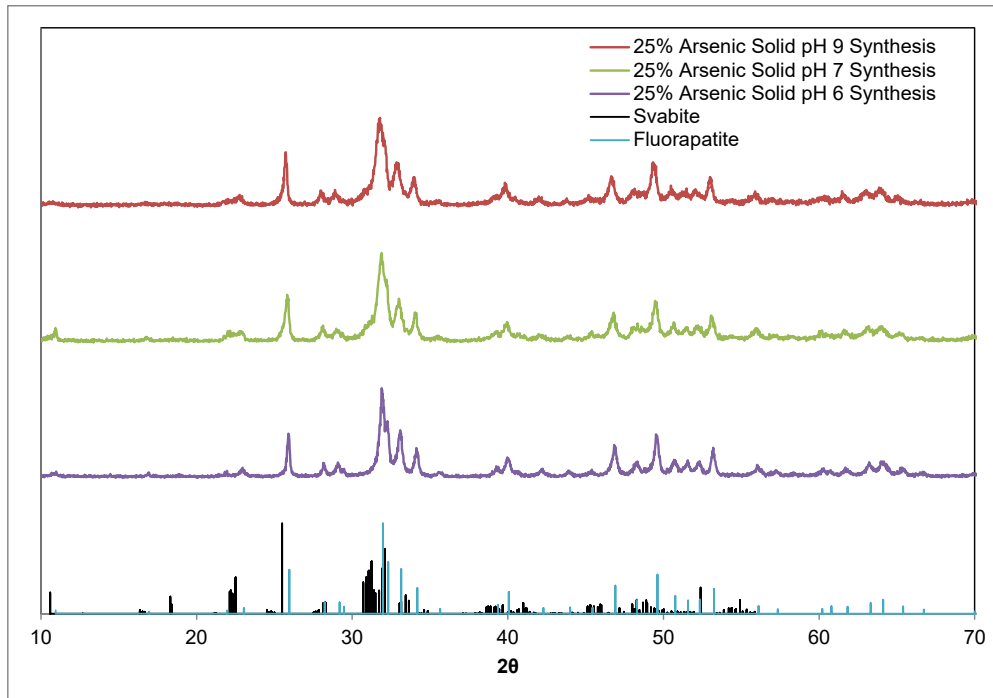
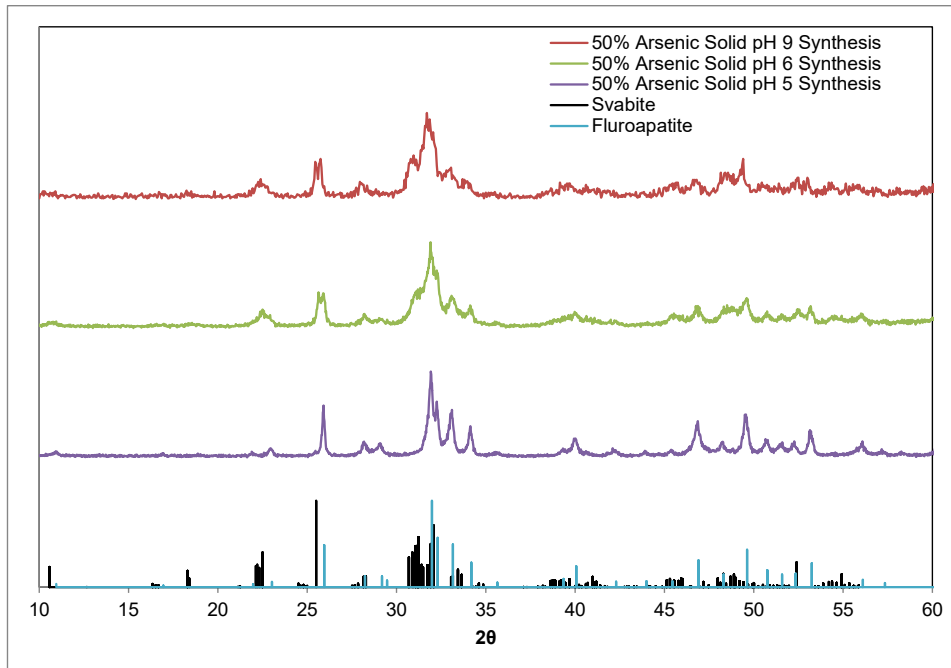


Figure B-1: XRD patterns for fluoroapatite synthesized at varied pH



**Figure B-2: XRD patterns for 25% arsenic synthesized mixed compounds at varied pH**

The XRD patterns for the solids formed with 50% arsenic in the initial solution at different pH are presented in Figure B-3. The pH 5 synthesis shows no peaks of svabite, while the synthesized solids at pH 6 and pH 9 show svabite peaks. Similarly, the pH 7 and pH 9 syntheses with 75% arsenic (presented in Figure A.12) show a greater similarity to svabite at higher pH. The transition between phases as the pH changed is not as smooth with a higher arsenic fraction. Perhaps syntheses at certain compositions do not result a solid solution, but are assemblies of fluoroapatite and svabite.



**Figure B-3: XRD patterns for solids precipitated with 50% arsenic at different pH**

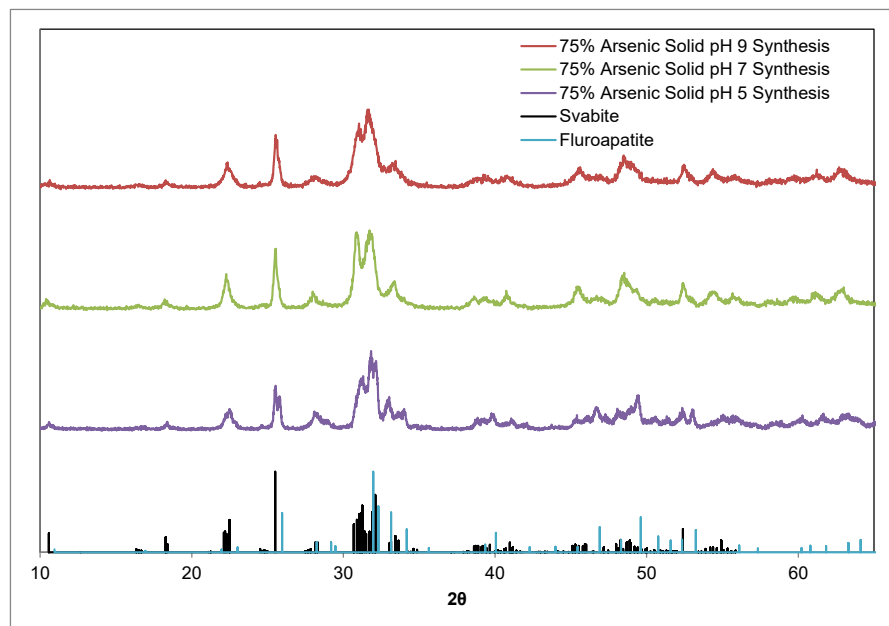


**Figure B-4: XRD patterns for solids precipitated with 75% arsenic at different pH**



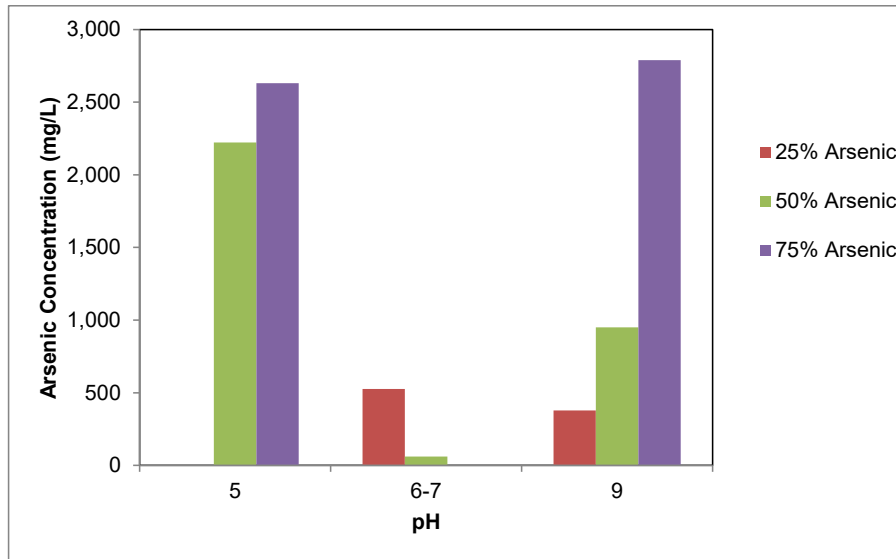


**Figure B-5: Residual arsenic concentrations after synthesis at different pH**

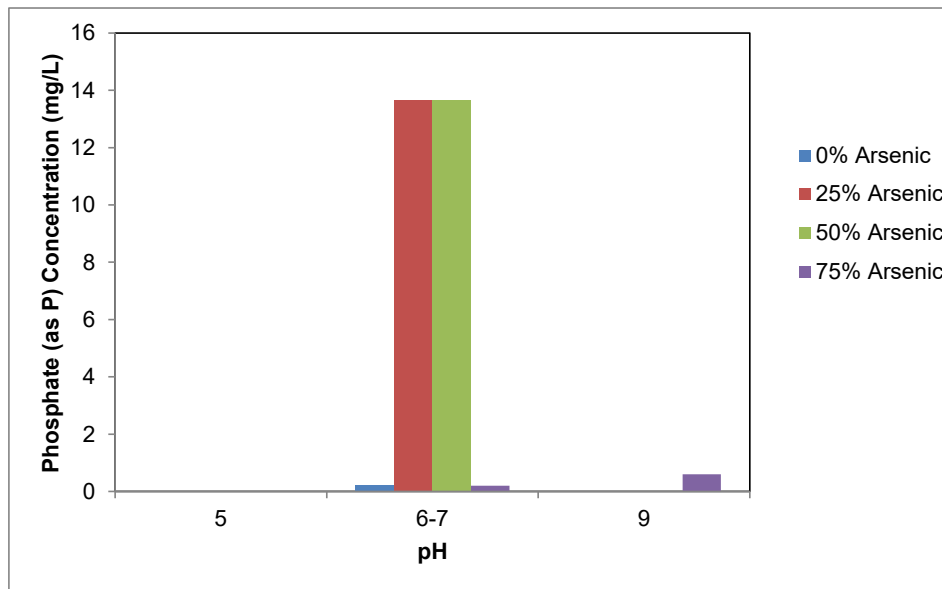


**Figure B-6: Residual phosphate concentrations after synthesis at different pH**

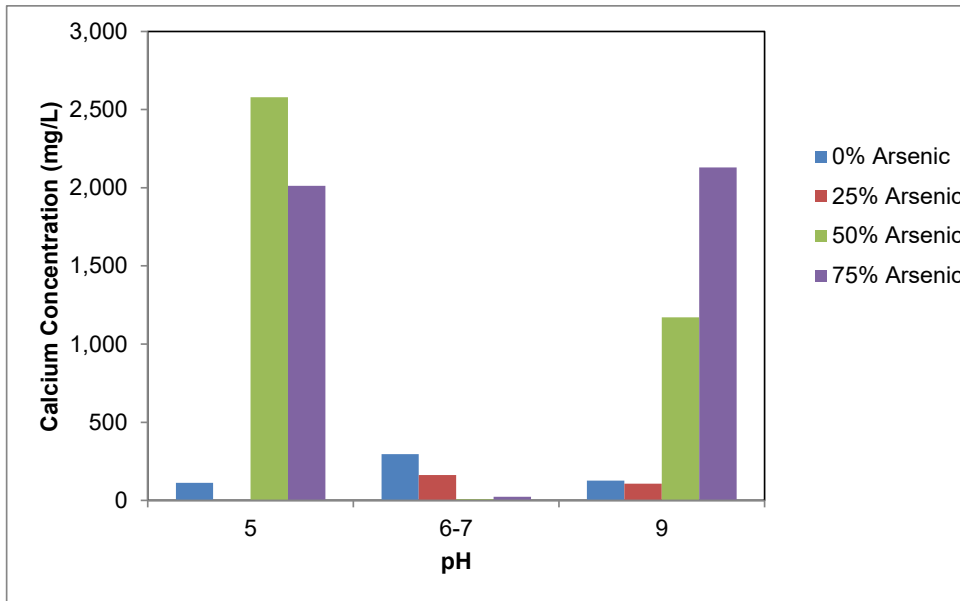


Figure B-7: Residual calcium concentrations after synthesis at different pH

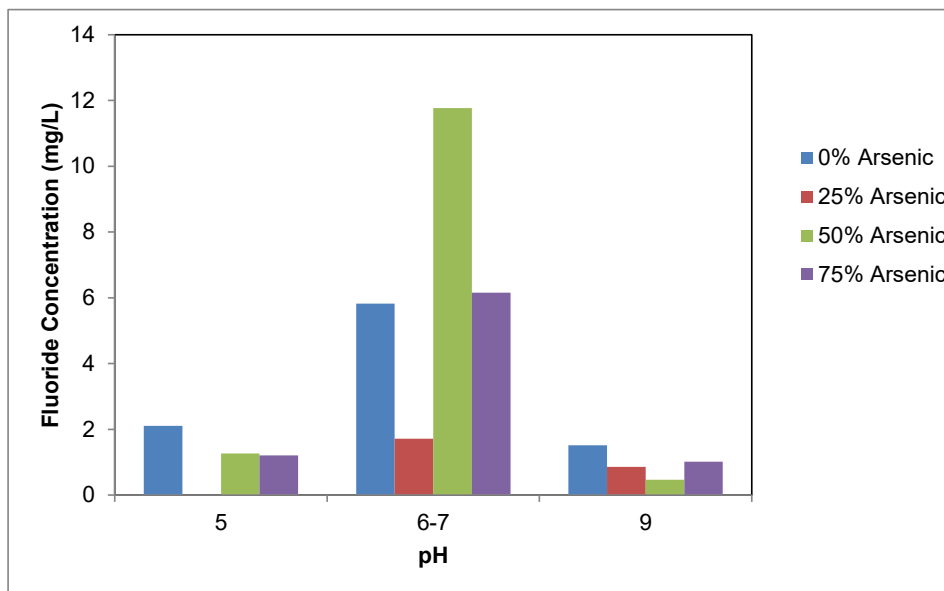


Figure B-8: Residual fluoride concentrations after synthesis at different pH

The concentrations in solution at the end of each synthesis were measured using ICP. The arsenic concentrations are presented in Figure B-5. Arsenic concentrations were lowest at pH 6-7. This decrease in concentration may be due to the presence of an immiscibility gap within the svabite/fluorapatite solid solution. Or potentially more Ca-As soluble phases are precipitated in this pH range. Further study is necessary. Phosphate concentrations are presented in Figure B-6. Phosphate concentrations are highest in pH 6-7, the opposite of the arsenate trend. The phosphate

concentrations are several orders of magnitude lower than the arsenate concentrations, i.e. phosphate is precipitating preferentially. Calcium concentrations are presented in Figure B-7. The calcium concentrations are lowest at pH 6-7. Fluoride concentrations are presented in Figure B-8, and are highest at pH 6-7. This may indicate the formation of fluoroapatite solids that are either not fully crystalline or they do not have the theoretical stoichiometric composition. Further characterization work including reproducibility measurements of solution concentrations to clarify the origin of this behaviour are required.